UNIVERSITA' DEGLI STUDI DI PADOVA

MASTER DEGREE IN CIVIL ENGINEERING

Analysis of multifractals downscaling method for urban scale rainfall

By

Paolo Leorin

Supervisor: Andrea Marion

Co-supervisor: Wang Li-Pen

Abstract

Localised storms with heavy rainfall can have disruptive consequences in cities for private lives and the urban economy. It is necessary to have accurate information about rainfall and flooding to be able to prevent such damage. This information, however is quite difficult to acquire, especially for cities with their highly variable urban landscapes that cause storms and water flows to move in unpredictable ways. Whether the final objective is to model flooding and explain occurred flood damage, accurate rainfall data are an absolute necessity and precisely this type of data is lacking for urban areas.

The aim of this work is to research methods to obtain reliable, urban scale rainfall values at areas smaller than 1 km^2, starting from the data given by the meteorological radar. In order to obtain these values, different techniques have been used: the advanced downscaling Multifractals method and different interpolation methods, the ordinary Kriging, the “Inverse distance weighting” and the “Inverse squared distance weighting”. Finally they have been compared with each other and, at the end, with the rain gauges which represent the only reliable devices. This study has taken into account different rainfall events, in terms of intensity, so different behaviours of the methods can be deduced. Interesting conclusions have been found despite the uncertainty given by the radar and its difficult correspondence with the rain gauges.

Contents

List of figures

List of tables

Chapter 1

Introduction

In this chapter, a brief background is firstly given and the motivation of this thesis is explained in order to define the aim of this research. Then, the main objective and consequent sub-objectives are precisely presented. Finally, the structure of this dissertation is summarised to provide a clear overview of this research.

1.1 Research motivation

Larger drainage area always suffers from frequent sewer pressurizations and occasional floods. Due to ongoing urbanization trends and climate change, it is expected that the frequency of sewer floods will significantly increase in the future. Many cities in the United Kingdom and other countries suffered from serious damages caused by floods; in the summer of 2007, for example, over 55,000 homes and businesses in the UK were flooded due to the fact that urban drains, river channels, and flood defences were unable to cope with the extreme quantities of water resulting from pluvial, fluvial and coastal causes. According to the post-flood study of 2007 summer floods conducted by the Environment Agency, around two-thirds of flooded properties were affected by pluvial (also known as surface water) floods, which are mainly induced by intense rainfall. Compared to coastal and fluvial flooding (which are induced respectively by the surge of sea and river water), pluvial flooding was given much less attention in the past and the associated forecasting and warning systems did not exist in the UK. Some follow-up studies further emphasised the importance of appropriately tackling pluvial floods as the associated statistics show that over 4 million properties in the UK are currently at risk from this type of flooding and

approximately 2 million people in the urban areas are at an annual pluvial risk of 0.5 % or greater. Pluvial (Surface water) floods caused serious disasters and massive losses particularly in urban areas because these areas are in general highly-populated and filled with businesses; in addition, these areas are usually small and a large percentage of surface is covered by impervious pavement and therefore the concentration time is short and the available response time to flooding is much less. This type of flooding usually happens quickly and locally and therefore advanced and reliable warning is difficult so that measures have to be taken: the first lies in the development of reliable and efficient hydraulic models so that they are able to effectively and timely reflect hydraulic behaviours of floods in urban areas in real time. The second lies in the generation of high-resolution rainfall forecasts, which will be used as inputs for the corresponding hydraulic modelling. Since the hydraulic modelling aspect is not the focus of this work, further discussion is not detailed here; It has been widely recognised that the uncertainty of rainfall forecasts propagates the overall hydrological processes and dominates the accuracy of urban pluvial flood modelling. Rainfall forecasting techniques therefore play a key role in obtaining reliable pluvial flood forecasts, and many related works have been carried out to provide better rainfall forecasts. There is however an inevitable trade-off between forecasting resolution and lead time. This lead time is however insufficient for the corresponding urban hydraulic modelling to accurately estimate the distribution of surface floods. It is therefore a challenging issue to retain the sufficient lead time for high-resolution rainfall forecasting. There are some cases in which the spatial and temporal resolutions such as 1 km/5 min with 3hr lead time could be enough; this achievement may not always satisfy the requirements for urban scale pluvial flood modelling, since the required spatial and temporal resolutions for rainfall estimates and forecasts are highly correlated to the concentration time (or the size) of the catchment and in some cases of very small areas the suggested resolutions could be 1-5 min and 100-500 m. In order to improve rainfall estimate and resolution, different techniques are currently subjects of research. Between these, higher resolution radars are studied and tested. In particular, the Rain Gain project which aims to obtain detailed data about peak precipitation and flooding at urban scale is moving in this direction. Another research technique is given by downscaling methods. New developments and tests are carried out on this technique, which is based upon the scale invariant properties of rainfall, that enable the generation of street scale (smaller than 1 km grid length in space) rainfall estimates. This research will analyse a kind of spatial downscaling method based upon the theory of left-sided multifractals, the (cascade) generating equation and the semi-deterministic cascade model, which will be exhaustively explained in chapter n° 4. A summary of the objectives research will be given in the following section.

1.2 Research objective

The main objective of this work is to bear an analysis on the downscaled rainfall estimates for urban scale resolution(particularly for 31.25x13.25m^2 areal estimates). In order to reach this objective, rainfall radar values have been used as data set for the downscaling method and, on the other hand, the values of the rain gauges have been used as "truth values". As a consequence other problems regarding the suitability of the radar and rain gauges values have been studied in order to understand the limits of the downscaling method. In addition, three different interpolation technique methods (Ordinary Kriging, Inverse distance weighting(IDW), Inverse squared distance weighting) have been involved in the attempt to improve the estimation of the rainfall spatial variability at the urban scale resolution and to understand if the interpolated values can provide better results instead of the downscaled values. Finally, a comparison between the interpolation methods is analysed, and their different behaviours in rainfall estimating are assessed. This leads to the detailed objectives of this research:

- Understand if the downscaling method used, is able to provide good order of magnitude and reliable estimation in relation to the values given by both the rain gauges and the radar.
- Understand if the downscaling method presents different behaviour according to the kind of rainfall events analysed, in terms of rainfall intensity.
- Find out solutions to improve the Downscaling method.
- Understand if the interpolation methods are able or not to give better values than the downscaling method. Understand if they can provide a reliable rainfall spatial variability. Make a comparison of the results obtained by the different interpolation methods.
- Make considerations about the suitability between radar and rain gauges and its variability according to the rainfall intensity and accumulation.

In the next chapter the methodology used to reach the objectives listed above is illustrated with also the relative limits. After, in the following chapters the downscaling method and the interpolation methods are deeply explained and finally the results and the conclusions are given.

Chapter 2

Research methodology

In this chapter, the interpolation and downscaling methods that have been used are explained and which are the possible limits and expectations of the methodology undertaken. Finally the rainfall events analysed are listed and their main features are explained, which can affect the working of both the downscaling and interpolation methods.

3.1 Devices and methods

The Bradford University is equipped with 16 rain gauges installed over the campus on the department roofs, and they are all concentrated in less than 500x500m^2; in total there are 8 measuring locations and in each one 2 pairs of rain gauges are positioned (Figure 2.1). The maximum distance between two rain gauges is 404 m. This unusual arrangement of the rain gauges gives the possibility to reliably analyse the rainfall variation on a sub kilometre scale; this is the essential input for the target of this research. In order to capture, at best, the rainfall variability three rain gauges have been chosen. In particular the points A,I,C was taken into account. The relative distance between the points A and C is the maximum (404 m as mentioned before). On the contrary the relative distances between C,I and I,A are respectively 88m and 380m. The two rain gauges in each position record the same values at each time step so that it was enough to consider just one of the two rain gauges. On the contrary, the rainfall in the three points showed some differences even if not so much to be considerable for some of the events analysed.

three points showed some differences even if not so much to be considerable for some of the events analysed.

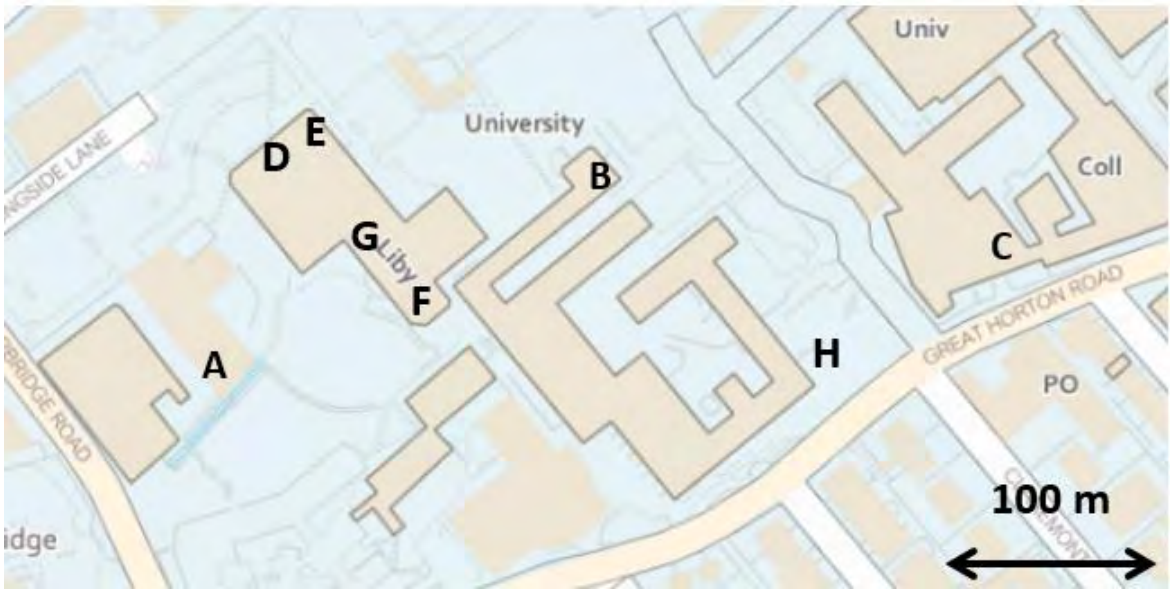

Figure 2. 1 : Rain gauge deployment at the University of Bradford.

One first comparison can be done using the estimation provided by the radar and in particular by its relative pixels. In this case, as it is shown in the figure 2.2, the rain gauges are all inside one pixel (with coordinates 415500;432500), so that there is just one reference. In order to compare the two data sets, they need to have the same resolution: the radar provides rainfall rate every 5 minutes on the other hand the rain gauges every minute. As a consequence, the rainfall rate measured by rain gauges, is averaged over 5 minutes. It has to be kept in mind that the type of data provided from the two devices are completely different. A rain gauge typically collects rainfall at ground level over a circular area of diameter 20 cm, on the contrary a radar scans the atmosphere over a volume whose projected area is roughly 1 km^2. Further, the two devices not only have different measurement systems but even different error characteristics. Potential problems and error sources in tipping bucket rain gauge data may occur, including blockages, wetting and evaporation, high rain rates, wind effects, position and shelter. On the other hand, different problems involve the radar working like occultation, spurious echoes, radar beam above the cloud and many others (in the chapter n°3 the working and error causes of the rain gauges and radar is briefly explained). Furthermore, this difference in the type of data is maintained even in the interpolation and downscaling method. Although they try to improve the radar values, they are always an elaboration of the same values.

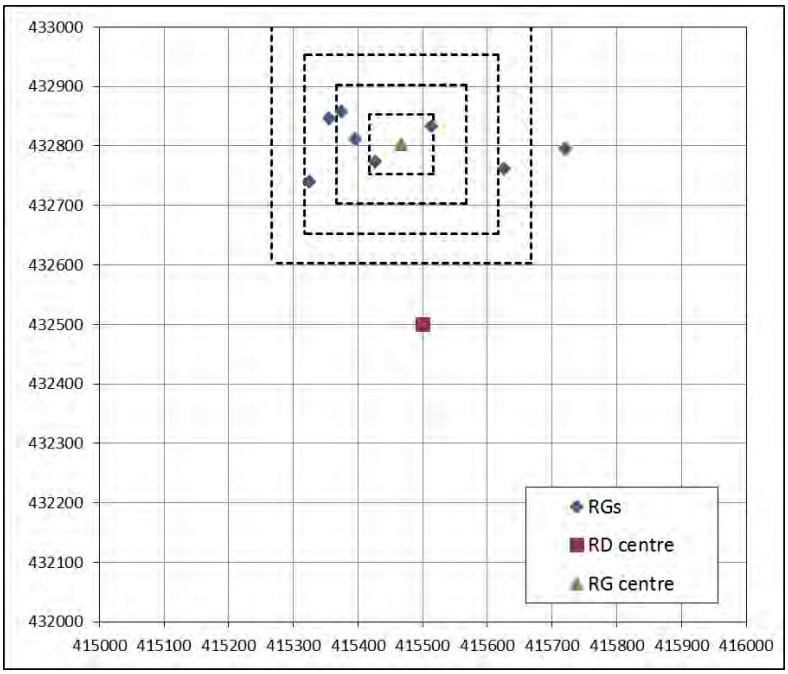

Figure 2. 2 Radar Pixel (coordinates 415500;432500) and rain gauges deployment.

In order to improve the estimation given by the radar a particular downscaling method has been used, based upon the theory of left-sided multifractals, the (cascade) generating equation and the semi-deterministic cascade mode (in chapter n° 4 the method is exhaustively explained). As mentioned before, the input is the radar data set 1x1km^2 and it is conducted with 5-level quad-nominal stochastic downscaling. It means that there are in total 5 levels (downscaled levels) and each one is divided in 4 equal sub-sections which, in turn, they are again sub-divided into 4 sub-sections. This entails that the 1 km^2 radar pixel was downscaled to 32 X 32 (in total 1024) grid squares, and each downscaled grid square size is 31.25 X 31.25 m^2. As it is shown in the figure 2.3, the three rain gauges taken into account fall within the respective 31.25 X 31.25 m^2 area. The rainfall values of these areas are the final output of the downscaling process, which are compared with the rain gauges and with the other methods later explained. The downscaling process is stochastic so 1024 (4x4x4x4x4=1024) realizations are generated for each area at the final level, at each time step. So the total number of realizations to take into account are 1024 x 3 (3 being the number of the areas which correspond with the points A,I,C (figure 2.1)). At the end, within the 1024 realizations, just 100 realizations are considered because they permit a good enough statistic analysis. Hence, at each time step(so every 5 minutes), 300 (100X3) values are taken into account for the downscaling process. In order to bear a satisfying analysis different statistic values have been calculated to represent at best the 100 realizations. In particular for each realizations series of each time step; the minimum, the first quartile, the median(the second quartile), the average, the third quartile and the maximum are found. Particularly important are the first and

the third quartile in which it is expected the rain gauge values to fall inside; this behaviour doesn't happen frequently, as it will be shown in chapter n°6, so that even the maximum and the minimum of each series are useful to find out. Being stochastic realizations, the downscaled values are not going to provide a spatial variation between the three areas considered; this behaviour will be clearer with the plot of the frequency distributions and the relative box plots (chapter n°6) of the realizations at each time step in the three areas. On the contrary, it is expected the downscaled value is able to provide an improved order of magnitude than the radar, that is able to better estimate the rain gauge values.

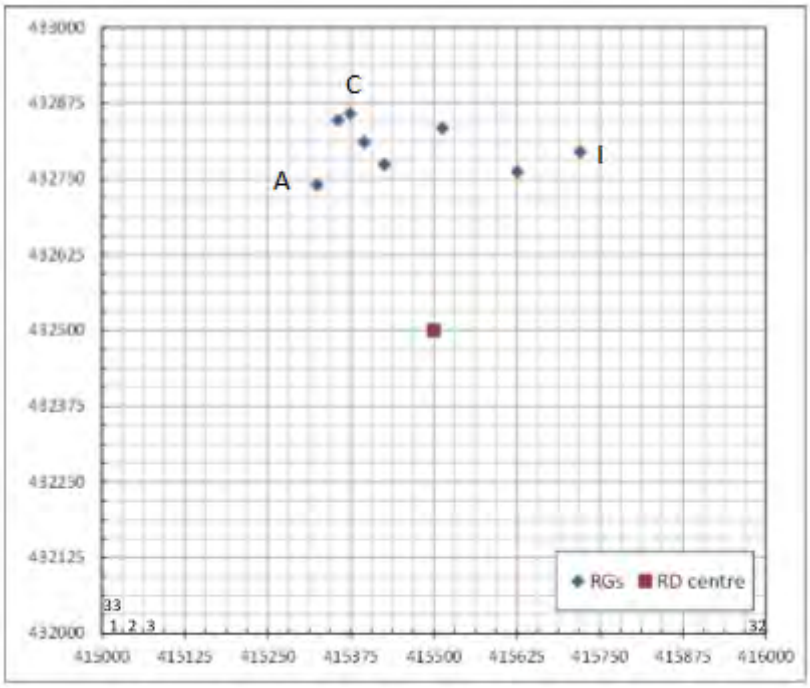

Figure 2. 3 The geometric deployment of the original (the dark-line boundary) and downscaled (the grey-line grids) radar grid squares and the rain gauge network (the blue markers).

Differently from the downscaling methods, it is expected that the interpolation methods are going to give a spatial variability and an order of magnitude similar to the radar values. Three kinds of interpolation methods have been utilized: the Kriging, the Inverse distance weighting and the Inverse squared distance weighting (they are all explained in chapter n°5). It is important to bear in mind, the interpolation methods have been invented with the necessity to obtain an estimation within a larger area starting from punctual values generally given by the rain gauges. In this case the interpolation methods are used differently, indeed they use radar data as starting values to estimate "smaller" area. Nonetheless an important assumption has to be done: even if radar data is areal estimation(spread on 1x1 km^2), it is considered as pointed in the centre of the relative pixels. Hence, in order to obtain the estimations in the A,I,C points with the interpolation

methods, a 9x9 radar grid square has been utilized centred with the pixel in which the rain gauges are localised (Figure2.4). Each pixel (in total 81) gives its contribution in the estimation according to its value and distance from the three points. Of course the central pixel and its neighbouring ones have more influence on the three target points differently from the others. In the analysis chapter n° 6 the comparison graphs between the three interpolation methods are reported and even their variability with the three points. Nonetheless, small differences are appreciable but interesting conclusions can be given for the concentrated rainfall events.

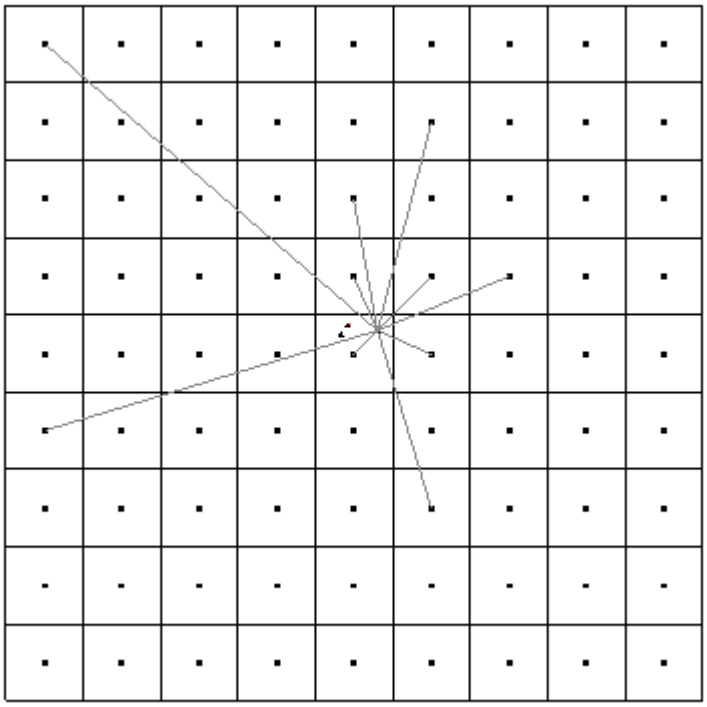

Figure 2.4 Interpolation process starting from the radar data considered as pointed in the relative pixel centre. In order to estimate the values in the three points, a 9x9 radar grid square is used. The squared points are the centres of the pixel, while the triangles are rain gauge location. More the line which join the centre of the pixel to the rain gauge location is short, more the relative radar estimate of that pixel is important on the interpolation process.

2.2 Rainfall Events

In total 5 rainfall events have been considered. They are all different for their intensities and some are similar for the duration. In the following table are shown their features:

Events	Rain gauge intensity (mm/5min)	Radar intensity(mm/5min)	Duration (h)
21/06/2012	1.67	*1.01*	00.20
07/07/2012	0.76	0.44	01.15
25/08/2012	0.50	0.3	01.15
06/07/2012	0.41	*0.24*	05.10
22/06/2012	0.08	*0.05*	21.30

Table 2.1 List of the events analysed. The average of the rain gauges intensities is shown, the radar intensity of the pixel located over the rain gauges and the duration.

The events are sorted according to the rain gauge intensities; indeed if they would have been sorted according to the radar intensities, the 25/08/2012 event would be the last. This fact is due to a malfunction of the radar device for problems that are briefly explained in the next chapter. It is clear that it is not an ordinary problem because the radar really underestimates the intensity about almost an order of magnitude. Indeed, it can be seen that in all the other events radar always underestimates the average of the rain gauge intensities but with proportionally similar rates. Some graphs and more precise considerations are discussed in Chapter n°6. As it could be expected the intensities of the events decreases with duration increase. The averaged rain gauge intensities represent the most important discriminating factor of this work. For example, decreasing this factor, downscaling method improves its estimations and even the radar device improves its working. Due to these trends, which change according to the intensity, some improvement in the downscaling method working will be suggested and tested.

Chapter 3

Rainfall Data Set

It is necessary to dedicate a chapter regarding the two rainfall devices because they affect all the work of this research. Both the downscaling and interpolation methods use the radar data as input in order to obtain as output, estimates more close as possible to the rain gauges records. The point is that the different workings, different error sources, and different kinds of data of the two devices affect this ambitious goal. In the following sections the two devices are briefly explained.

3.1 Introduction

Rain gauges remain the most reliable sensors providing direct and accurate point rainfall measurements over the ground surface, which are widely used as “ground truth”. The major drawback of rain gauge data lies in its limited ability to characterise the spatial variation in rainfall. Radar sensors have been widely used to compensate for this drawback, in the necessity to accurately determine the performance of urban drainage systems both in terms of urban flood risk. To better understand the response of drainage systems to rainfall there is considerable interest in the use of rainfall data recorded by radar. This is especially so when attempts are made to predict the future performance of systems. Urban catchments are usually relatively small when compared to upland and river basin catchments. Thus, in response to rainfall, the reaction speed of urban catchments is faster and the reaction threshold is lower when compared to a rural catchment. Hence, the application of weather radar to the urban area requires that the rainfall data are of high frequency and high spatial resolution. The use of weather radar systems may be considered advantageous over the use of traditional rain gauges, as they provide spatial rainfall

data over an entire region compared to the sparse multiple single point measurements that are usually available from rain gauges. Furthermore, rain gauges and radar are fundamentally different types of measurement systems: the first, typically collects rainfall at ground level over a circular area of diameter 20 cm whereas a radar scans the atmosphere over a volume whose projected area is roughly 1 km^2 (for standard C-band radar operated by most of the western Europe meteorological national services). Hence, observation scales are in a ratio of more than 103 between the two devices. A basic consequence, is that direct comparison of the outputs of the two sensors is at least problematic. Moreover, the two devices have different problems and error sources: blockages, wetting and evaporation, high rain rates, wind effects, position and shelter for rain gauges and occultation, spurious echoes, radar beam above the precipitation at long ranges and many others for the radar. The two devices used in this work will be briefly described in the next sections.

3.2 Meteorological Radar

Radar is an echo-sounding system, which uses the same aerial for transmitting a signal and receiving the returned echo. Short pulses of electro-magnetic waves, which travel at the speed of light (approx. 186000 miles per second), are transmitted in a narrow beam for a very short time (typically 2 microseconds). When the beam hits a suitable target, some of the energy is reflected back to the radar, which 'listens' out for it for a much longer period (3300 microseconds in the case of Met Office radars) before transmitting a new pulse(Figure 3.1). The distance of the target from the transmitter can be worked out from the time taken by a pulse to travel there and back. Since radars cannot send and receive at the same time, the transmitted pulse must be very short (or echoes from close range will be lost), and the listening time must be as long as possible, for detecting distant echoes. Increasingly the transmitted power is subject to engineering constraints and cost. A longer transmission pulse would give more power and better long-range performance, but would reduce the close-range capability. The returning echo is very much weaker than the transmitted pulse, and depends on several factors. There is attenuation, or absorption of energy, by particles of dust or cloud droplets in the atmosphere. There is also an inverse square relationship with range (i.e. doubling the range cuts the return power to one quarter) due to the increasing spread of the radar beam. The beam width of many modern radars is approximately 1° and, as the target distance increases, only an increasingly small part of the transmitted beam is reflected back to the radar. Each radar completes a series of scans about a vertical axis between

four and eight low-elevation angles every 5 minutes (typically between 0.5 and 4.0 degrees, depending on the height of surrounding hills). Each scan gives good, quantitative data (1 and 2 km resolutions) out to a range of about 75 km and useful qualitative data (5 km resolution) to 255 km.

- 5 km resolution data provides a good overall picture of the extent of precipitation at a national/regional scale.
- 2 km data is suitable for more demanding rainfall monitoring and hydrological applications.
- 1 km resolution provides the most detailed information, down to the scale of individual convective clouds. It is designed to assist real-time monitoring of small urban catchments and sewers (The data used in this work is 1-km, 5-min)

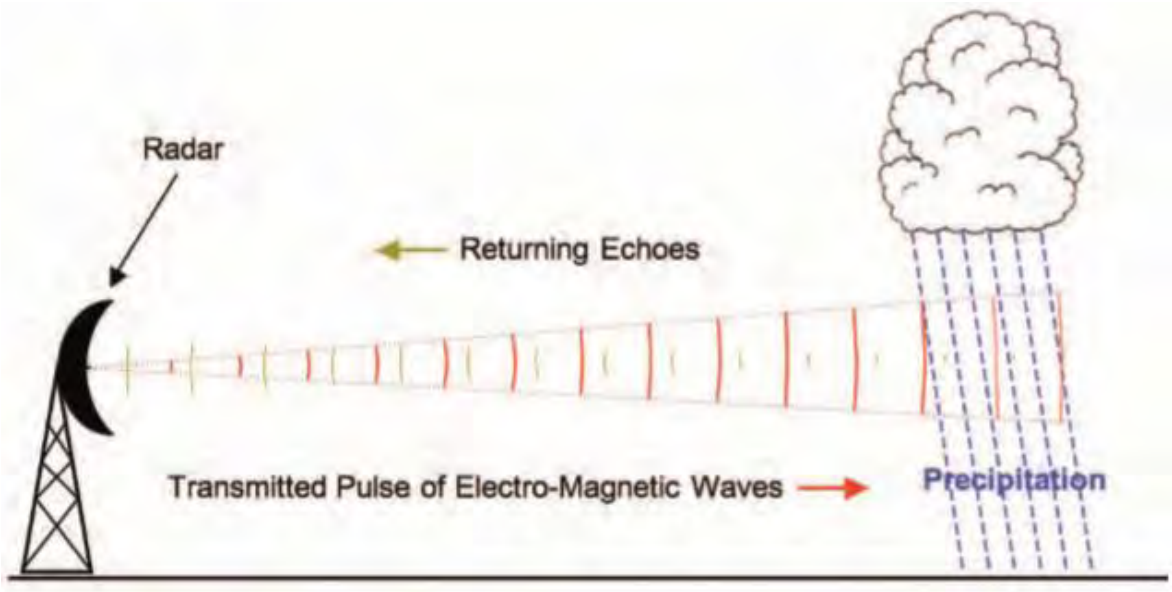

Figure 3.1 Working of the Meteorological Radar.

Depending on the equipment installed it is possible to obtain direction and speed information on the droplets observed. Using this data it is then possible to calculate wind speed and elevation data within the rain cloud, out to a range of 100 km from the radar. The way Doppler radar works is that two pulses of electromagnetic radiation are transmitted. The first pulse is sent from the radar and the returning echoes are received, then almost immediately, a second pulse is sent from the radar and again the returning echo is received. The computer then analyses these two returned echoes and the movement of the droplets of water is calculated. This movement is only very slight but it is enough to calculate the wind speed within the cloud and the direction of the water droplets.

3.2.1 Meteorological causes of errors

The radars do not receive echoes from tiny cloud particles, but only from the precipitation-sized droplets. Drizzle is generally too small to be reliably observed, unless close to the radar, but rain, snow and hail are all observed without difficulty. It is important to interpret the radar imagery in terms of the beam's elevation and 'width' and the earth's curvature. The latter, for example, means that echoes come from an increasingly higher level the further away precipitation is from the radar. Thus at a range of 100 km, the radar beam is being reflected from the raindrops in a cloud at a height of 1.5 km, but beneath that level rain may be falling from the cloud which the radar misses. For this and other reasons (listed below), the radar rainfall display may not fully represent the rainfall observed at the ground.

- Permanent echoes (occultation): These are caused by hills or surface obstacles blocking the radar beam, and are often referred to as clutter. Clutter is rarely seen on radar imagery as it can be mapped on a cloudless day, and then taken out or subsequent pictures by the on-site computer. Occultation is caused by the radar beam being obstructed by a hill or building. A network of overlapping radars helps to minimise this problem.
- Spurious echoes: These may be caused by ships, aircraft, sea waves, chaff in use on military exercises, technical problems or interference from other radars. The pattern formed by spurious echoes are short-lived, and can usually be identified as they look very different from genuine precipitation echoes.
- Radar beam above the precipitation at long ranges: Even with a beam elevation of only 1°, an individual radar may not detect low-level rain clouds at long distances. A network of overlapping radars helps to minimise this problems.
- Evaporation of rainfall at lower levels beneath the beam: Precipitation detected by the radar at high levels may evaporate if it falls through drier air nearer the ground. The radar rainfall display will then give an over-estimate of the actual rainfall.
- Orographic enhancement of rainfall at low levels: The rather light precipitation which is generated in layers of medium-level frontal cloud can increase in intensity by sweeping up other small droplets as it falls through moist, cloudy layers at low levels. This seeder-feeder mechanism is very common over hills, resulting in very high rainfall rates and accumulations. Even with a network of radars, the screening effect of hills can make the detection of this orographic enhancement difficult, resulting in an under-estimate of the actual rainfall.
- Bright band: Radar echoes from both raindrops and snowflakes are calibrated to give correct intensities on the rainfall display. But at the level where the temperature is near 0 °C, melting snowflakes with large, wet, reflective surfaces give strong echoes. These produce a false band of heavier rain, or bright band, on the radar picture.

- Drop sizes of precipitation within a cloud: Every cloud has a different composition of droplets; in particular, frontal rainfall clouds differ from convective shower clouds. In deriving rainfall rates from radar echo intensities, average values for cloud compositions are used. Radars under-estimate the rain from clouds composed of smaller-than-average drops (e.g drizzle), and over estimate the rain falling from clouds very large drops (e.g.shower). However, averaging the rain over 5 km squares on the radar rainfall display reduces the peak intensities in convective cells.
- Anomalous propagation (anaprop): Radar beams are like light beams, in that they travel in straight lines through a uniform medium but will be bent (refracted) when passing through air of varying density. When a low-level temperature inversion exists , the radar beam is bent downwards and strong echoes are returned from the ground, in a manner akin to the formation of mirages. This usually occurs in anticyclones, where rain is unlikely and so anaprop is normally recognised without difficulty.

3.3 Rain gauge

A rain gauge is simply an instrument that is designed to measure the amount of rain that reaches the ground surface during a storm. Rain gauges are considered the most traditional method for measuring rainfall. They have been used historically to provide rainfall quantities and rates at a single point in space. The basic idea of most rain gauges is to collect rainwater into a cylindrical vessel of a fixed diameter. Rainfall measurements are usually provided in units of water depth (inches or millimeters). The volume of collected water is divided by the area of the cylinder opening and converted into a depth or rain. There are different types of rain gauges that can be classified into two main categories: non-recording gauges, and recording gauges. The first type is a basic storage device that measures the cumulative amount of rain. A common type of this gauge is called the 8-inch Standard Rain Gauge (SRG) which is simply a large cylinder with a funnel and a plastic measuring tube inside the cylinder. Differently, the second type is designed to automatically record the amount of rainfall reaching the surface as a function of time during the lifespan of a storm. The most common types of recording gauges are: Tipping-bucket rain gauge (this is the device used in this work that will be briefly explained below), Weighing rain gauge (it measures the weight of the water accumulation on a vessel located on a scale), Optical rain gauge (it measures rain rate as proportional to the disturbance by raindrops to an optical beam), Disdrometer (it measures the drop size distribution and falling velocity of rain drops and it is based upon the either optical or acoustic technologies).

3.3.1 Tipping-bucket rain gauge

The tipping bucket rain gauge consists of a cylinder (typically 8 or 12-inch diameter) with a funnel that drains into a pair of buckets that are balanced on a horizontal axis(in figure 3.2 a pair of the University of Bradford rain gauges are shown). When a predetermined amount of rainwater (commonly 0.01 inches) has been collected into one of the buckets, the bucket tips causing the other bucket to move quickly into position and catch the incoming rain. With each tip, an electronic signal is sent to a data logger that records the time of tip occurrence. The known amount of each tip and its occurrence time makes it possible to calculate the incremental amounts of rain over variable or fixed intervals of time. These measurements can also be used to estimate the rainfall rates during the life of the storm.

Figure 3.2 Tipping-bucket rain gauge of the University of Bradford located in the point C (see figure 2.1)

3.3.2 Sources of errors in rain gauge measurements

Although rain gauges present the most simple and direct way for measuring rainfall amounts and rates, they are subject to several sources of uncertainties and errors. Nevertheless, the largest source of error is due to wind effect which is discussed as first:

- Wind-induced errors

  Since most rain gauges are elevated above the ground, wind eddies form around their orifices which reduces the catch of small rain drops. This problem is known as wind-induced gauge under-catch and is considered the most common and serious source of rainfall-measurement errors. Wind effect can

be minimized by placing wind-shields around the gauges. Several studies have developed and assessed different formulae to correct rainfall amounts due to wind effects for unshielded and shielded gauges. Research has shown that for the 8-inch standard rain gauge (SRG), wind under-catch can be in the order of 5 to 10% on an annual basis but can be relatively larger on individual storm scales. Therefore, it is recommended to perform wind corrections on a monthly or daily basis.

- Evaporation and Wetting Losses

  These losses are encountered in storage-type non-recording gauges, and recording gauges at long intervals (several days). The magnitude of these losses depends on temperature, humidity, and time between rain and collection of the measurement. However, such errors are usually small and can be often neglected except for low-intensity rainfall events

- Calibration Errors

  This error is encountered in tipping-bucket rain gauges. These gauges require calibration and adjustment of the tipping mechanism which is mostly done at a fixed small or intermediate rain rate (usually referred to as static calibration). However, at high rain rates a tipping-bucket gauge may suffer from underestimation problems due to the fact that the tipping buckets cannot keep up with heavy rain during a severe thunderstorm. To correct for such problems, rain rate-dependent calibration procedure should be developed; however, this can be time consuming and only static calibration is developed and provided by the gauge manufacturer. The user of such gauges should be aware of possible underestimation at high rainfall intensities (>50 mm/h).

- Other sources of errors in gauge measurements

  Other sources of errors include rainfall splashing, possible electronic and mechanical breakdown of gauges, clogging of gauge orifices and funnels, and observer mistakes in recording, processing and publishing rainfall measurements. Also, improper sitting configuration of rain gauges near trees or building can cause significant losses of rainfall amounts. As a general rule, an obstruction object should not be closer to the gauge than twice its height above the ground.

Chapter 4

Rainfall Downscaling

This method is used for generating rainfall estimates with finer spatial-resolution. It is a stochastic generator and is developed based upon the theory of left-sided multifractals, the (cascade) generating equation and the semi-deterministic cascade model. The basic idea of this multifractal-based downscaling model is to characterise the scaling feature of spatial rainfall data (e.g. radar rainfall observations) over a specific range of spatial scales (e.g. from 1 to 8 km spatial resolution), and then to assume that this scaling feature does not change at a finer scale (smaller than 1 km^2) and can be further used to generate finer-resolution rainfall estimates. In this chapter, a theoretical background is firstly given in order to understand better the new downscaling method used in this work

4.1 Euclidean dimension

In Euclidean geometry, any object has a characteristic number associated with it called a dimension. The estimation of the Euclidean dimension requires complex mathematical formalism but can be explained using a simple example as follows. There are for example a line (1-dimension, length L), a square (2-dimension, sidelength L and area L^2) and a cube (3-dimension, sidelength L and volume L^3). If the line is divided into m equal segments, the length of each segment is L/m; in other words, it needs N = m segments (length L/m) to cover the line and the contracting ratio (or called the scaling ratio) against the original line is r = (L/m)/L = 1/m = 1/N. If each side of the square is divided into m segments, it needs N = m^2 small squares (area $(L/m)^2$) to

cover the original square and the contracting ratio for each side is $r = \sqrt[2]{(L/m)^2/L^2} = \sqrt{(1/N)}$. Similarly, it needs N = m^2 small cubes (volume $(L/m)^3$) to cover the original cube (the contracting ratio of each side is $r = \sqrt[3]{(1/N)}$) if each side of the cube is subdivided into m segments. This example can be extended to a E-dimension object, and it needs N = m^E small objects to cover the original object. Based upon this derivation, it can be found that,

$$N = m^E = \left(1/r\right)^E \qquad (4.1)$$

Or

$$E = \frac{\ln N}{\ln \frac{1}{r}} \qquad (4.2)$$

Based upon this definition, we may however meet some problems, such as the Cantor set, which is constructed by repeatedly deleting the open middle thirds of a set of line segments. The associated Euclidean dimension is therefore E = lnN / ln1/r = ln2/ln3 = 0.631, which conflicts with the definition of integer dimension in Euclidean Geometry. Therefore, further theories were developed to explain dimension in a more general idea.

4.2 Monofractals

Fractals, or Monofractals, provide a simple framework to characterise the scale-invariant features of a given natural process primarily based upon a simple scaling relationship:

$$N(\epsilon) \sim \epsilon^{-D_F} \qquad (4.3)$$

where N(ϵ) is some property of the natural process observed at a specific scale ϵ (or so-called box, which is the same as r in Eq.(4.1)), and D_F is a scaling exponent. This relationship has been widely used to analyse the geometric structures of certain processes by defining N(ϵ) as the number of boxes needed to cover the whole structure. The corresponding scaling exponent D_F thus is known as a fractal dimension. It is obvious that this dimension is not necessarily an integer; in other words, it could be a fraction, which is an extension of the dimension defined in Euclidean Geometry (Eq. (4.2)). The fractal dimension of the Cantor set, i.e., ln2/ln3 = 0.631, which is estimated by rearranging Eq. (4.3), no longer conflicts with the definition of fractal dimension. The structure of rainfall quantities and the fluctuations thereof have been studied based upon this simple scaling relationship. For example, Lovejoy and Mandelbrot (1985) defined this simple scaling feature in terms of the probability distribution of a random function X(t) and its fluctuations ΔX(t) respectively as $X(\lambda t) =^d \lambda^H X(t)$ and $\Delta X(\lambda \Delta t) =^d \lambda^H \Delta X(\Delta t)$. Here, for arbitrary t0 and t1, $\Delta t = t_1 - t_0$, $\Delta X = X(t_1) - X(t_0)$, $t_2 = t_0 + \lambda(t_1 - t_0)$ and $\Delta X(\lambda \Delta t) = X(t_2) - X(t_0)$. The parameter λ is the resolution with corresponding scale ϵ = L/λ, where L is the largest scale of the structure and is

obtained when λ = 1; H is a scaling exponent related to the fractal dimension (D_F); and the symbol $=^d$ denotes identity statistical distribution. This definition indicates a relation that the probability distribution of rainfall or its fluctuations will change according to the ratio λ_H when the measurement scale or its fluctuations are rescaled by a factor λ. Olsson et al. (1992) also analysed the simple scaling feature of rainfall sequences observed in Lund, Sweden, using box-counting methods. The results showed that the same fractal dimensions were investigated in minute, daily, and monthly observations when proper threshold values were respectively applied. These works generally conclude that the scale invariance that is characterised by a single fractal dimension indeed exists at a specific scale interval; however, for the structures of most natural phenomena, scaling features cannot be entirely illustrated using merely one quantity, or a set of them. The theory of Multifractal Measures, or Multifractals, therefore was developed to generalise the concept of fractal sets to measures. This generalisation is implemented by characterising the scale-invariant features of multifractal measures by a function instead of a single number.

4.3 Multifractals

In order to explain Multifractals, a quantity, namely the coarse H¨older exponent, is intro- duced herein:

$$\alpha = -\frac{\log \mu(\epsilon)}{\log \epsilon} \qquad (4.4)$$

which is the logarithm of the measure within a given box, μ(ϵ), divided by the logarithm of the sidelength of that box ϵ. This quantity describes the scaling behaviour of a local μ located within a certain finite interval ϵ in the support of the measure. Whilst fractals are useful to represent whether an event belongs to a fractal set or not, multifractals represent how intensely an event behaves fractally. This intensity is generally measured by counting the number of boxes of side ϵ having a coarse Holder exponent equal to a given α. Based upon this number $N_\epsilon(\alpha)$, an analysis of the frequency distribution of this α could be carried out by introducing

$$f(\alpha) = -\frac{\log N_\epsilon(\alpha)}{\log \epsilon} \qquad (4.5)$$

where $f_\epsilon(\alpha)$ is the logarithm of $N\epsilon(\alpha)$ divided by the logarithm of the box size ϵ. The points $(\alpha, f_\epsilon(\alpha))$ compose a plane domain of singular measures, of which the upper boundary is a concave curve shaped like the symbol ∩ and leaning to one side in most cases (shown as Figure 4.1).

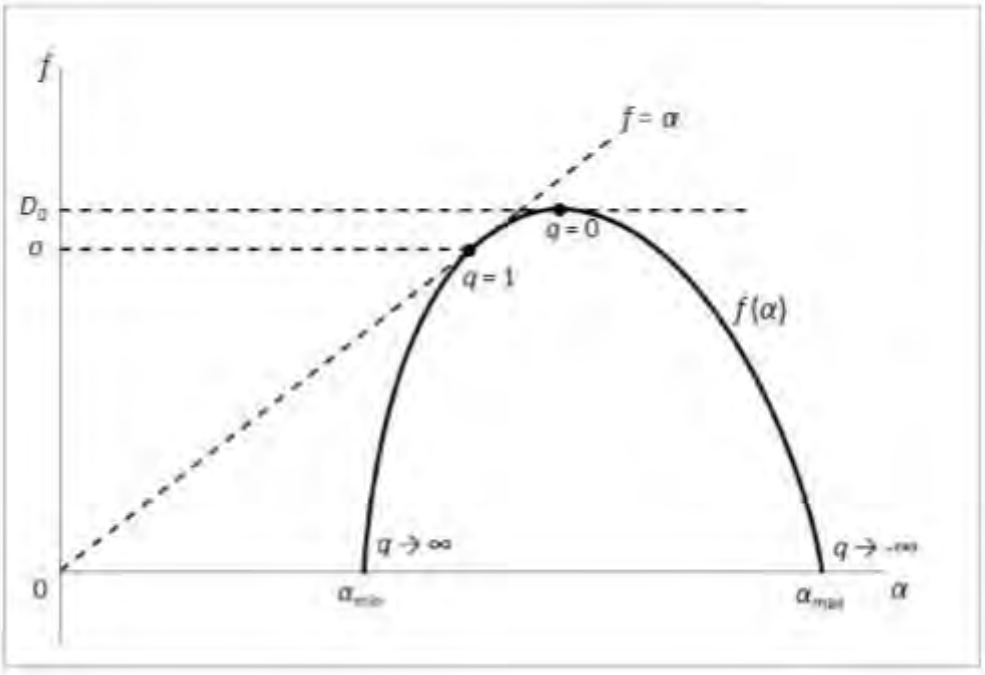

Figure 4.1 The multifractal spectrum f(α) estimated from a typical self-similar measure.

This upper boundary defines the function f(α), which is loosely similar to the fractal dimension D_F but is defined within the subsets of the size ϵ having coarse Holder exponent α. In other words, the whole f(α) curve, known as a multifractal spectrum, represents an infinite number of fractal dimensions. Some basic properties of the f(α) curve can be briefly reviewed herein by letting $A^{\alpha}(\epsilon)$ be a subset of boxes covering the support of the measure having a coarse Holder exponent between α and α + dα; then, the corresponding measure within this subset is $\mu(A^{\alpha}(\epsilon)) = N_{\epsilon}(\alpha)\epsilon^{\alpha}d\alpha = \epsilon^{-f(\alpha)\epsilon+\alpha}d\alpha \sim \epsilon^{-f(\alpha)+\alpha}d\alpha$. Due to the fact that the total measure in all boxes is one, a relation $f(\alpha) \leq \alpha$ can be derived. This implies that the f(α) curve always lies under the bisector (i.e. the straight dotted line α = f(α), shown in Figure 4.4), and there is a unique point intersecting this bisector where f'(α) = 1. Further mathematical formalism of the function f(α), has been well established. If the size of the space that supports the whole measure is assumed to be unity, the probability of having the coarse Holder exponent equal to α can be derived as $P_{\epsilon}(\alpha) = N_{\epsilon}(\alpha)/\epsilon^{-E}$, where E denotes a Euclidean dimension and ϵ^{-E} is proportional to the total number of the boxes (with the side ϵ). Replace the $N_{\epsilon}(\alpha)$ term in Eq. (4.5) by this probability term; then a domain of singular densities can be estimated by defining

$$C_{\epsilon}(\alpha) = \frac{\log P_{\epsilon}(\alpha)}{\log \epsilon} \qquad (4.6)$$

As $\epsilon \rightarrow 0$, the exponent $C_{\epsilon}(\alpha)$ converges to the limit C(α). This function C(α) is termed the codimension function of singular measures due to its simple relation to f(α), i.e., C(α) = E –f(α). A detailed formalism of C(α) and its further relations to f(α) have been well studied in previous

research. Note that, according to the convention in previous research related to hydrological or geophysical applications, the codimension function is usually termed C(γ) instead of C(α), where γ is a quantity with similar idea to α and termed the order of singularity. A modified relationship of the codimension function and probability distributions of measures then is expressed as:

$$P(\mu(\epsilon) \geq \lambda^{\gamma}) \sim \lambda^{-C(\gamma)} \quad (4.7)$$

This equation entails that the probability distribution of the measure above a threshold quantity λ^{γ} (namely a singularity of order γ, where λ, the same as aforementioned, is the resolution) could be characterised by the associated codimension function. This relation provides a theoretical framework for constructing random cascade models. A prototype of this type of models can be demonstrated by introducing a simplified equality deduced from Eq. (4.7):

$$P\left(\frac{\mu(\epsilon)}{\epsilon} = \lambda^{\gamma}\right) = P(\epsilon, \gamma) = \lambda^{-C(\gamma)} \quad (4.8)$$

where μ(ϵ), in a physical sense, can be explained as (normalised) rainfall quantities at a given temporal/spatial scale (ϵ) and μ(ϵ)/ ϵ is the associated intensity. This equation has been evolved into various rainfall models which are used to generate rainfall sequences or fields. A β-model, for example, was implemented based upon Eq. (4.8) to define two states:

$$P\left(\frac{\mu(\epsilon)}{\epsilon} = \lambda^{\beta}\right) = \lambda^{-\beta}$$

$$P\left(\frac{\mu(\epsilon)}{\epsilon} = 0\right) = 1 - \lambda^{-\beta} \quad (4.9)$$

This β-model was originally developed to simulate the complex turbulent process of generating eddies and has been further used to construct space-time mesoscale rainfall generators based upon the with/without rainfall dichotomy determined by the exponent β. Although being substantially simplified, this model produces acceptable results. Similar to the β-model that was developed based upon Eq. (4.6), the α-model and the log-Poisson model are discrete- in-scale random cascade models but are constructed by characterising cascade processes based upon more complex probability distributions; particularly the latter (the log-Poisson model) was widely used in hydrological and geophysical applications. However, most of this type of models preserve only the statistical ensemble while generating successive cascades, which means that the measures (e.g. rainfall quantities) are not exactly conserved between successive cascades in these models. This inconsistency of measures may be amplified as a finer scale or/and a short-term event is studied, which may massively increase the input uncertainty for urban pluvial flood modelling or forecasting. Unlike the wide applications of codimension function C(γ) in the realm of natural phenomena, the applications of multifractal spectrum f(α) seem to be relatively limited due to its being deterministic. This feature could be traced back to the earlier development of the multifractal spectrum, which was based upon the study of multiplicative cascades. A deterministic

multiplicative cascade is a process to generate random sequences. This process fragments a geometric set into smaller and smaller components according to a given set of ratios (s_1 and s_2) and at the same time fragments the associated measure of the components (e.g., the rainfall intensity or depth) by another set of ratios (w_1 and w_2). However, these ratios are unnecessary to be applied in sequence when used to fragment scales and measures. This means the sequence of ratios could be randomly altered at each branching. Nonetheless, due to the fact that the ratios used are fixed, this process can be satisfactorily characterised by the theory of self-similar multifractals and the complexities induced by randomness can be therefore circumvented through working with non-random measures.

4.4 Self-similar and Left-sided Multifractals

The connection between multiplicative cascade and the theory of multifractals can be linked by characterising an important feature of cascade process: self-similarity. In this section, self-similar multifractals are derived by considering a self-similar measure μ supported by a self-similar subset F of R, where the self-similar measure and subset respectively represent the fragmented measure and geometric set in a self-similar multiplicative cascade process. Let $S_1,...,S_b : R \rightarrow R$ be contracting similarities with ratios $s_1,...,s_b$, where $b \geq 2$. These ratios are used to fragment the self-similar set by repeatedly divide a given interval on F into a series of subintervals, of which each is a closed interval I such that $S_i(I) \subset I$ for all i, and $S_i(I) \cap S_j(I) = \emptyset$ whenever $i \neq j$. These subintervals could be then indexed by the finite sequences $\mathbf{I}_k = \{(i_1,...,i_k) : 1 \leq i_j \leq b\}$. Thus:

$$\mathbf{I}_i = \mathbf{I}_{i1,i2,...,ik} = S_{i1} \circ \cdots \circ S_{ik}(\mathbf{I}) \quad (4.10)$$

where ○ denotes the composition operator, and **i** = $(i_1,...,i_k)$, termed "address**,** is a typical *b*-adic sequence of $\mathbf{I}$. The address helps determine the whereabouts of each interval, and the length of the address (k) indicates the number of times that subdivision is carried out on subset F. If $|\mathbf{I}| = 1$ is further assumed herein, thus

$$|\mathbf{I}_i| = s_i = s_{i1} s_{i2} \cdots s_{ik} \quad (4.11)$$

Let $w_1,...,w_b$ be fragmentation ratios, satisfying $w_i > 0$ for all i and $\sum_{i=1}^{b} w_i = 1$. The pertinent measure with support F then can be derived as:

$$\mu(\mathbf{I}_{i1,i2,...,ik}) = w_{\mathbf{i}} = w_{i1} w_{i2} \cdots w_{ik} \quad (4.12)$$

This measure can be easily regarded as a self-similar measure, in the sense that

$$\mu(A) = \sum_{i=1}^{m} w_i \, \mu(S_i^{-1}(A)) \quad (4.13)$$

for all sets A. This equation represents the process to evaluate the measure for a given subset A at a specific level in a self-similar multiplicative cascade (**shown as Figure 4.3 stesso di prima**). First

the measure of the associated subset at the previous level is obtained by evaluating μ on the "presubset" of A, i.e., $S_i^{-1}(A)$. Then, multiply this previous measure with fragmentation ratios w_i and finally add up the results to obtain the measure of A.

$$\chi(q,\epsilon) = \sum_j \mu_j^q(\epsilon) \sim \epsilon^{\tau(q)} \qquad (4.14)$$

where the partition function χ(q,ϵ) is the q-th order moment of the measures within a box of side ϵ. In a physical sense, χ(q, ϵ) represents specific statistical features of the measures at the scale ϵ; for example, the first two moments (i.e. q = 1 and q = 2) of the measures are respectively related to the mean and the variance of the measures. This scaling relation performs an important feature of self-similar multifractals that the moment of measures χ(q, ϵ) scales a power law of the form $\epsilon^{\tau(q)}$ for all $-\infty < q < \infty$. By applying with various sizes of the box and orders of moments, the curve τ(q), shown as Figure (4.5) then can be estimated and has been known as the characteristic function of multifractal measures.

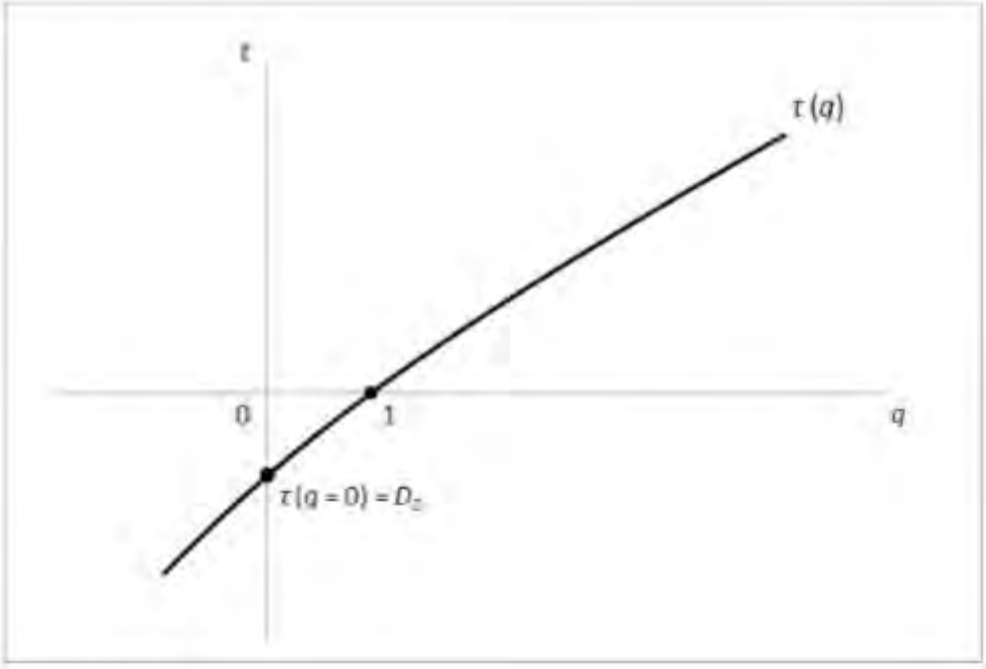

Figure 4.2 The associated Legendre transform (τ(q)) of the multifractal spectrum in Figure (4.1)

Moreover, the function τ(q) has been further proved to be the Legendre transform of the multifractal spectrum f(α), and vice versa:

$$f(\alpha) = \min_{-\infty<q<\infty} \{q\alpha - \tau(q)\} \qquad (4.15)$$

Analogous to multifractal spectra, codimension functions C(γ) also has the associated Legendre transform, which is usually denoted as K(q) [1] and has been widely used to demonstrate the scaling features of rainfall. Since τ(q) curve is strictly convex, for a given α there is a unique $q_\alpha = q(\alpha)$ to

attain the minimum in equation (4.15). Differentiate qα−τ(q) with respect to q and equate it to 0, thus:

$$\alpha = \frac{d\tau}{dq}|_{q=q_\alpha} = \alpha(q_\alpha) \qquad (4.16)$$

Substituting it into Eq. (4.15) gives

$$f(\alpha) = q_\alpha\, \alpha(q_\alpha) - \tau(q_\alpha) \qquad (4.17)$$

This equation helps understand properties of the f(α) curve; for example, the extremum of the f(α) curve for the value α = α(q) can be derived by satisfying

$$\frac{\partial}{\partial\alpha} f(\alpha)|_{\alpha=\alpha_q} = q \qquad (4.18)$$

If the f(α) curve is differentiable, the maximum of it can be attained where q = 0 (shown in Figure 4.1). Due to the fact that τ(q) is a unique mapping to its corresponding multifractal spectrum, the features of f(α) could be indirectly determined by profiling the function τ(q). Previous research has studied the function τ(q) in two senses according to the range of q. In a restricted sense, the function τ(q) is defined for all $-\infty < q < \infty$, which indicates that the scale-invariant relation depicted by equation (4.14) is required to hold for all real number q, and its corresponding "restricted" multifractal spectrum is shown as Figure 4.2. However, in a general sense, the function τ(q) is defined only for $0 \le q < \infty$, which means that the scaling relation in equation (4.14) fails to hold for q < 0. As for f(α), only the left side of a "general" multifractal spectrum looks like it does in a "restricted" multifractal spectrum (i.e., the segment between $q \to \infty$ and q = 0 of the curve in Figure 4.2). The multifractal spectrum in a general sense, thus, is named the left-sided multifractal spectrum, which could be characterised by $\alpha_{max} = \infty$ with $f(\alpha_{max}) = D_0$ (a constant) and, in theory, the constant D_0 could be obtained from equation (4.14) and (4.15) as q = 0. A deterministic multiplicative cascade has been proved to behave "left-sided" in previous research. This suggests that the left-sided multifractal spectrum may provide a theoretically reliable framework for studying rainfall, which is implicitly consistent with previous research which considered merely the case q > 0 when analysing rainfall based upon the scaling relation in equation (4.14). However, it is still an open problem to generate rainfall sequences or fields based upon these left-sided multifractal features even though the theory has been well established.

4.5 The Generating Equation

A possible solution to deriving a general generator/generating methodology in synergy with left-sided multifractals is the "generating equation":

$$\sum_{i=1}^{b} s_i^{-\tau(q)} w_i^q = 1 \qquad (4.19)$$

where $s_1,...,s_b$ and $w_1,...,w_b$ are the fragmentation ratios respectively for the set and measure, the same as those in Eqs. (4.11) and (4.12), to repeatedly divide a self-similar set and its associated self-similar measure into b subsets and sub-measures. This equation is a simple framework to describe a multiplicative cascade with deterministic fragmentation ratios and was derived from the process of rescaling transformation on self-similar measures. The reason Eq. (4.19) is known as the generating equation is that one could implicitly generate the theoretical values of τ(q) via numerically solving it if all the values of s_i and w_i were known; whilst the inverse task, i.e., to derive the s_i and w_i from known τ(q), is relatively difficult and seldom explored. These ratios are the key elements to construct a general rainfall generator/generating methodology; an explicit/analytic solution of these ratios cannot, however, be obtained. A further study therefore is necessary to profile this generating equation, particularly focusing on the composition of these ratios. It is obvious that difficulties primarily arise out of the unknown branching number b and the quantities and orders of these fragmentation ratios. An assumption of single-scaled multifractal measures (i.e., $s_i = 1/b$ for all i) is made herein to simplify these parametric problems, which gives:

$$\tau(q) = -\log_b \sum_{i=1}^{b} w_i^q \qquad (4.20)$$

This equation has been discussed using an example considering the case of the multinomial measure with b = 10 to implicitly demonstrate the links between a τ(q) curve and the associated fragmentation ratios. Three scenarios were considered: the first was where $w_i = s_i = 1/b = 0.1$ for all i, which would produce a uniform distribution. The associated τ(q) curve, by substituting $w_i = 1/b$ into Eq. (4.20) could be derived as

$$\tau(q) = q-1 \qquad (4.21)$$

a straight line with slope one (the solid line in Figure 4.3). The second scenario was where all values of $w_i = 0.111$, except one equal to 0.001, of which the distribution was uniform but with small areas having very small (non-zero) measures. The associated τ(q) curve was a line substantially dropping for $q < 0$ but similar to that of the first scenario for $q > 0$ (shown as the dashed line in Figure 4.3). The last scenario was all w_i's equal to 0.07, except one equal to 0.37. The corresponding plot of τ(q) sharply dropped for $q > 0$, but was somewhat similar to that of the first scenario for $q < 0$ (the dotted line in Figure 4.3).

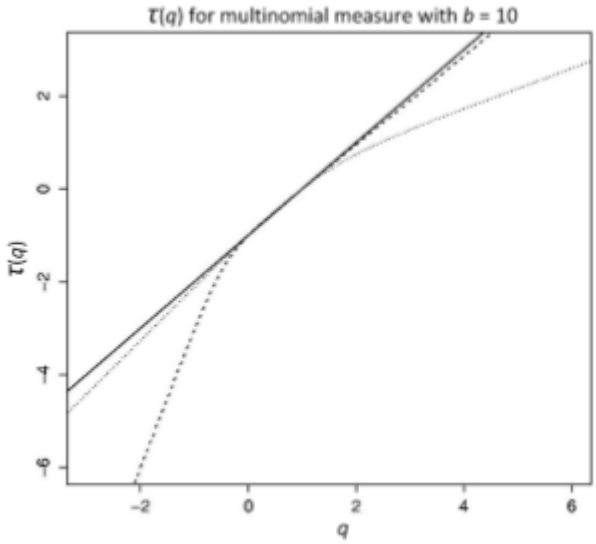

Figure 4.3 The solid line denotes the first scenario where wi = 0.1 for all i; the dashed line represents the second scenario where wi = 0.111 for all i, except one equal to 0.001; and the dotted line is where wi = 0.07 for all i, except one equal to 0.37.

These examples provides an understanding of the behaviour of the generating equation. They also provides guidance as to the possible composition of the associated fragmentation ratios. When all values of w_i are equal, the measure is expected to be uniformly distributed over the support set and the associated τ(q) curve is a straight line. However, when the measure is not uniformly distributed, the associated τ(q) curve is concave downwards. According to the section where τ(q) drops down, the relative composition of w_i's values could be roughly foreseen. For q > 0, it is expected that the relatively large measures would dominate the trend of the τ(q); whilst for q < 0, the relatively small non-zero measures would dominate it. In other words, the τ(q) curve can be used to investigate the extent to which the measure deviates from a uniformly distributed measure. This information may help reduce the solution domain when numerically solving Eq. (4.19)

4.6 Semi-deterministic, quad-nomial cascade model

A new cascade model, called semi-deterministic cascade model (denoted SD model in the following context), is used in this work. Employing the generating equation as the cascade generator, this model is able to produce random cascade processes by using deterministic fragmentation ratios (i.e. s_i and w_i); the statistical features (e.g. mean and variance) of the produced processes are therefore invariant (hence named the semi- deterministic cascade model). In the generating equation (Eq.(4.19)), it is intuitive that the τ(q) curve could be obtained if s_i and w_i were known. However, the inverse task, i.e., to derive the s_i and w_i from known τ(q), is relatively difficult because of the non-linearity of the generating equation and the unknown number of s_i and w_i (i.e. unknown b); but this inverse derivation is the key to constructing the cascade generator of the SD model. Following the general methodology of applying the theory of multifractals to cascade-based rainfall downscaling, the proposed SD model first analyses the scaling features of historical rainfall data over the scales of interest to obtain the empirical τ(q) curve. This curve is then substituted into the generating equation to iteratively and inversely derive the "best" set of s_i and w_i by fitting the theoretical and empirical τ(q) curves (e.g. the likelihood method) subject to the constraints $\sum_{i=1}^{b} s_i = 1$, $\sum_{i=1}^{b} w_i = 1$. Finally, this set of s_i and w_i is further used to synthesise (or downscale) rainfall estimates that have similar structures (i.e. statistical features) to the associated historical observations through the cascade process. To implement the SD model, one of the key parameters that needs to be identified is b, which largely dominates the applicability of the theoretical τ(q) curve and consequently affects the fitting results of the τ(q) curves. In conventional discrete- in-scale random cascade models, the value of b is in general assumed to be 2 because it can directly generate more intermediate cascade levels (i.e. more intermediate timescales) and is easier to be implemented and formalised 2. However, based upon the analyses in Wang et al. (2009a,b), a better fitting is obtained if the branching number is assumed to be 4 (this is the motivation of the so called Quad-nomial cascade model). To simplify the complexity of solving the generating equation, the value of s_i is assumed to be constant (i.e. equal to 1/b, where b = 4). The cascade generator used in this model is therefore the single-scaled generating equation (i.e. Eq. (4.20)). The cascadings between successive levels over the range of spatial scales of interest in this work (8×8 km^2 to 1×1 km^2) is shown in Figure 4.4. As a consequence, the generation of street-scale rainfall estimates is conducted based upon the assumption that the scale-invariance feature, establishing over the spatial scales ranging from 8 km to 1 km, can be extended to finer scales. This means that the associated fragmentation ratios can be directly applied to the 1-km radar data to produce finer scale rainfall estimates.

Standard deviations (or spatial variability) reasonably increase when higher-resolution rainfall estimates are studied. Unfortunately,this quantitative increment of standard deviations between any two successive scales however is not invariant. This is due to the nonlinear nature of the SD model. In addition, for some time steps, it is observed that the patterns of standard deviations are gradually altering. This is because, in the SD model, the fragmentation ratios are obtained from an optimal fitting process between scales 8 km and 1 km. For those time steps at which the patterns change, the forcing from coarser- resolution rainfall is stronger than the 1-km rainfall and therefore the patterns are gradually altered in order to follow the theoretically optimal patterns at given scales.

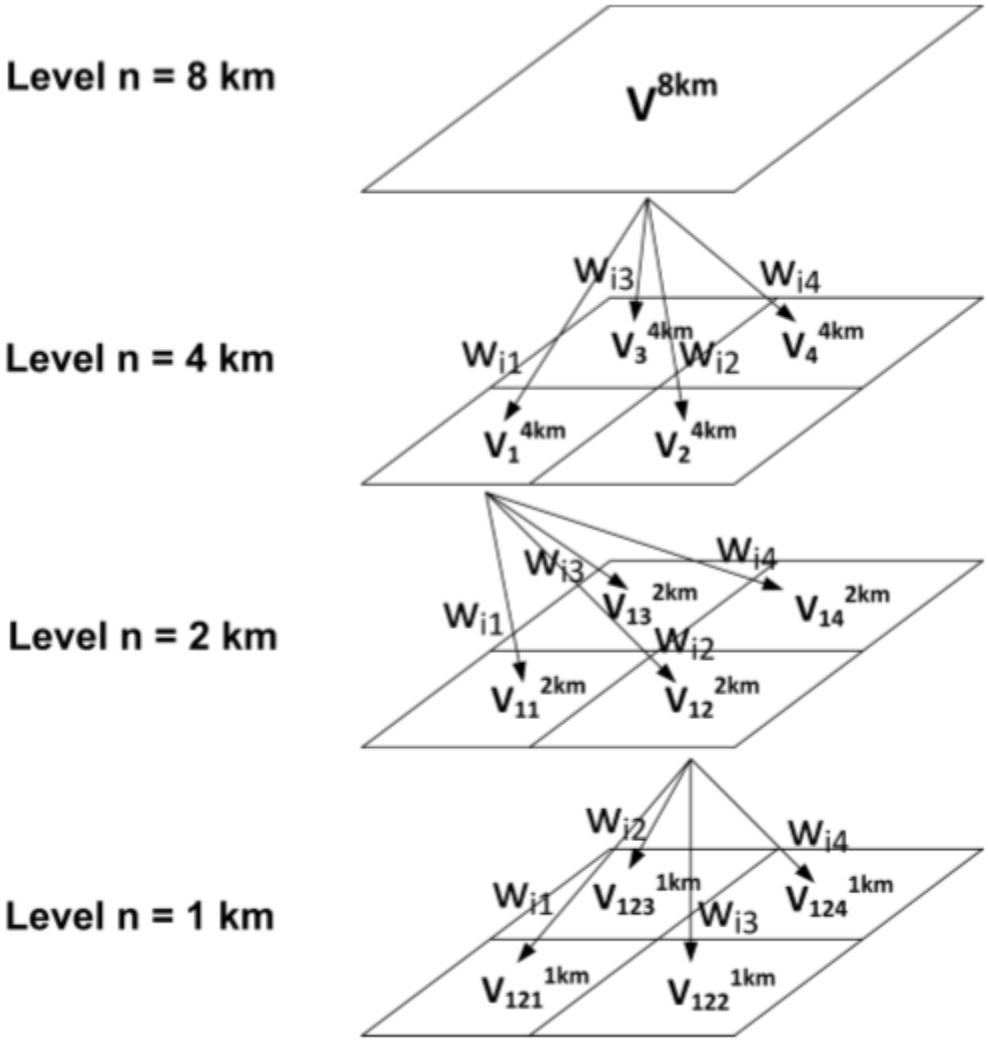

Figure 4.4 Application of the quad-nomial cascade to rainfall field downscaling

Chapter 5

Rainfall interpolation

In this chapter a background about the interpolation methods are firstly given and then the interpolation method used in this work are explained in the respective sections.

5.1 Interpolation methods

Interpolation is a method of constructing new data points within the range of a discrete set of known data points. One often has a number of data points, obtained by sampling or experimentation, which represent the values of a function for a limited number of values of the independent variable. It is often required to interpolate (i.e. estimate) the value of that function for an intermediate value of the independent variable. This may be achieved by curve fitting or regression analysis. There are many different interpolation methods, some of which are described in the next section. Some concerns come out in the kind of interpolation method taken into account for instance how much it is accurate or wow much it smooths the interpolant or even how many data points are needed. The simplest interpolation method is to locate the nearest data value, and assign the same value. In simple problems, this method is unlikely to be used, as linear interpolation is almost as easy, but in higher dimensional multivariate interpolation, this could be a favourable choice for its speed and simplicity. Linear interpolation is quick and easy, but it is not very precise. The error is proportional to the square of the distance between the data points. The error in some other methods, including polynomial interpolation and spline interpolation (described below), is proportional to higher powers of the distance between the data points. These methods also produce smoother interpolants. Polynomial interpolation is a generalization of linear

interpolation; now, the linear interpolant of linear method, is replaced with a polynomial interpolant of higher degree. if n data points are given The interpolation error is proportional to the distance between the data points to the power n. Furthermore, the interpolant is a polynomial and thus infinitely differentiable. So, we see that polynomial interpolation overcomes most of the problems of linear interpolation. However, polynomial interpolation also has some disadvantages. Calculating the interpolating polynomial is computationally expensive (see computational complexity) compared to linear interpolation. Furthermore, polynomial interpolation may exhibit oscillatory artifacts, especially at the end points. More generally, the shape of the resulting curve, especially for very high or low values of the independent variable, may be contrary to commonsense, i.e. to what is known about the experimental system which has generated the data points. These disadvantages can be reduced by using spline interpolation. Spline interpolation uses low-degree polynomials in each of the intervals, and chooses the polynomial pieces such that they fit smoothly together. The resulting function is called a spline. Like polynomial interpolation, spline interpolation incurs a smaller error than linear interpolation and the interpolant is smoother. However, the interpolant is easier to evaluate than the high-degree polynomials used in polynomial interpolation. Even, other kind of interpolations are based upon the algorithms of averaged weights. Generally the latter are all equal for all the points to interpolate or they can change according to the distances from the interpolated points (as the Inverse distance weighting interpolation method). Therefore , they can change according to a Gaussian process which is a powerful non-linear interpolation tool. Gaussian processes can be used not only for fitting an interpolant that passes exactly through the given data points but also for regression, i.e., for fitting a curve through noisy data. In the geostatistics community Gaussian process regression is also known as Kriging.

5.2 Inverse distance weighting and the Inverse squared distance weighting interpolation methods

Inverse Distance Weighting (IDW) is a type of deterministic method for multivariate interpolation with a known scattered set of points. The assigned values to unknown points are calculated with a weighted average of the values available at the known points. The name given to this type of methods was motivated by the weighted average applied since it resorts to the inverse of the distance to each known point ("amount of proximity") when assigning weights. The expected result is a discrete assignment of the unknown function u in a study region:

$u(x) : x \rightarrow \mathbb{R},\ x \in D \subset \mathbb{R}^n$

Where D is the study region and x the spatial variable. The set of N known data points can be described as:

$[(x_1, u_1), (x_2, u_2), \ldots., (x_N, u_N)]$

The function is to be "smooth" (continuous and once differentiable), to be exact $(u(x_i) = u_i)$ and to meet the user's intuitive expectations about the phenomenon under investigation. A general form of finding an interpolated value u at a given point x based on samples $u_i = u(x_i)$ for $i = 0, 1,\ldots,N$ using IDW is an interpolating function:

$$u(x) = \sum_{i=0}^{N} \frac{w_i(x)u_i}{\sum_{j=0}^{N} w_j(x)}$$

Where:

$$w_i(x) = \frac{1}{d(x, x_i)^p}$$

w_i is a simple IDW weighting function, x denotes an interpolated (arbitrary) point, x_i is an interpolating (known) point, d is a given distance (metric operator) from the known point x_i to the unknown point x, N is the total number of known points used in interpolation and p is a positive real number, called the power parameter. The weight decreases as distance increases from the interpolated points; therefore, greater values of p assign greater influence to values closest to the interpolated point, with the result turning into a mosaic of tiles with nearly constant interpolated value for large values of p. For two dimensions, power parameters $p \leq 2$, cause the interpolated values to be dominated by points far away, since with a density ρ of data points and neighboring points between distances r_0 to R, the summed weight is approximately:

$$\sum_j w_j \approx \int_{r_0}^{R} \frac{2\pi r \rho dr}{r^p} = 2\pi\rho \int_{r_0}^{R} r^{1-p}\, dr$$

which diverges for $R \rightarrow \infty$ and $p \leq 2$. For N dimensions, the same argument holds for $p \leq 2$. For the choice of value for p, one can consider the degree of smoothing desired in the interpolation, the density and distribution of samples being interpolated, and the maximum distance over which an individual sample is allowed to influence the surrounding ones. In this work two kinds of power parameters was taken into account in order to understand if the rainfall values change according to it. The first p=1 (Inverse distance weighting) and the second p=2 (Inverse squared distance weighting). It is expected that the method, with the first kind of power parameter, is going to provide more variable rainfall values according to the detections of the pixels close to the central pixel in which the rain gauges are located.

5.3 Ordinary Kriging

In statistics, originally in geostatistics, kriging or Gaussian process regression is a method of interpolation for which the interpolated values are modeled by a Gaussian process governed by prior covariances, as opposed to a piecewise-polynomial spline chosen to values. Interpolating methods based on other criteria such as smoothness need not yield the most likely intermediate optimize smoothness of the fitted values. Under suitable assumptions on the priors, kriging gives the best linear unbiased prediction of the intermediate values. The method is widely used in the domain of spatial analysis as the rainfall variable. The basic idea of kriging is to predict the value of a function at a given point by computing a weighted average of the known values of the function in the neighborhood of the point. The method is mathematically closely related toregression analysis. Both theories derive a best linear unbiased estimator, based on assumptions on covariances, make use of Gauss-Markov theorem to prove independence of the estimate and error, and make use of very similar formulae. They are nevertheless, useful in different frameworks: kriging is made for estimation of a single realization of a random field, while regression models are based on multiple observations of a multivariate dataset. Kriging can also be understood as a form of Bayesian inference. Kriging starts with a prior distribution over functions. This prior takes the form of a Gaussian process: N samples from a function will be normally distributed, where the covariance between any two samples is the covariance function of the Gaussian process evaluated at the spatial location of two points. A set of values is then observed, each value associated with a spatial location. Now, a new value can be predicted at any new spatial location, by combining the Gaussian prior with a Gaussian likelihood function for each of the observed values. The resulting posterior distribution is also Gaussian, with a mean and covariance that can be simply computed from the observed values, their variance, and the kernel matrix derived from the prior. In geostatistical models, sampled data is interpreted as a result of a random process. The fact that these models incorporate uncertainty in their conceptualization doesn't mean that the phenomenon - the forest, the aquifer, the mineral deposit - has resulted from a random process, but solely allows to build a methodological basis for the spatial inference of quantities in unobserved locations and to the quantification of the uncertainty associated with the estimator. A stochastic process is simply, in the context of this model, a way to approach the set of data collected from the samples. The first step in geostatistical modulation is the creation of a random process that best describes the set of experimental observed data. In geostatistical models, sampled data is interpreted as a result of a random process. The fact that these models incorporate uncertainty in their conceptualization doesn't mean that the phenomenon the forest, the aquifer, the mineral deposit has resulted from a random process, but solely allows to build a methodological basis for the spatial inference of quantities in unobserved locations and to the quantification of the uncertainty associated with the estimator. A stochastic process is simply, in the context of this model, a way to

approach the set of data collected from the samples. The first step in geostatistical modulation is the creation of a random process that best describes the set of experimental observed data. A value spatially located at x_1 (generic denomination of a set of geographic coordinates) is interpreted as a realization $z(x_1)$ of the random variable $Z(x_1)$. In the space A , where the set of samples is dispersed, exists N realizations of the random variables $Z(x_1)$, $Z(x_2)$,…, $Z(x_N)$, correlated between themselves. The set of random variables, constitutes a random function of which only one realization is known $z(x_1)$ the set of experimental data. With only one realization of each random variable it's theoretically impossible to determine any statistical parameter of the individual variables or the function. The proposed solution in the geostatistical formalism consists in assuming various degrees of stationarity in the random function, in order to make possible the inference of some statistic values. For instance, if a workgroup of scientists assumes appropriate, based on the homogeneity of samples in area A where the variable is distributed, the hypothesis that the first moment is stationary (i.e. all random variables have the same mean), than, they are implying that the mean can be estimated by the arithmetic mean of sampled values. Judging an hypothesis like this as appropriate is the same as considering that sample values are sufficiently homogeneous to validate that representativity. The hypothesis of stationarity related to the second moment is defined in the following way: the correlation between two random variables solely depends on the spatial distance that separates them and is independent of its location:

$$C(Z(x_1), Z(x_2)) = C\left(Z(x_i), Z(x_i + \boldsymbol{h})\right) = C(\boldsymbol{h})$$

$$\gamma(Z(x_1), Z(x_2)) = \gamma\left(Z(x_i), Z(x_i + \boldsymbol{h})\right) = \gamma(\boldsymbol{h})$$

Where:

$$\boldsymbol{h} = (x_1, x_2) = (x_1, x_i + \boldsymbol{h})$$

This hypothesis allows to infer those two measures: the variogram and the covariogram based on the N samples:

$$\gamma(\boldsymbol{h}) = \frac{1}{2N(h)} \sum_{i=1}^{N(h)} (Z(x_i) - Z(x_i + h))^2$$

$$C(\boldsymbol{h}) = \frac{1}{N(h)} \sum_{i=1}^{N(h)} (Z(x_i) Z(x_i + \boldsymbol{h})) - m(x_i) m(x_i + \boldsymbol{h})$$

Where:

$$m(x_i) = \frac{1}{N(h)} \sum_{i=1}^{N(h)} Z(x_i)$$

Spatial inference, or estimation, of a quantity Z : $Z : \mathbb{R}^n \to \mathbb{R}$, at an unobserved location x_0, is calculated from a linear combination of the observed values $z_i = Z(x_1)$ and weights $w_i(x_0)$, i= 1,…,N :

$$\hat{Z}(x_0) = [w_1 \quad \cdots \quad w_N] \cdot \begin{bmatrix} z_1 \\ \vdots \\ z_N \end{bmatrix} = \sum_{i=1}^{n} w(x_0) \times Z(x_i)$$

The weights w_i are intended to summarize two extremely important procedures in a spatial inference process:

- reflect the structural "proximity" of samples to the estimation location, x_0
- at the same time, they should have a desegregation effect, in order to avoid bias caused by eventual sample clusters

When calculating the weights w_i, there are two objectives in the geostatistical formalism: unbias and minimal variance of estimation. If the cloud of real values $Z(x_0)$ is plotted against the estimated values $\hat{Z}(x_0)$, the criterion for global unbias, intrinsic stationarity or wide sense stationarity of the field, implies that the mean of the estimations must be equal to mean of the real values. The second criterion says that the mean of the squared deviations ($\hat{Z}(x_0) - Z(x)$), must be minimal, which means that when the cloud of estimated values versus the cloud real values is more disperse, the estimator is more imprecise. Depending on the stochastic properties of the random field and the various degrees of stationarity assumed, different methods for calculating the weights can be deducted, i.e. different types of kriging apply. Classical methods are: Ordinary kriging (assumes stationarity of the first moment of all random variables), Simple kriging (assumes a known stationary mean), Universal kriging (assumes a general polynomial trend model, such as linear trend model). Below, the type of kriging used in this work will be explain.

- Ordinary Kriging

The unknown value $z(x_0)$ is interpreted as a random variable located in x_0, as well as the values of neighbors samples $z(x_i)$, i= 1,…,N . The estimator $\hat{z}(x_0)$ is also interpreted as a random variable located in x_0, a result of the linear combination of variables. In order to deduce the kriging system for the assumptions of the model, the following error committed while estimating z(x) in x_0 is declared:

$$\epsilon(x_0) = \hat{Z}(x_0) - Z(x_0) = [W^T - 1] \cdot [Z(x_i) \cdots Z(x_N)\, Z(x_0)]^T = \sum_{i=1}^{N} w_i(x_0) \times Z(x_i) - Z(x_0)$$

The two quality criteria referred previously can now be expressed in terms of the mean and variance of the new random variable $\epsilon(x_0)$.

- Unbias

Since the random function is stationary $E(Z(x_i)) = E(Z(x_0)) = m$, the following constraint is observed:

$$E(\epsilon(x_0)) = 0 \Leftrightarrow \sum_{i=1}^{N} w_i(x_0) \times E\left(Z(x_i)\right) - E\left(Z(x_0)\right) = 0 \Leftrightarrow m \sum_{i=1}^{N} w_i(x_0) - m = 0$$

$$\Leftrightarrow \sum_{i=1}^{N} w_i(x_0) = 1 \Leftrightarrow 1^T \cdot W = 1$$

In order to ensure that the model is unbiased, the sum of weights needs to be one.

- Minimal Variance: minimize $E(\epsilon(x_0)^2)$

Two estimators can have $\epsilon(x_0) = 0$, but the dispersion around their mean determines the difference between the quality of estimators.

$$Var\big(\epsilon(x_0)\big) = Var\left([W^T - 1] \cdot [Z(x_i) \cdots Z(x_N)\, Z(x_0)]^T\right) =$$

$$= [W^T - 1] \cdot Var\left([Z(x_i) \cdots Z(x_N)\, Z(x_0)]^T\right) \cdot \begin{bmatrix} W \\ -1 \end{bmatrix}$$

$$Var\left(\epsilon(x_0)\right) = [W^T - 1] \cdot \begin{bmatrix} Var_{x_i} & Cov_{x_i x_0} \\ Cov_{x_i x_0}^T & Var_{x0_i} \end{bmatrix} \cdot \begin{bmatrix} W \\ -1 \end{bmatrix}$$

Where the literals $\{Var_{x_i},\ Var_{x_i}, Cov_{x_i x_0}\ \}$ stand for:

$$\{Var\left([Z(x_i) \cdots Z(x_N)]^T\right), Var\big(Z(x_0)\big), Cov\left([Z(x_i) \cdots Z(x_N)]^T, Z(x_0)\right)\}$$

.Once defined the covariance model or variogram, C(h) or γ(h), valid in all field of analysis of Z(x), than we can write an expression for the estimation variance of any estimator in function of the covariance between the samples and the covariances between the samples and the point to estimate:

$$Var\left(\epsilon(x_0)\right) = W^T \cdot Var_{x_i} \cdot W - Cov_{x_i x_0}^T \cdot W - W^T \cdot Cov_{x_i x_0}^T + Var_{x_0}$$

$$Var\left(\epsilon(x_0)\right) = Cov(0) + \sum_i \sum_j w_i\, w_j Cov\big(x_i, x_j\big) - 2 \sum_i w_i\, C(x_i . x_0)$$

Some conclusions can be asserted from this expressions. The variance of estimation is not quantifiable to any linear estimator, once the stationarity of the mean and of the spatial covariances, or variograms, are assumed. Furher, it grows with the covariance between samples $C(x_i . x_j)$, i.e. to the same distance to the estimating point, if the samples are proximal to each other, than the clustering effect, or informational redundancy, is bigger, so the estimation is worst. This conclusion is valid to any value of the weights: a preferential grouping of samples is always worst, which means that for the same number of samples the estimation variance grows with the relative weight of the sample clusters. The variance of estimation grows when the covariance between the samples and the point to estimate decreases. This means that, when the samples are more far away from x_0, the worst is the estimation. Again it grows with the a priori variance C(0) of the variable Z(x) . When the variable is less disperse, the variance is lower in any point of the area A. Finally, always the variance of estimation does not depend on the values of the samples. This means that the same spatial configuration (with the same geometrical relations between samples and the point to estimate) always reproduces the same estimation variance in any part of the area A. This way, the variance does not measures the uncertainty of estimation produced by the local variable.

Chapter 6

Analysis

In this chapter, the results obtained with the downscaling and interpolation methods are finally shown. Firstly, a comparison between the radar and rain gauges is given because it affects all the other following sections. The limits of the downscaling method are shown and a solution to improve its applicability is given. Then, even the limits of the interpolation methods are explained and, at the end, their application to the rainfall spatial variability is analysed.

6.1 Radar and rain gauge data suitability

Even if the suitability between radar and rain gauges data is not the aim of this work, it is necessary to provide a brief analysis. This necessity comes from the fact both the interpolation and the downscaling methods have as input the radar data. This means that if the radar provides wrong data, as a consequence the methods do the same; furthermore, it is even more important to understand if the radar commits systematic errors so that the true values can be estimated; or understand if the radar errors change according to some features of the rainfall events such as the intensity for example. According to the rainfall events analysed (table 3.1), the intensity recorded by the radar is always lower than the intensity recorded by the rain gauges. In order to be as exhaustive as possible in the figure 6.1, 6.2 and 6.3 the rain gauge accumulations respectively of the A,I,C points, are reported compared with the radar accumulation; the averaged rain gauge intensities of the analysed events is put as a variable in the x-axis. The three charts are really similar to each other; the small dissimilarities are due to the different records of the three rain gauges because the radar data remains the same. From the same graphs, it can be seen that for the rain gauge intensity equal to 0.5025, which corresponds to the 25/8/2012 event, the radar

didn't work properly and one or more of the causes mentioned in chapter n°3 have occurred. As a consequence, for this event the interpolation and downscaling methods are completely affected by the deficiency of the radar so that a reliable comparison with the rain gauge estimations cannot be done.

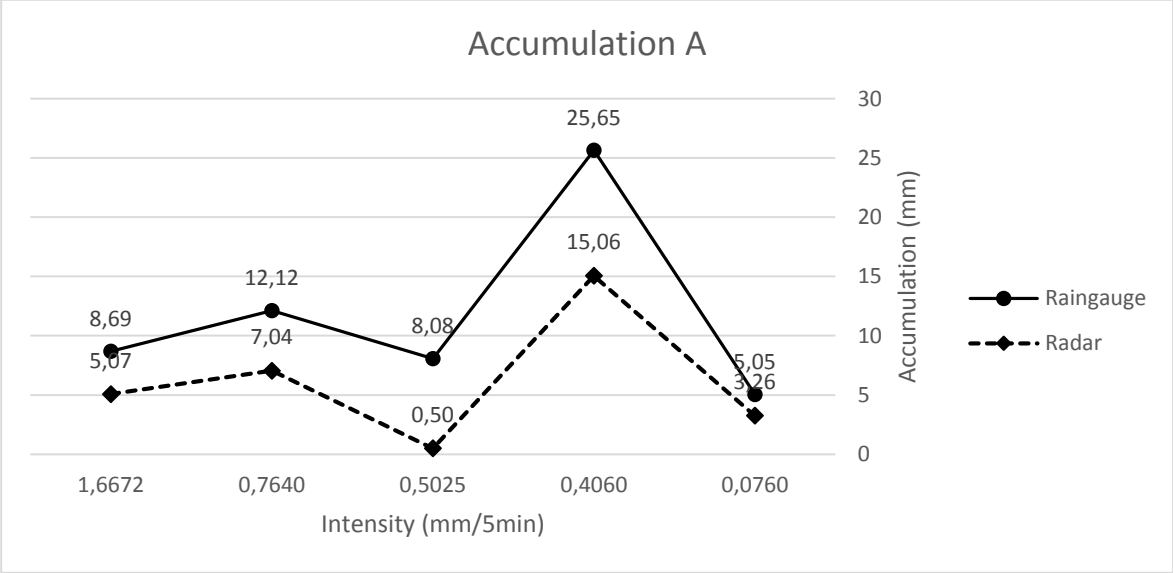

Figure 6.1 Radar and rain gauge accumulation in the point A, at rain gauge intensity variation.

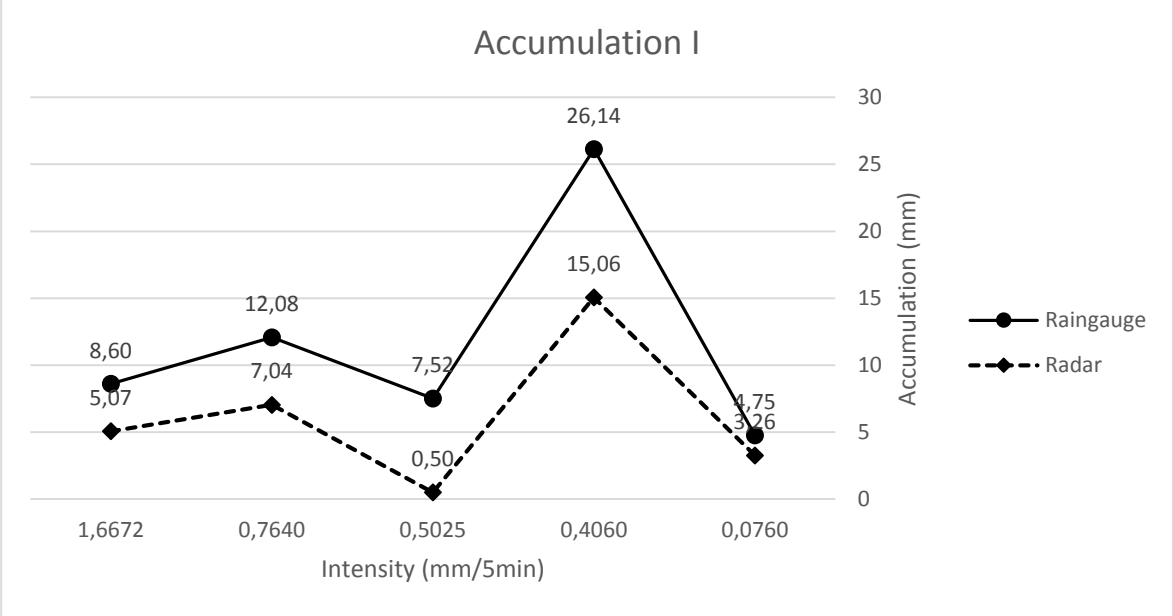

Figure 6.2 Radar and rain gauge accumulation in the point I, at rain gauge intensity variation.

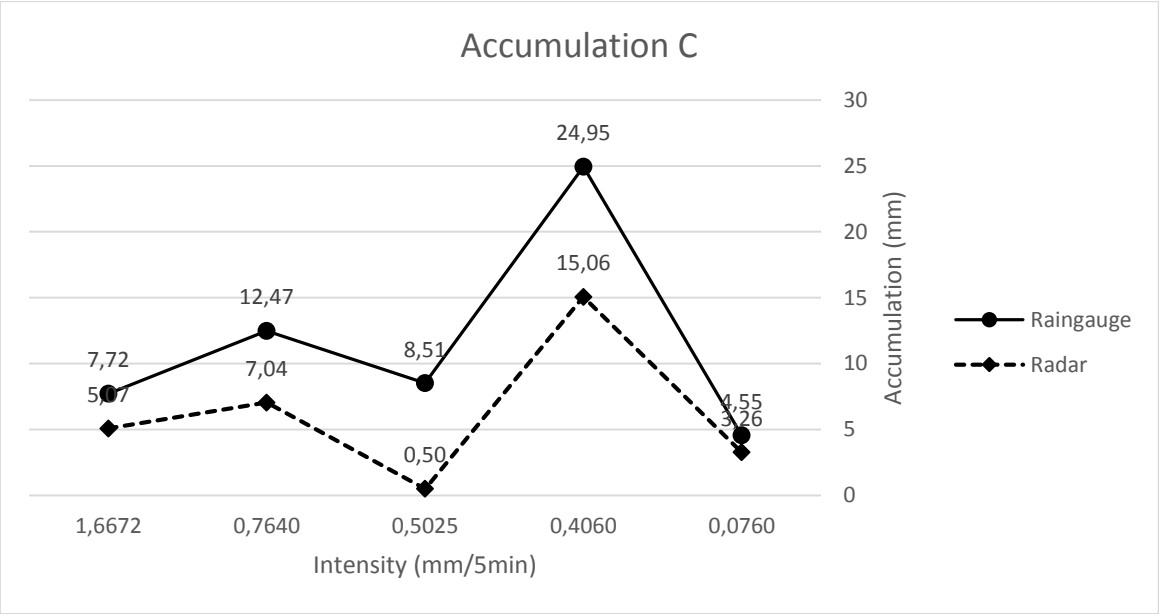

Figure 6.3 Radar and rain gauge accumulation in the point C, at rain gauge intensity variation

The order of magnitude provided by the two devices is the same; this is not true just for the 25/8 event. Further, the graphs show that the rainfall intensities of the events are not the main discriminating factor, indeed the accumulation difference between the two devices doesn't change according to its increase or decrease. However, if the percentage of error is calculated (table 6.1) it can be seen that there is a trend with the rainfall intensity changing (figure 6.4).

Event	Averaged rain gauge accumulation (mm)	Radar accumulation (mm)	Averaged rain gauge intensity(mm/5min)	Percentage Radar-Rain gauge error
21/6	8,336	5,073	1,67	39
7/7	12,224	7,042	0,76	42
25/8	8,039	0,497	0,50	94
6/7	25,579	15,063	0,41	41
22/6	4,785	3,258	0,08	32

Table 6.1 Radar-Rain gauges accumulation percentage error.

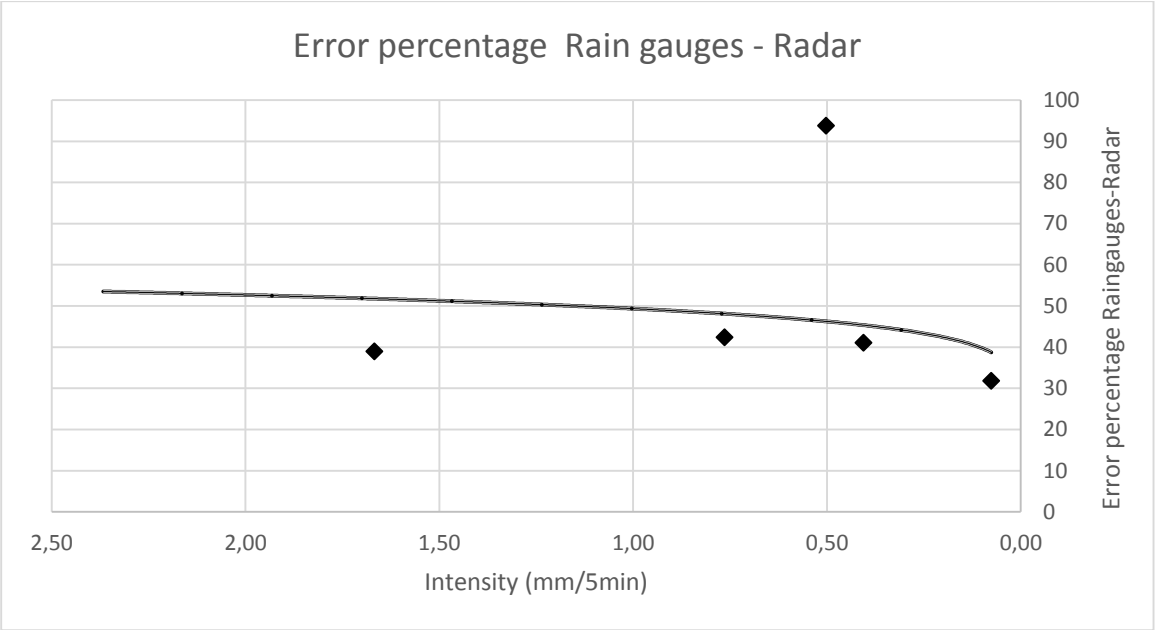

Figure 6.4 Radar-Rain gauges accumulation percentage error varying the intensities of the events. The power trend line shows the radar improves with the intensity decrease.

In particular, if the intensity decreases, the radar improves its working. This is predictable because for the radar it is more easy to detect a spread rainfall than a localised storm; this is due to the problems mentioned in chapter n°3, as for example the beam above the cloud at long ranges or the spatial shift due to wind effect. Another factor which affects the working of the radar is just the same rainfall accumulation, whereas the error percentage committed by the radar enhances with its increasing. In table 6.2 the events are sorted according to the decreasing rainfall accumulation so that the error percentage decreases as well. This behaviour is even more evident in figure 6.6 in which a power trendline is plotted. The 25/8 event is dismissed because it is an anomaly for this analysis. In graph 6.5 the averaged differences between radar and rain gauges change according to the averaged rain gauge accumulation. The lines which join the points slightly trend to increase their slopes with the averaged rain gauge accumulation, except for the last line for which a small decrease is seen (this is consistent with the values of table 6.2).

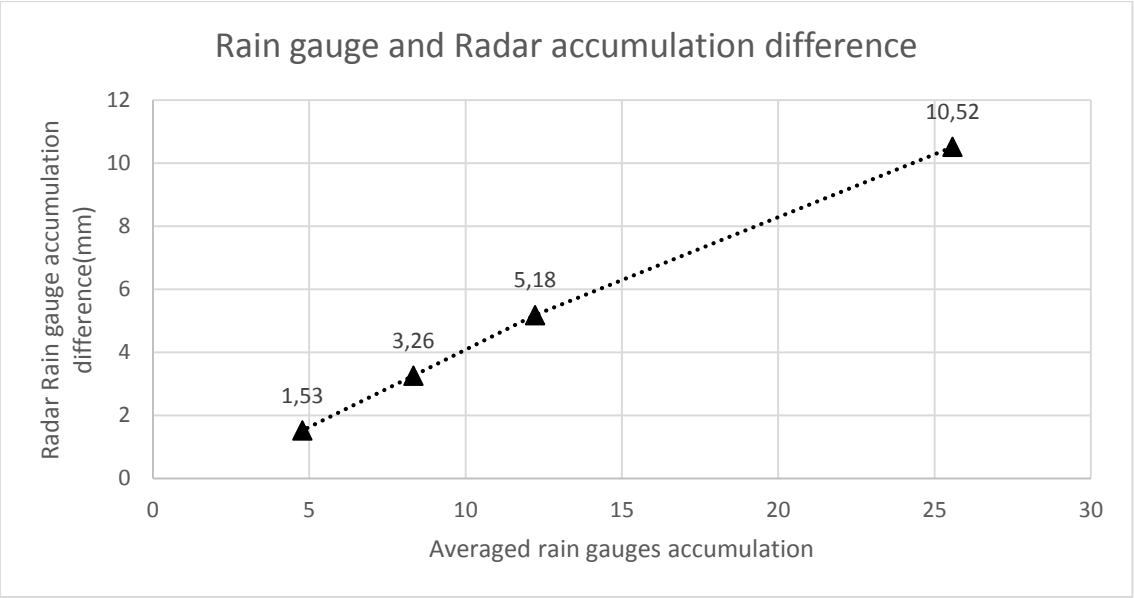

Figure 6.5 Radar and averaged rain gauge accumulations difference with the averaged rain gauge accumulations changing.

Events	Averaged rain gauges accumulation (mm)	Radar accumulation (mm)	Percentage Radar-Rain gauges error
6/7	25,579	15,063	41
7/7	12,224	7,042	42
21/6	8,336	5,073	39
22/6	4,785	3,258	32

Table 6.2 Events sorted according to the rain gauges accumulations and relative accumulation percentage error commited by the radar

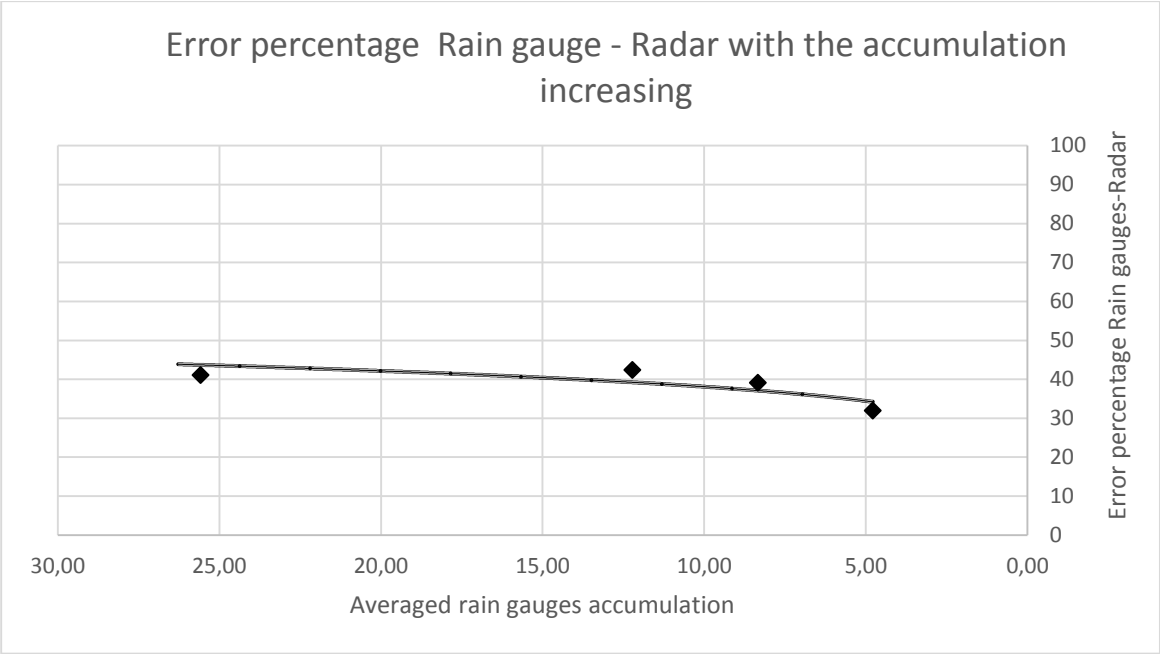

Figure 6.6 Radar-Rain gauges accumulation percentage error varying with the averaged rain gauges accumulation. The power trendline shows the radar improves with the averaged rain gauges accumulation decrease.

It can be deduced that the radar commits a systematic error because it always underestimates the rainfall. Further, the analysis showed that the radar working tends to improve for lower intensity events and for lower accumulation events. Despite this, more events should be taken into account to study the radar- rain gauge data suitability and finally to plot more reliable trendlines; but, this is not the aim of this work, as a consequence this analysis is not further expanded on. Anyway, being that the interpolation and downscaling methods are directly dependent on the radar values, it can be deduced that their efficacies vary according to these two parameters changing. For the events analysed in this thesis, the 22/6 event commits less radar-rain gauge percentage error, 32%; on the contrary the 6/7, 7/7, 22/6 events commit an error almost stable on 40% and finally 94 % for the 25/8 event.

6.1 Downscaling method results

As mentioned in chapter n°2, in order to represent at best the downscaled values, it is necessary to use statistical function because a stochastic downscaling method is used(chapter 4). The more important statistical functions for this work are the 1st and the 3rd quartiles which represent respectively the 25% and the 75% positions of all realizations. It is expected that the rain gauge values will fall inside this range. The results of all the rainfall events are shown in the following figures, in which even the radar and rain gauge values are reported. Just the outputs in point A is shown because the downscaling method is a stochastic method and as a consequence it is able to provide an order of magnitude of all the possible realizations which could occur. So it is not useful to also report the downscaled values in the other points I,C, because they provide similar realizations. Further, for the same reason, the downscaling method is dismissed in the rainfall spatial variability section.

- 22/6 Event

  The first and the third quartiles are not able to contain the rain gauge record at all and just in the last part of the event, the rain gauge estimation falls inside the range. On the contrary, the radar estimation is in the middle of the 2 quartiles; it entails that in this event the downscaling estimation is really consistent with the radar data and its difference with the rain gauge values is due to the radar deficiency.

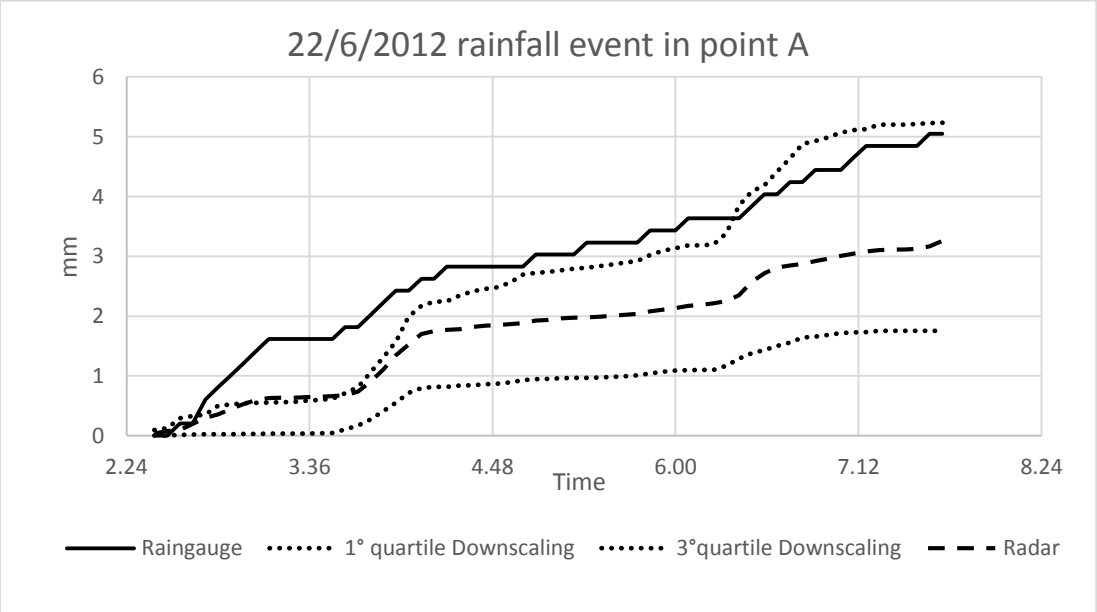

Figure 6.7 1st quartile and 3rd quartile of downscaled values, rain gauge and radar estimations rainfall comparison for the event 22/6 in point A.

- 6/7 Event

  Again, in this event the downscaled values are quite consistent with the radar estimations even if the latter is clearly closer to the third quartile. This entails that the downscaling method, in this case, slightly underestimates the radar values. The rain gauge estimation is really distant from the two quartiles range for approximately all the event.

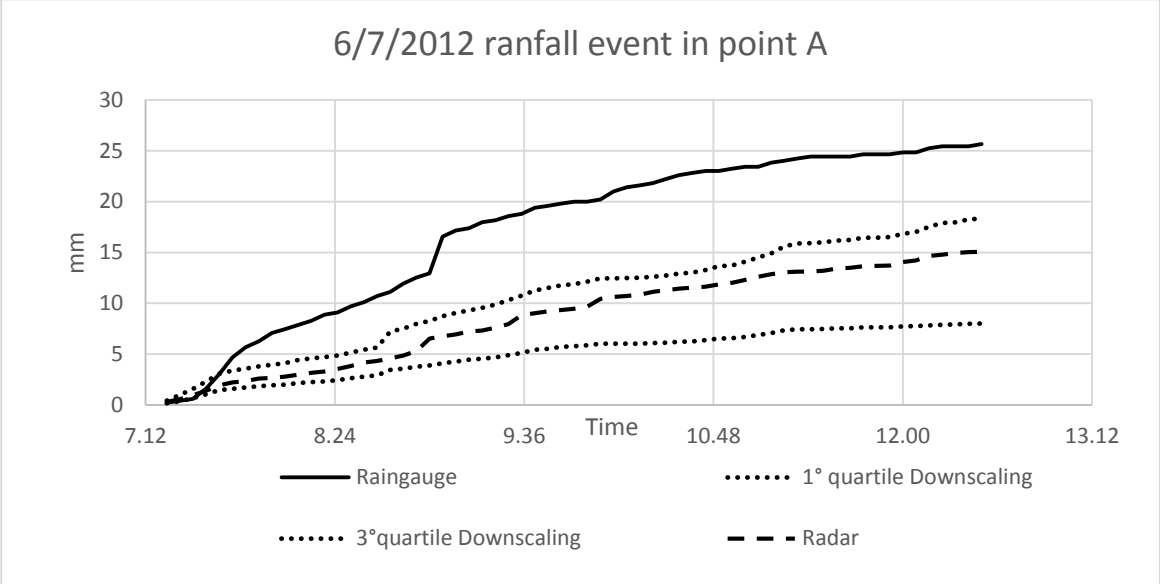

Figure 6.8 1st quartile and 3rd quartile of downscaled values, rain gauge and radar estimations rainfall comparison for the 6/7 event in point A.

- Event 25/8

  In this event, the radar clearly didn't work and even the downscaling method does the same. As a consequence, the consistency between the radar and downscaling method is confirmed and so no comparison is possible with the rain gauge.

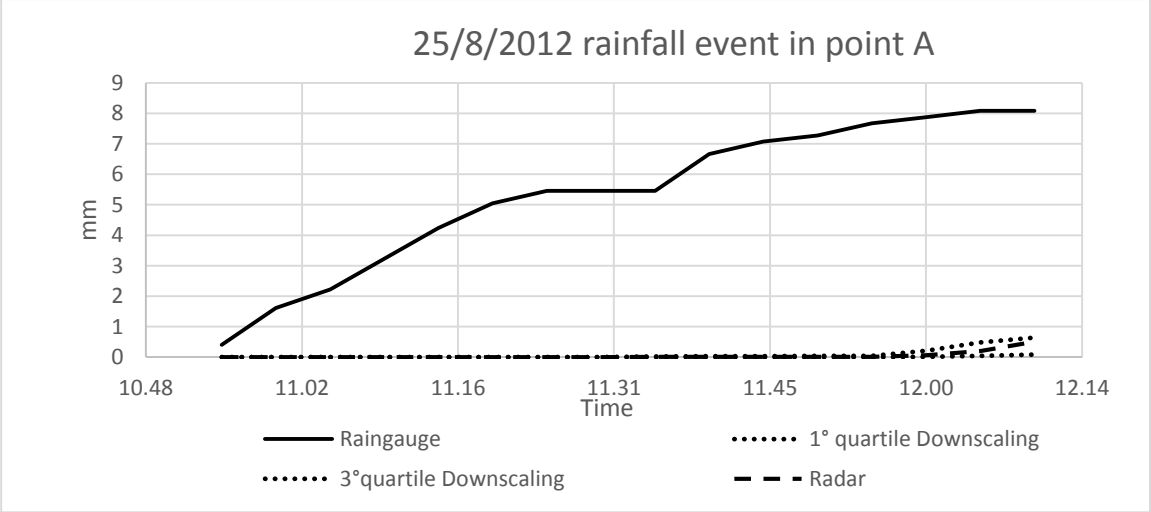

Figure 6.9 1st quartile and 3rd quartile of downscaled values, rain gauge and radar estimations rainfall comparison for the event 25/8 in the point A.

- Event 7/7

  In this event, the downscaled values really underestimate both the radar and the rain gauge values. There is almost an order of magnitude of difference between the rain gauge and the downscaled estimation. Further, it is curious that in the initial time step the radar detects really high intensity while the downscaling method ignores it. Until now, this is the first event in which the downscaling method is inconsistent, even with the radar; it seems that just in the first time step the method is not able to "read" the high intensity detected by the radar. Other than the downscaling method analysis it can be seen there is a temporal shift between the radar and the rain gauge because the first device detects high intensity at 18:30 while the second one at 18:35 and 18:40.

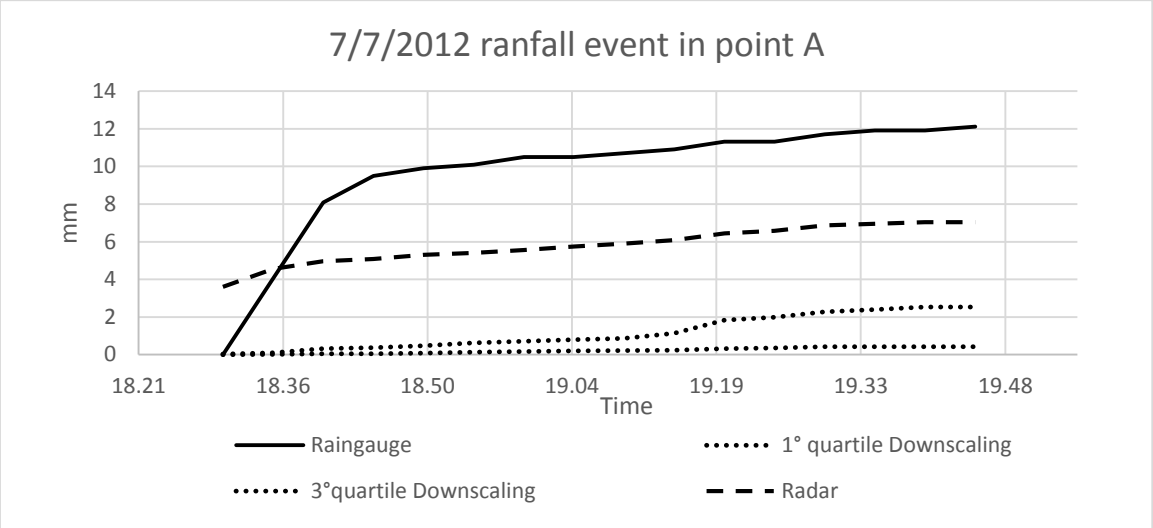

Figure 6.10 1st quartile and 3rd quartile of downscaled values, rain gauge and radar estimations rainfall comparison for the event 7/7 in the point A.

- Event 21/6

  Like the previous event, the downscaling method really underestimates the rain gauge and the radar event. Even here the method is not able to calculate high intensity and for this reason, it is neither consistent with the radar estimations. Differently from the previous event, the radar doesn't seem to show temporal shift but only underestimation.

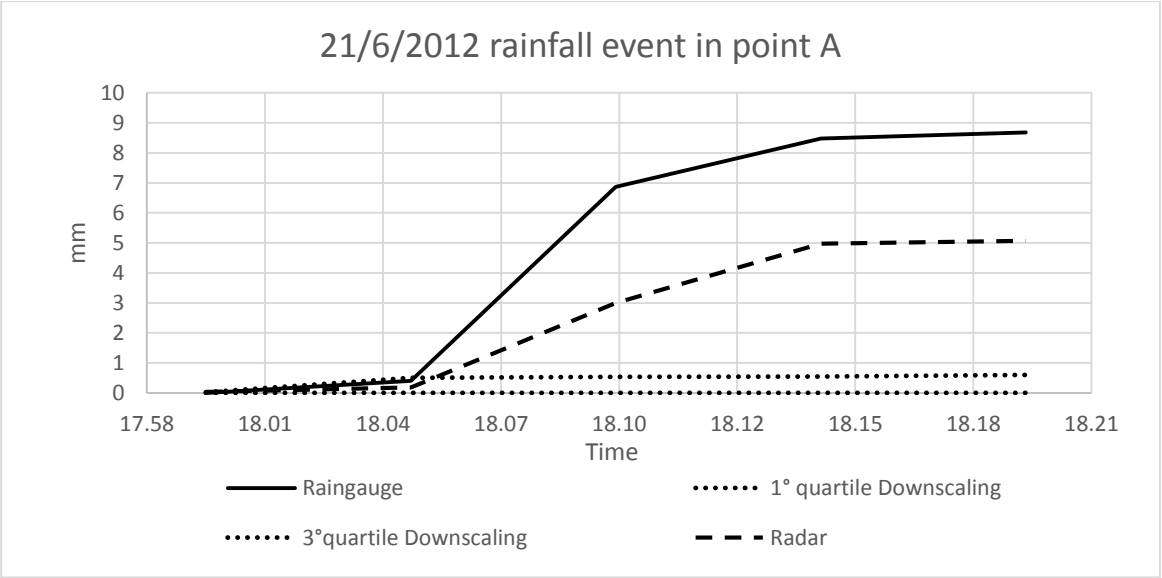

Figure 6.11 1st quartile and 3rd quartile of downscaled values, rain gauge and radar estimations rainfall comparison for the event 21/6 in the point A.

As a consequence of this analysis, some features of the downscaling method can be deduced. The method is strictly conditioned by the radar data and if the latter is not able to detect the rainfall for its working limits, it affects even the downscaled values. The downscaling method always underestimates the rain gauge and this deficiency increases with higher rainfall intensities. Also, the method is consistent with the radar detections only for low intensities, while it starts to underestimate it with the intensity increasing. So, an important conclusion is that the method doesn't underestimate the rain gauge values just for the radar deficiency but even for the intrinsic method limit in the case of high intensities. In figure 6.12, the order of magnitude of the rain gauge, radar and 1st,2nd,3rd quartiles of the downscaling methods are plotted; it is obtained by dividing the accumulations of each series for the number of time steps. It is clear how the order of magnitude changes for the intensity increasing. The lines, which join the markers, are plotted just to show their positions better.

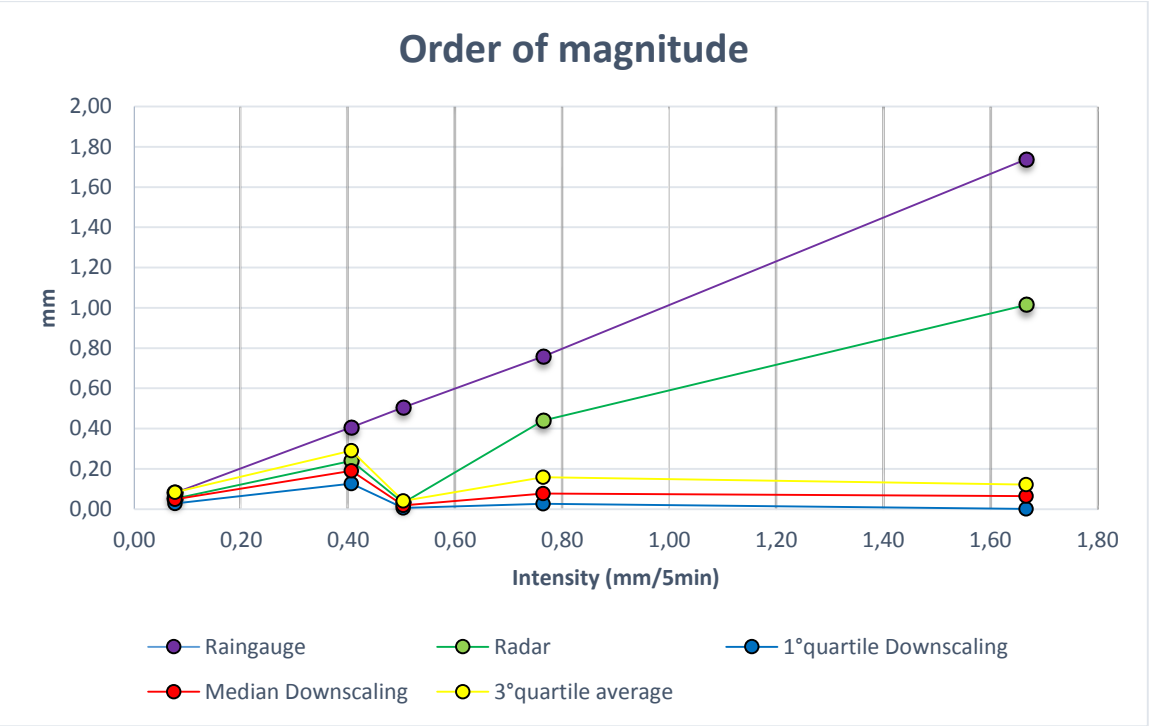

Figure 6.12 Order of magnitude of the rain gauge, radar, 1st,2nd ,3rd quartiles of the downscaling method with the intensity events changing.

6.3 Downscaling method improvement

It seems that the downscaling method is not able to provide high values when high intensities occur. This is true, if only the positions until the 3rd quartile are considered in the realization series. If the frequency distributions are extrapolated from the rainfall realizations at each time step, it is clear how they change with the intensity (and the kind of event) varying. Indeed, if low intensities and consequently spread and long events occur, types of normal and concentrated distributions appear; the contrary happens for heavy and localised events. Some examples of the long and low rainfall intensity in 22/6/2012 and 6/7/2012 events are reported respectively in figure 6.13 and in figure 6.14. On the contrary, in figures 6.15 and 6.16 respectively two examples from the shorter and localised 7/7/2012 and 21/6/2012 events are reported. The important difference between the first and the second type of distributions is that the latter shows high frequencies even for values far from the median value and as a consequence the values are spread and not concentrated. It is possible to see this feature even better from the respective box plot: the box is clearly larger in the second type of realizations and the "whiskers" are even much bigger. This feature suggests that the downscaling method is able to obtain consistent values for high intensity but for higher positions that are not within the range purposed by the 1st and 3rd quartiles.

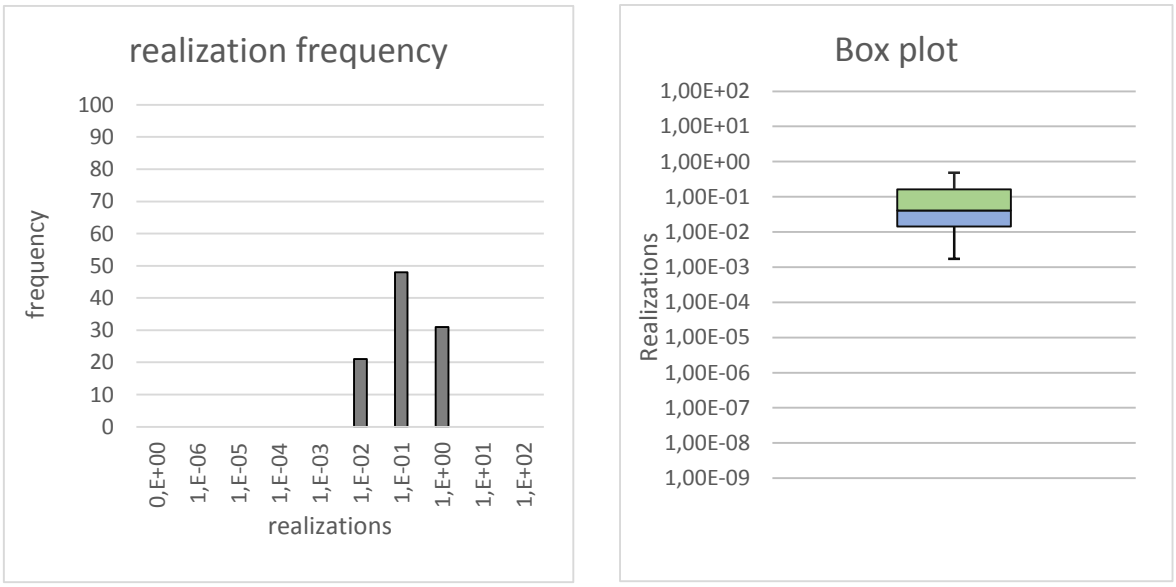

Figure 6.13 Frequency and respective Box plot of a characteristic realization series at one time step of the 22/6/2012 event.

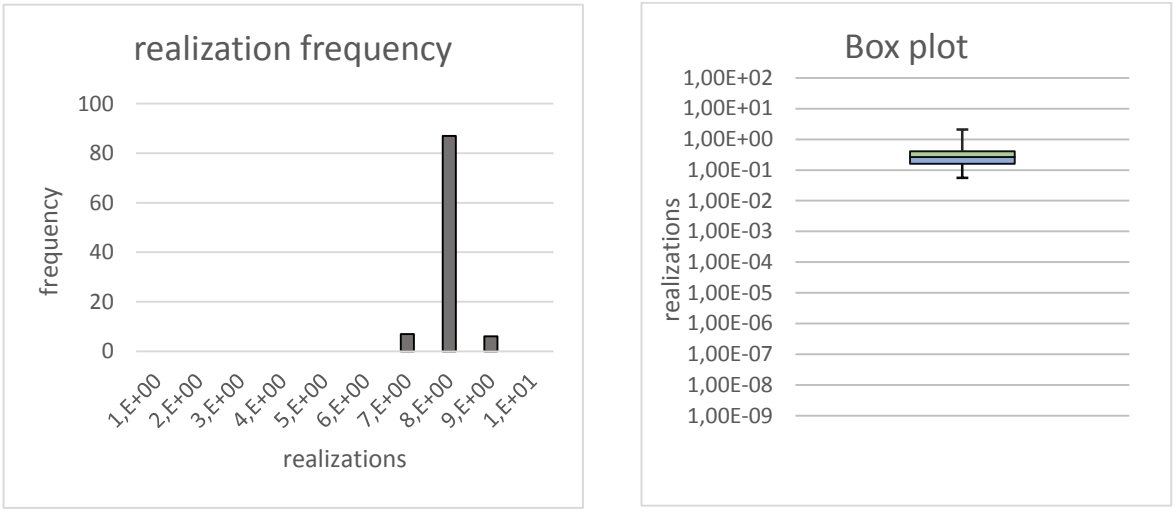

Figure 6.14 Frequency and respective Box plot of a characteristic realization series at one time step of the 6/7/2012 event

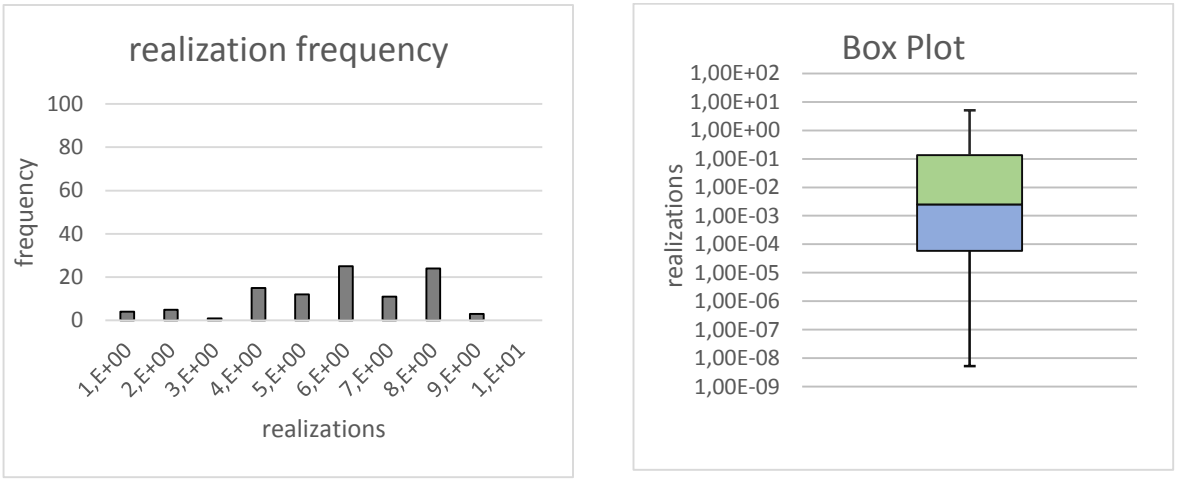

Figure 6.15 Frequency and respective Box plot of a characteristic realization series at one time step of the 7/7/2012 event

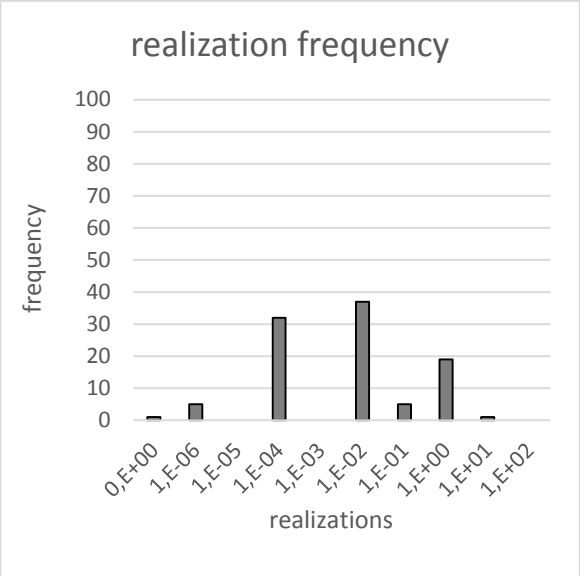

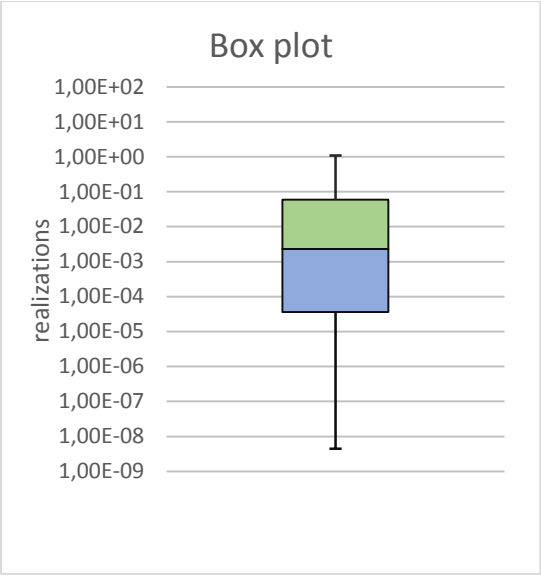

Figure 6.16 Frequency and respective Box plot of a characteristic realization series at one time step of the 21/6/2012 event

This downscaling method deficiency is due both to the radar malfunction with the intensity increasing and to the downscaling method feature. In order to improve the downscaling method estimations, it is necessary to understand the rate of these two problems with the rainfall intensity changing. In order to do this, the best fits of the downscaled realization positions according to the radar and the rain gauge estimations are calculated (table 6.3). They are estimated so that the sum of the errors at each time step, with both the rain gauge and the radar estimations, is minimized. In the table below, the position indicate the which number between 1 and 100 of the sorted downscaled realization series has been taken into account in order to minimize the sum of the errors with the rain gauges and the radar estimates.

Events	Downscaled realization position equal to rain gauges	Downscaled realization position equal to radar	Rain gauges intensity (mm/5min)	Radar intensity (mm/5min)
21/6	78	76	1.667	1.015
7/7	99	75	0.764	0,440
25/8	100	65	0.502	0.031
6/7	90	66	0.406	0.239
22/6	75	50	0.076	0.052

Table 6.3 Best fit downscaled realization position for rain gauges and radar.

Based upon the analysis conducted in the previous sections, it is clear that the positions for the best fit for the rain gauges are all over the best fit for the radar. It is possible to appreciate it better in the next figure, in which the best fits for the downscaled realization positions are plotted for both rain gauge and radar with their respective intensities. The two power trendlines are also plotted. In the case of the radar, even the 25/8/2012 event is considered in the graph, while it is dismissed for the rain gauge because it represents an anomaly. Contrarily it would be expected for the analysis conducted in the radar and rain gauge suitabilty, the trendlines slightly diverge from each other for low intensities; unfortunately, this is due probably to an insufficient number of points on which to plot the trendlines. However, the two trendlines show that the best fit positions of the downscaled realizations change with the rainfall intensity and in particular they both decrease for low intensities. As it has been found in the previous section, downscaling method is really consistent with the radar for really low intensities.

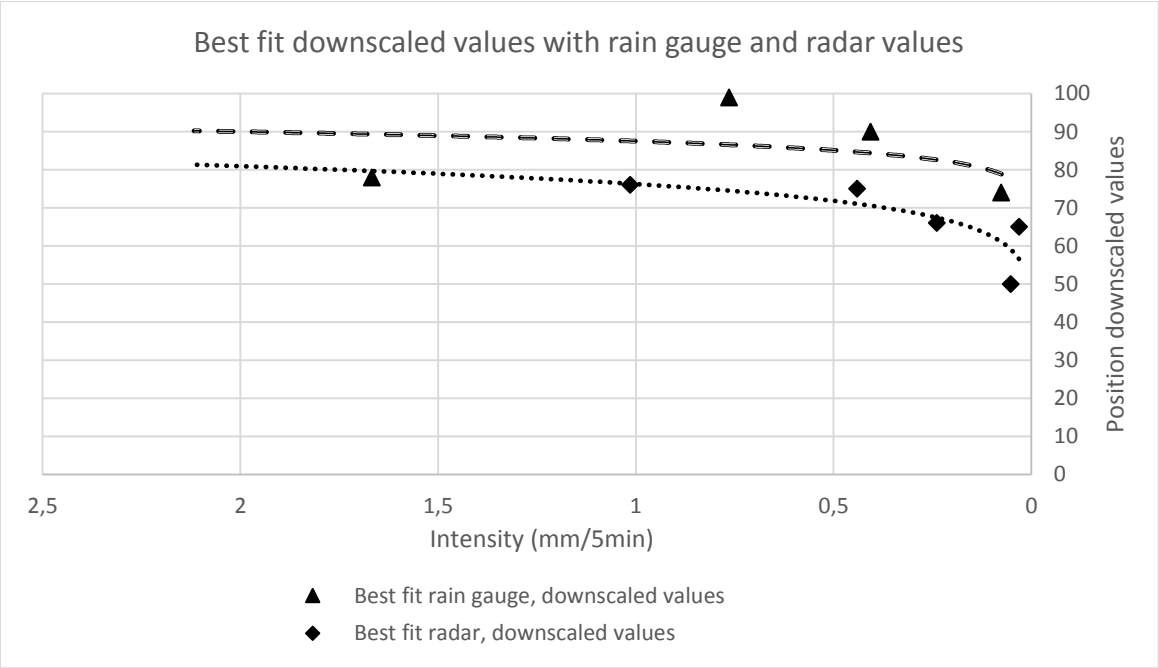

Figure 6.17 Best downscaled values fit according to the rain gauge and radar values with the intensity changing

In order to improve the downscaled estimations for forecasting, the radar intensity is the only possible parameter to obtain in advance. So, the idea is to extract an algorithm which can give the best position for the downscaled realizations in order to better estimate the rain gauge values according to the radar intensity. So the best fit for rain gauge and downscaled best positions can

be plotted according to the radar intensities and the power trendline can be found which approximates at best the points (figure 6.18).

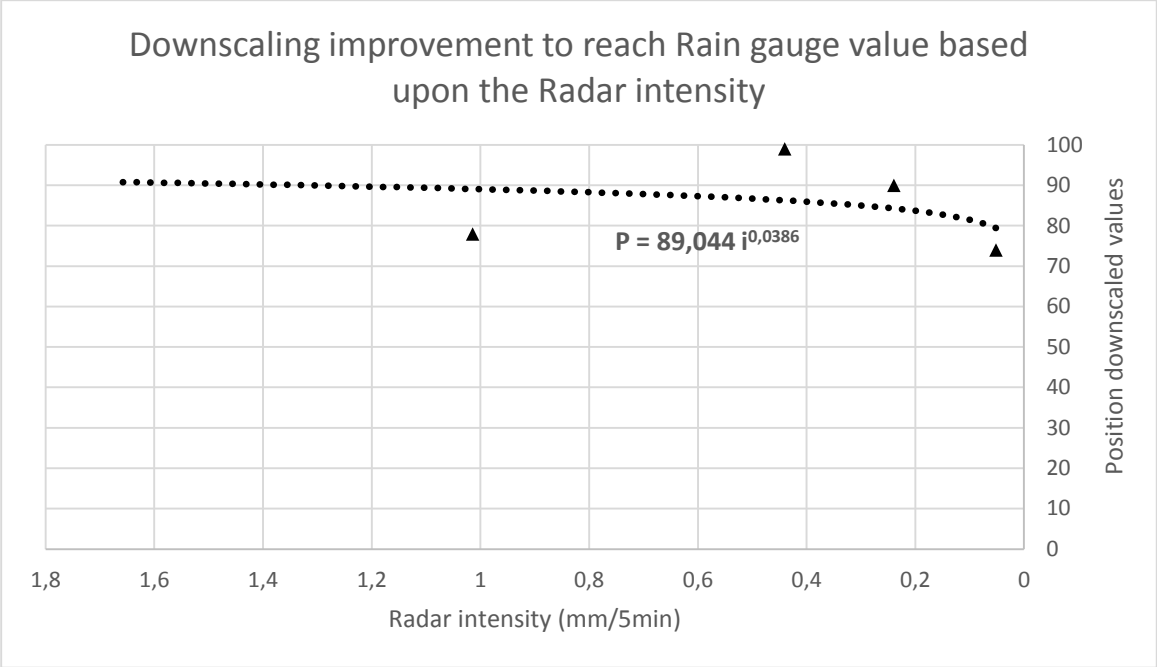

Figure 6.18 Best downscaled values fit according to the rain gauge values with the radar intensity changing

The algorithm which results from the trendline equation is:

$$\mathbf{P = 89{,}044\ I^{\,0{,}0386}}$$

P being the approximation of the best position of the downscaled realizations and I, the radar intensity in mm/5min. In the next table P is calculated and then compared with the real best position; as a consequence it can be understood how much the algorithm approximates the solution.

Event	Radar intensity(mm/5min)	Position obtained with the algorithm	Best fit (obtained with rain gauge)
21/6	1.014	**89**	78
7/7	0.440	**86**	99
25/8	0.0310	**80**	100
6/7	0.239	**84**	90
22/6	0.051	**80**	75

Table 6.4 Improvement of the position of the downscaling method realization with the radar intensity

The intensity used in the algorithm is averaged in all the rainfall events; surely the approximation improves if the intensity is referred to parts of the event. It can be seen that the best positions obtained with the algorithm are not sorted (in the central column of the previous table), because the central value is referred to the 25/8/2012 event in which the radar didn't work. This could be a limit of this improvement method because it is always dependent on the radar working. In the following figures the results obtained firstly with the algorithm and secondly with the best downscaled values are reported which minimize the error with the rain gauge for each events; the radar and rain gauge values and the 1st and the 3rd quartiles are also reported. For the 22/6/2012 event the best downscaled solution is dismissed because it coincides with the 3rd quartile.

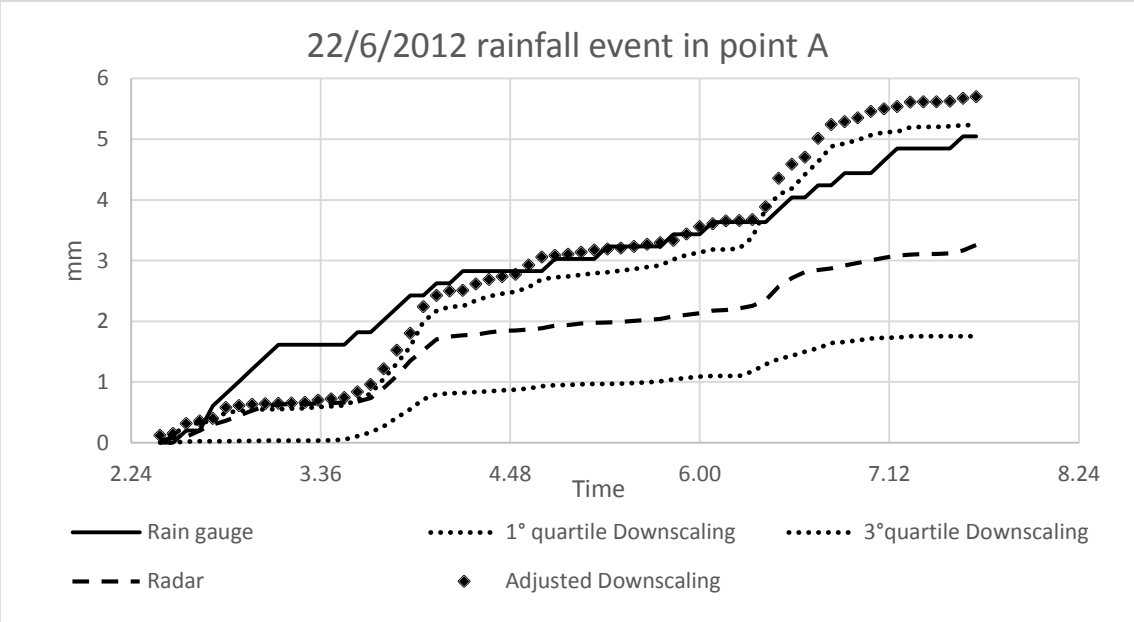

Figure 6.19 Adjusted downscaling method for the 22/6/2012 event

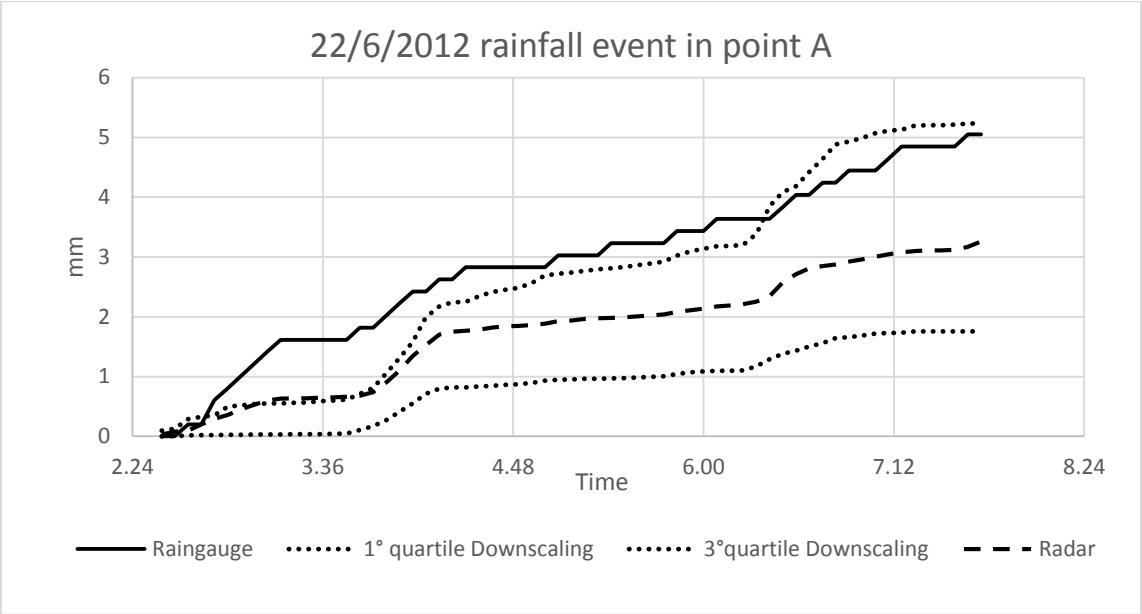

Figure 6.20 Best downscaled values which minimize the error with the rain gauge for the 22/6/2012 event

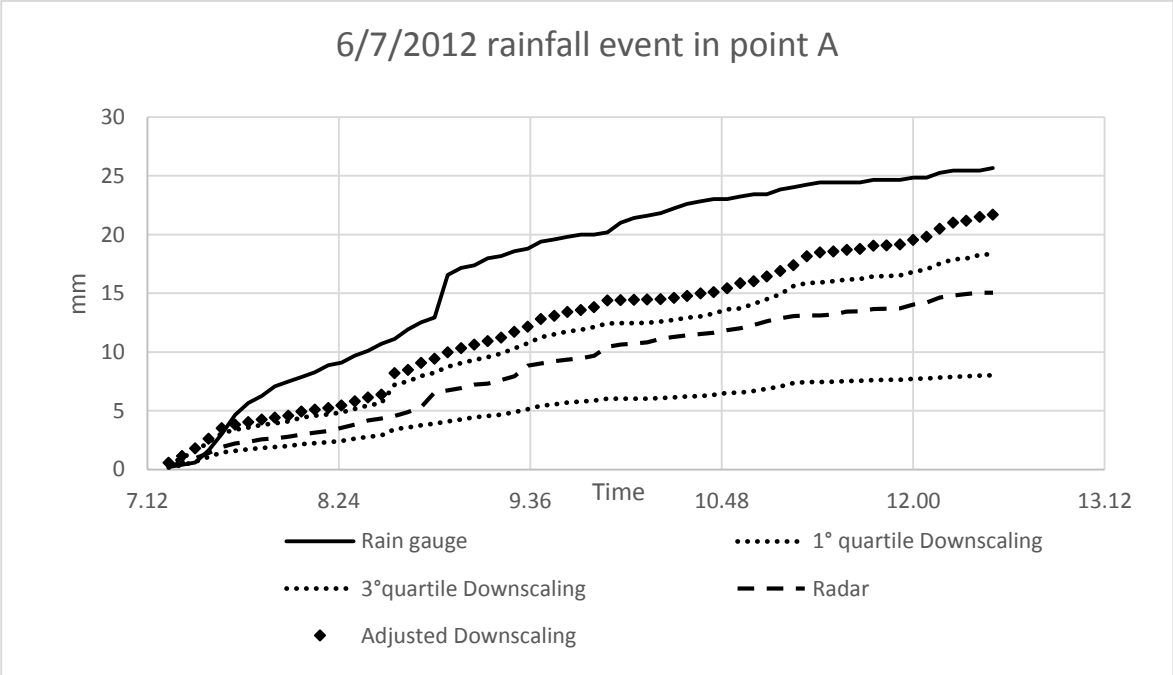

Figure 6.21 Adjusted downscaling method for the 6/7/2012 event

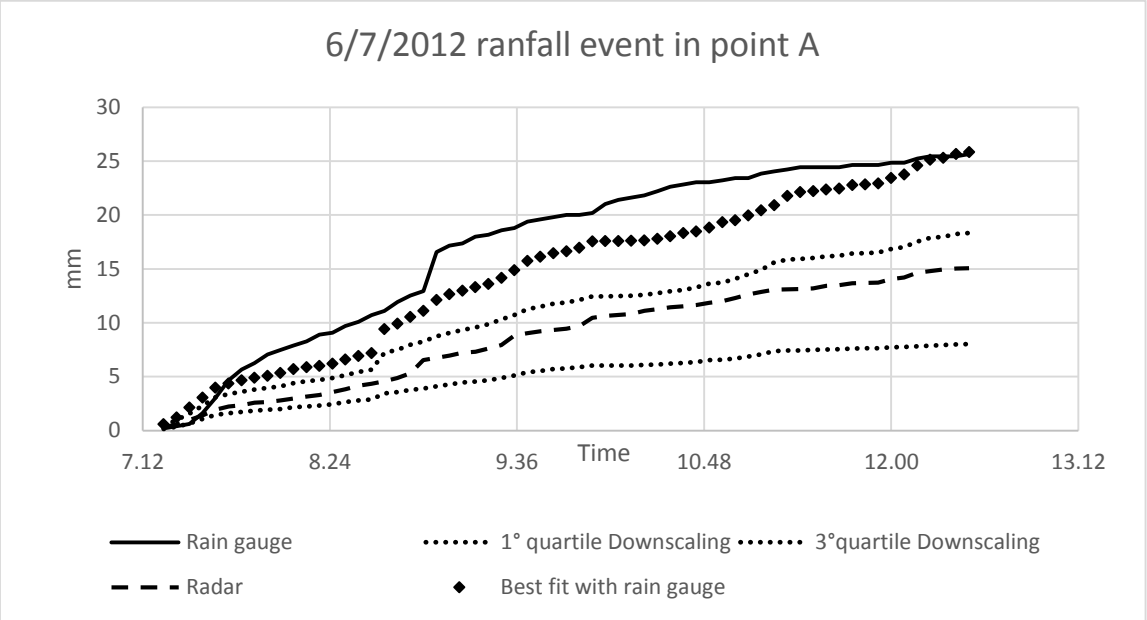

Figure 6.22 Best downscaled value which minimize the error with the rain gauge for the 6/7/2012 event

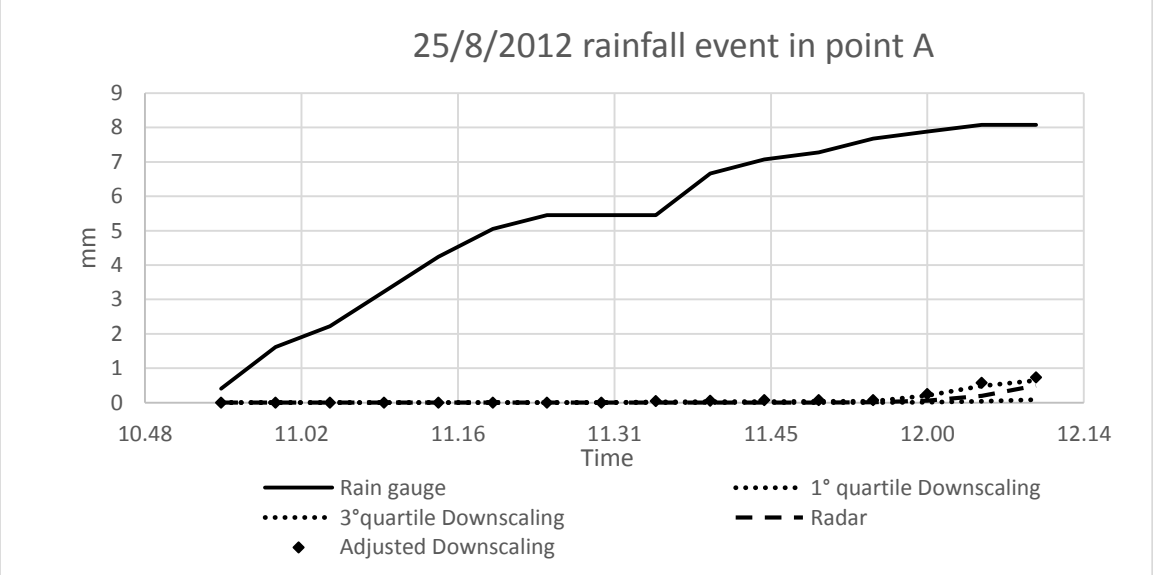

Figure 6.23 Adjusted downscaling method for the 25/8/2012 event

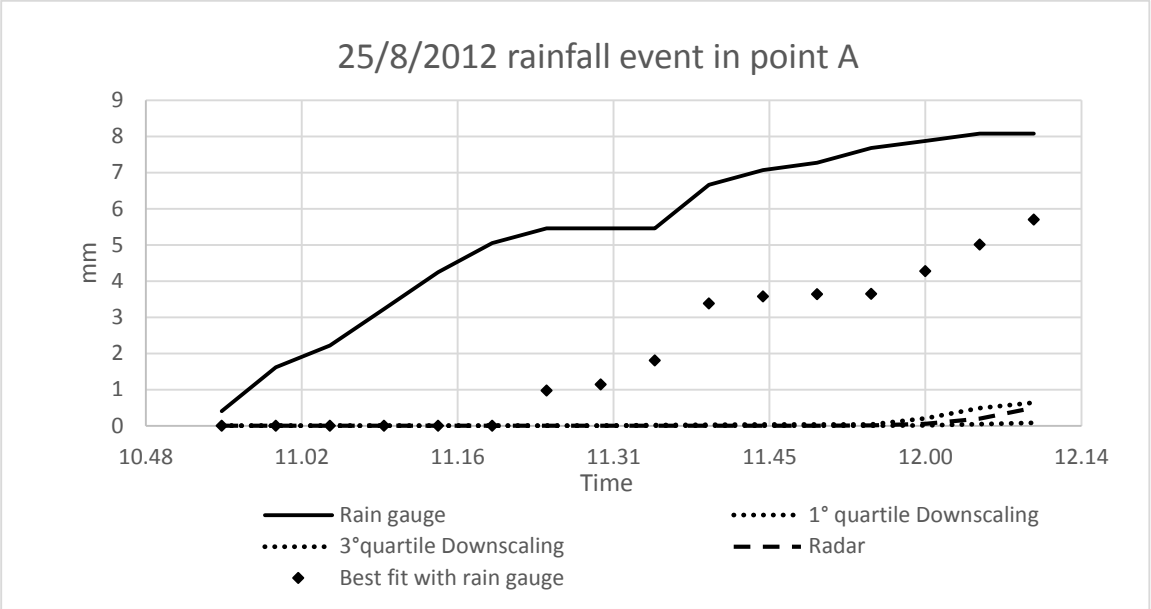

Figure 6.24 Best downscaled values which minimize the error with the rain gauge for the 25/8/2012 event

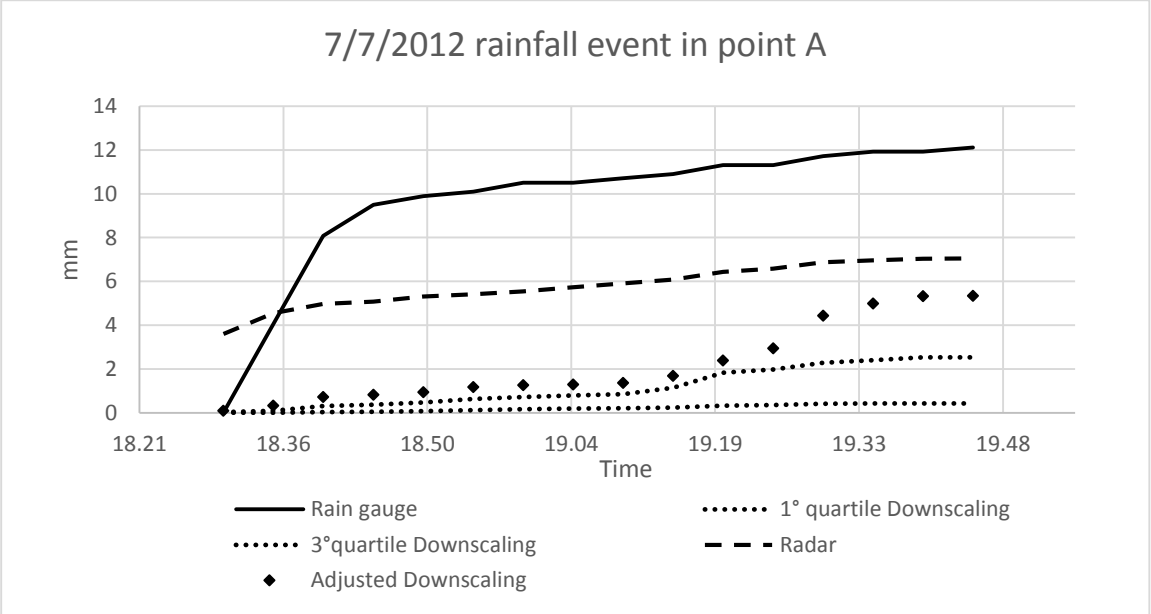

Figure 6.25 Adjusted downscaling method for the 7/7/2012 event

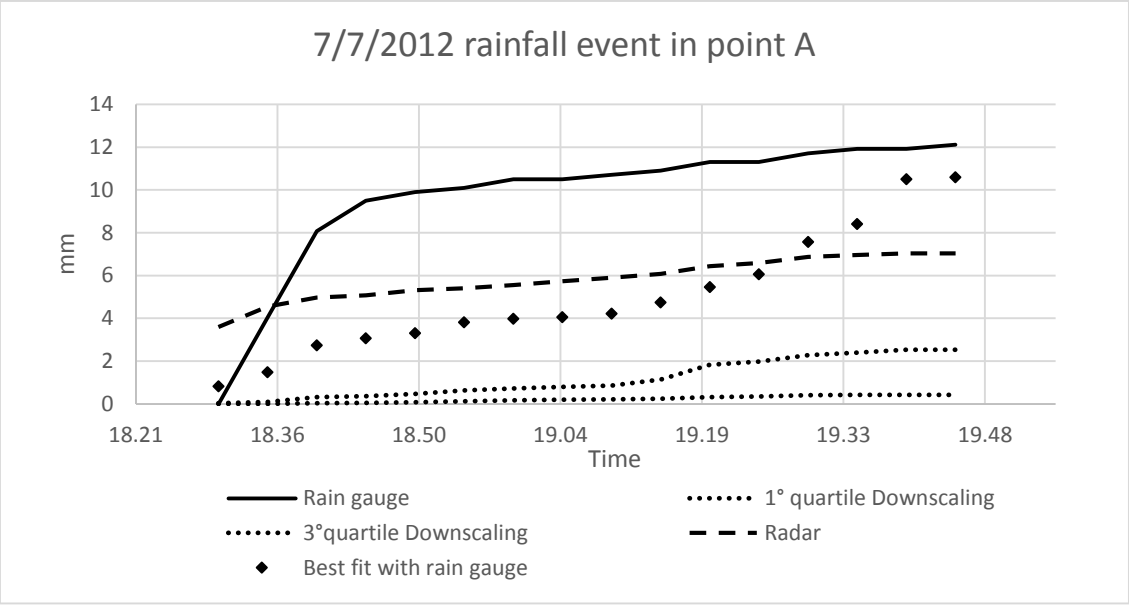

Figure6.26 Best downscaled values which minimize the error with the rain gauge for the 7/7/2012 event

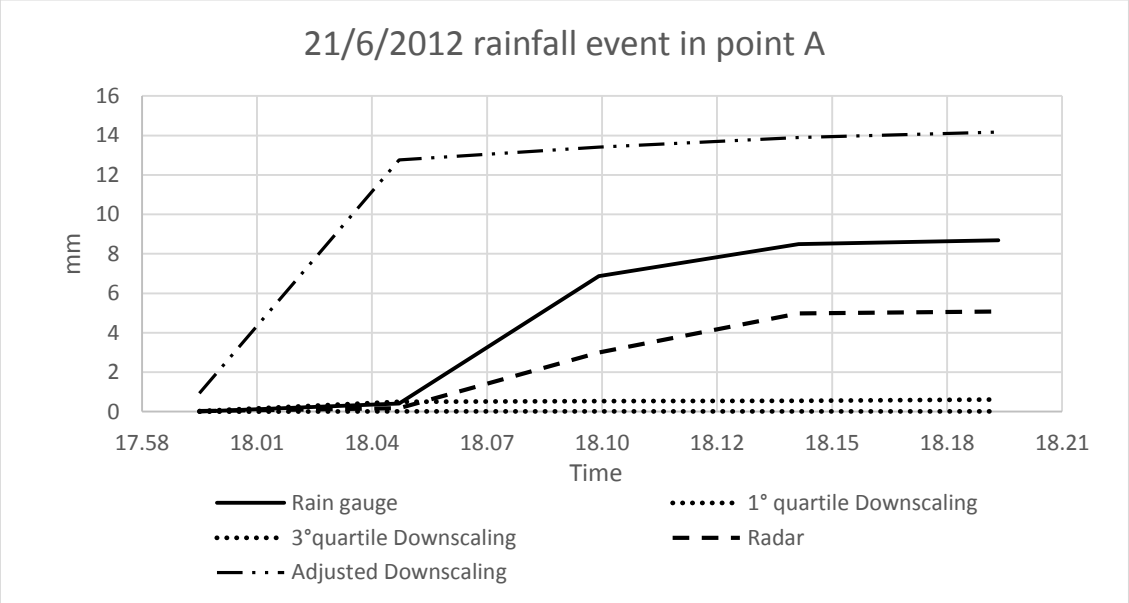

Figure 6.27 Adjusted downscaling method for the 21/6/2012 event

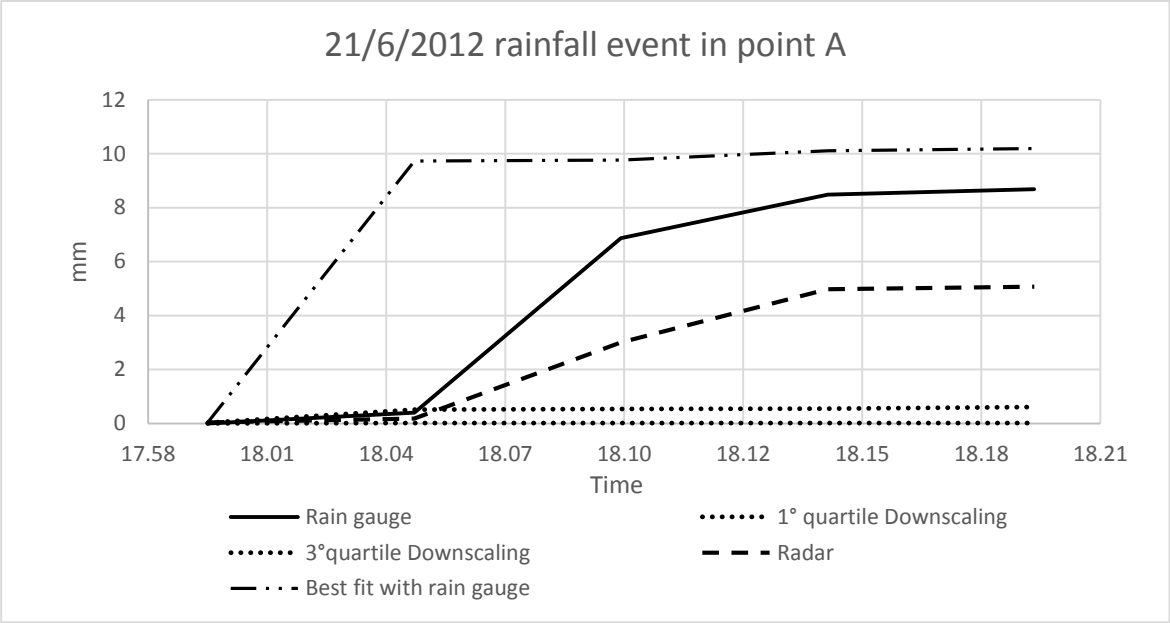

Figure 6.28 Best downscaled values which minimize the error with the rain gauge for the 21/6/2012 event

The downscaled accumulation obtained with the estimated best position, underestimates the rain gauge accumulation for the 21/6/2012 and 22/6/2012, in fact the corresponding points stay under the trendline (figure 6.18). The contrary happens for 6/7/2012 and 7/7/2012 events. Surely, a better trendline could be calculated if more rainfall events are taken into account; in fact it has been plotted, considering just four rainfall events because the 25/8/2012 event has been dismissed. In table 6.5 the rainfall accumulation of the rain gauge and of the downscaling method are reported using the best position of the realization which minimizes the error with the rain gauge(best downscaling method), the best estimated position with the algorithm (best estimated downscaling method) and the 2nd quartile; as consequence their relative percentage on the rain gauge value is shown. The percentages obtained with the improvement of the downscaling method using the algorithm are really better than those ones obtained with the second quartile. A difference of almost about 50% is appreciable.

events	Rain gauge accumulation (mm)	best downscaling method rainfall accumulation (mm)	best estimated downscaling method rainfall accumulation (mm)	2nd quartile rainfall accumulation (mm)	best downscaling method percentage referred to rain gauge estimate	best estimated downscaling method percentage referred to rain gauge estimate	2nd quartile percentage referred to rain gauge estimate
21/6	8,69	10,19	14,17	0,32	117	163	4
7/7	12,12	10,58	5,34	1,23	87	44	10
25/8	8,08	5,70	0,73	0,31	71	9	4
6/7	25,65	25,82	21,68	12,00	101	84	47
22/6	5,05	4,77	5,70	3,09	94	113	61

Table 6.5 Comparison of the cumulative rainfall given by the rain gauge and the downscaling method using the best position of the realization which minimizes the error with the rain gauge(best downscaling method), the best estimated position with the algorithm(best estimated downscaling method) and the 2nd quartile.

6.4 Interpolation methods results

The methodology used to obtain the interpolated values is really questionable because it expects to obtain punctual values starting from areal values(1x1km^2) which are considered as pointed in the centre of the pixels. This procedure is lead in the attempt to improve the spatial rainfall variability and to provide a finer resolution scale. Nonetheless, the results obtained are very poor; indeed, often the interpolated values are really close to the radar estimation of the central pixel in which the rain gauges are located. As for instance, in figure 6.29 the order of magnitude of the interpolation methods compared with the radar and the rain gauge for the point C is reported. The lines are plotted just to better understand the position of the marks. Moreover, the Inverse squared distance weighting interpolation method is dismissed because it gives the same values as the Idw (Inverse distance weighting). Just some small differences are appreciable for the higher intensities and the contrary happens for low intensities in which the marks of the radar and the interpolation methods are all overlapped. Further, it can be seen that for high rainfall intensities the radar values is higher than the interpolated values. This behaviour can be due to the "smooth" process of the interpolation methods which average the rainfall peaks between all the rainfall radar data involved in the calculation. As a consequence, the interpolated field is more variable but, at the same time, the rainfall peaks are mitigated.

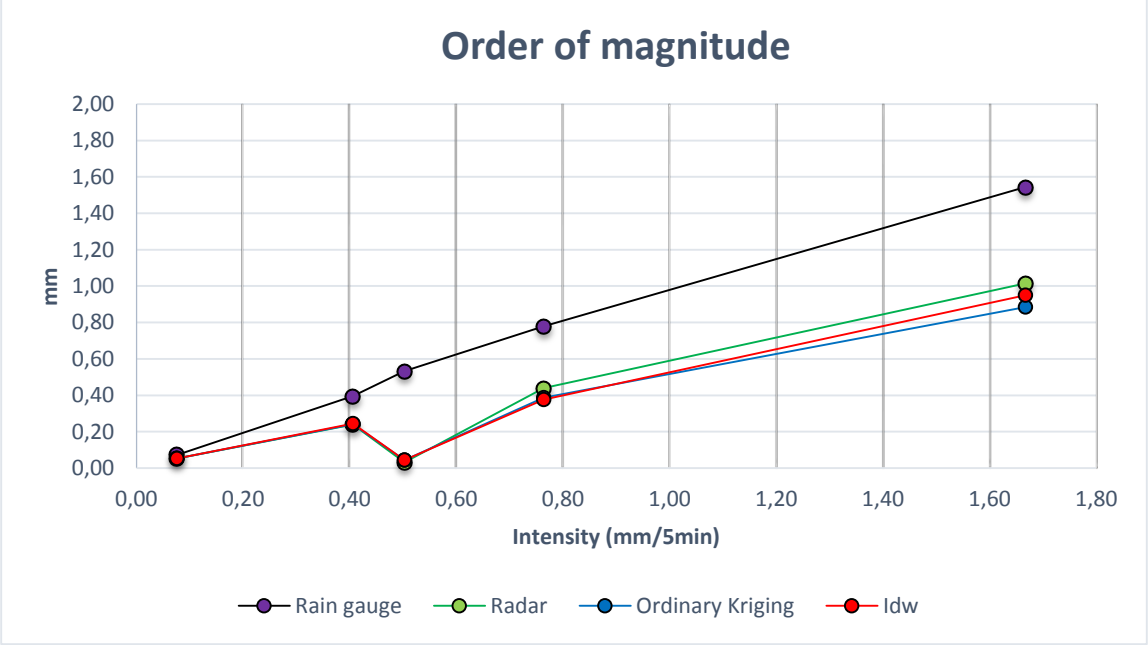

Figure 6.29 Order of magnitude of the Rain gauge, Radar and the Interpolation methods in the point C with rainfall intensity changing

In the next figures the rainfall accumulations of the radar and the interpolation methods in the point C are reported. Also in this case the Inverse squared distance weighting interpolation method is dismissed for the same reason as before. As it is clear in the order of magnitude graph, the values are really close for the 22/6/2012 and 6/7/2012 events in which there is low intensity; on the contrary the differences enhance for the other events with the intensity increasing. Particularly meaningful is the last event 21/6/2012 in which it is appreciable the interpolation method behaviour of "smoothing"; indeed when radar detects low rainfall rate the interpolation methods increase it and the contrary happens for high rainfall rate. This "contrary" effect is reasonable because the high intensity event are also localised so that it is supposed that probably in the neighbouring pixels, it is raining with different intensities. Further in the previous event 7/7/2012 it is curious that in the first rainfall rate the radar value is sensibly over the interpolated value. This is always due to the fact that the interpolation methods "smooth" the rainfall peaks. The rainfall accumulation graphs of points A and I are dismissed because they are really similar to the graphs of point C.

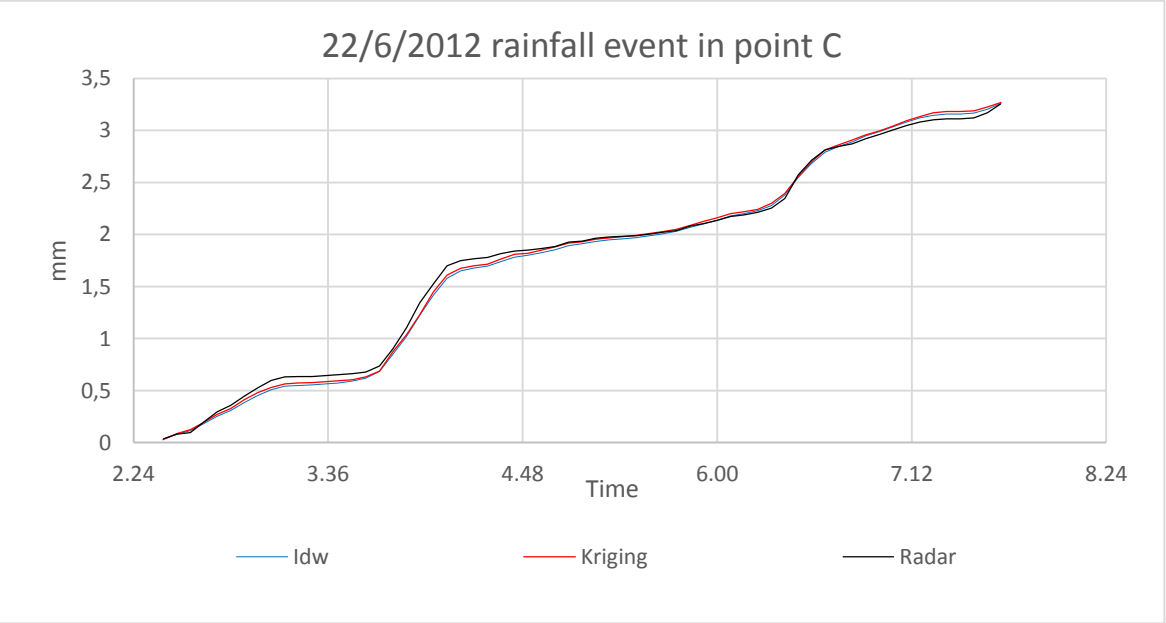

Figure 6.30 Rainfall accumulations obtained with the radar, kriging and idw method in the point C in the 22/6/2012.

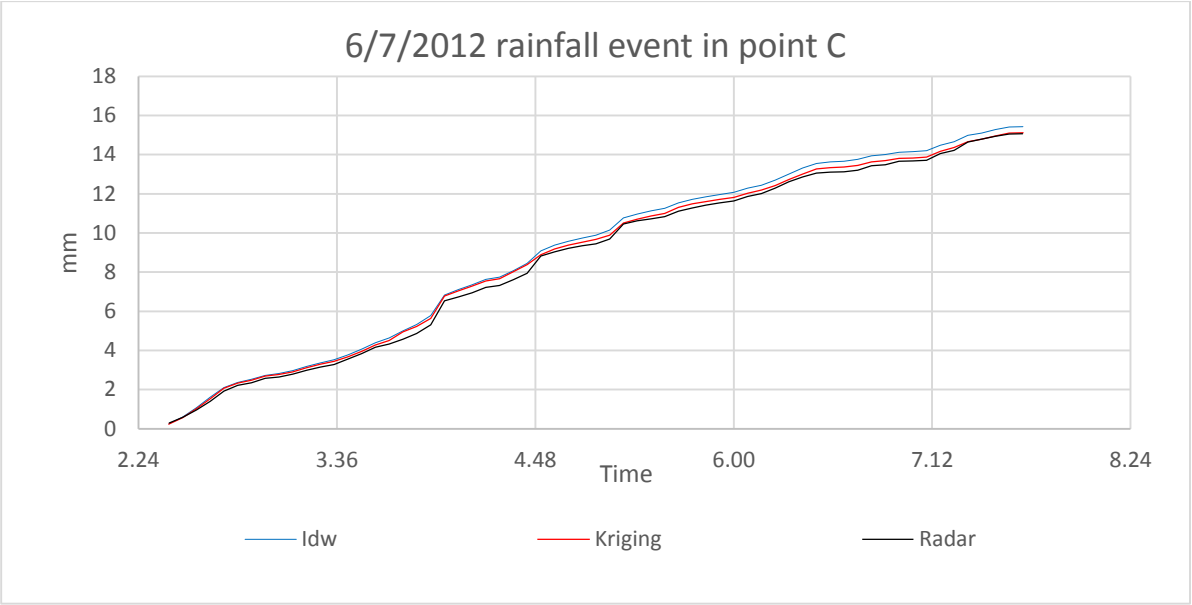

Figure 6.31 Rainfall accumulations obtained with the radar, kriging and idw method in the point C in the 6/7/2012.

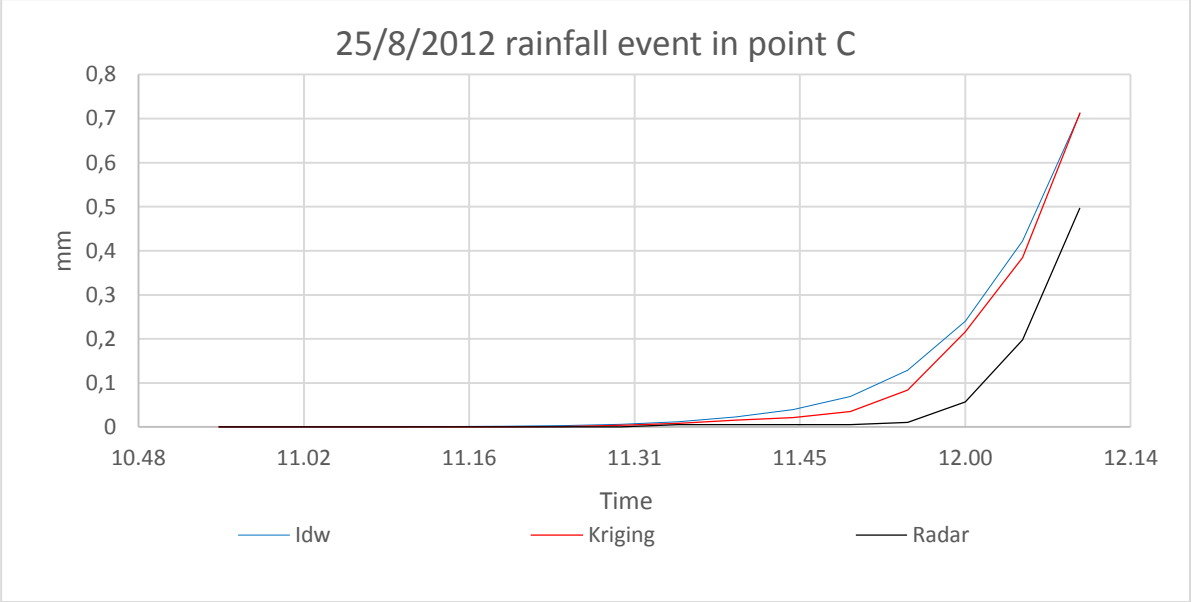

Figure 6.32 Rainfall accumulations obtained with the radar, kriging and idw method in the point C in the 25/8/2012.

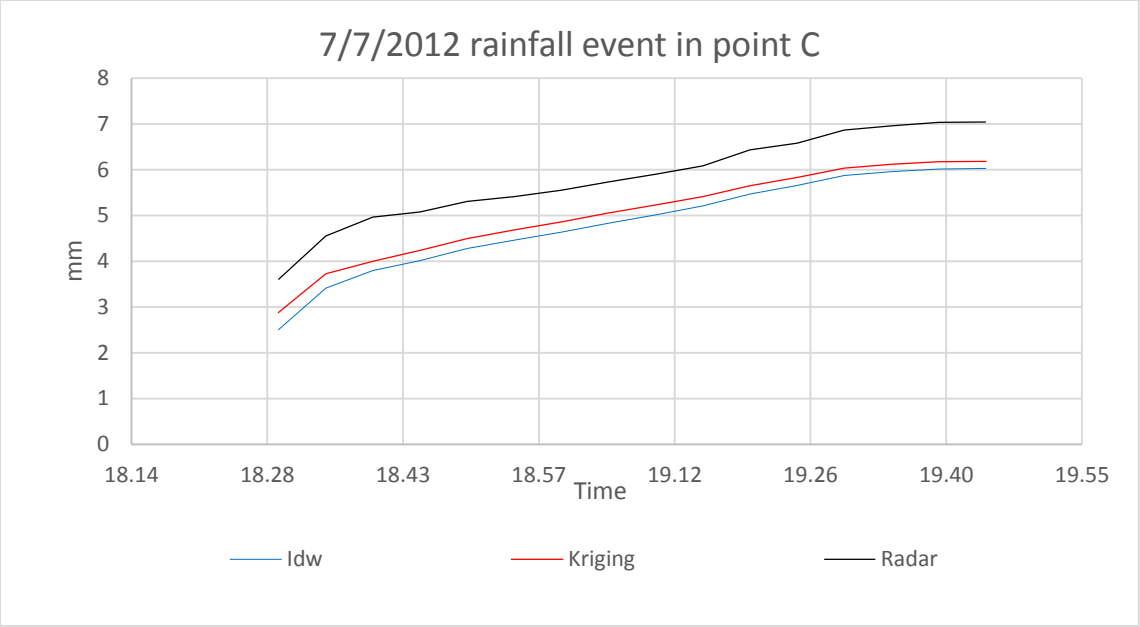

Figure 6.33 Rainfall accumulations obtained with the radar, kriging and idw method in the point C in the 7/7/2012.

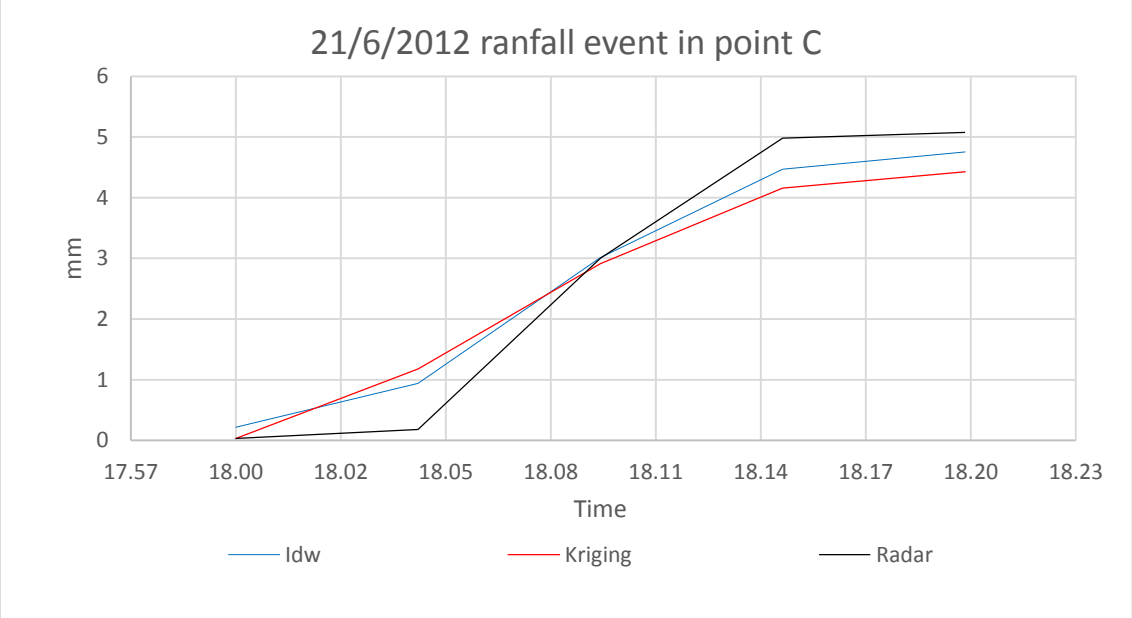

Figure 6.34 Rainfall accumulations obtained with the radar, kriging and idw method in the point C in the 21/6/2012.

6.5 Rainfall spatial variability

In order to understand the capabilities of interpolation methods to capture the rainfall spatial variability, first of all the comparison graphs between the rain gauges in the points A, I, C are analysed (figure 6.35,6.37, 6.39, 6.41, 6.43). Of course, the records of the rain gauges are similar and, as it is expected, the differences increase for higher rainfall intensities. The common feature in all the graphs is that the records in point C are generally different from the other two. This is due to the position of the rain gauge C, which is the furthest from the other two gauges. For instance, in the event 25/8/2012 the rain gauge C records much less rainfall than the other two but suddenly in the 11.35 and 11.40 time steps it reaches and overtakes them. Further, in the event 7/7 at the 18:35 time step in the rain gauge C it has rained 2 mm more than the other two rain gauges; this difference is maintained until the end of the event. Finally, in the last event the rain gauges A and I, have similar accumulation lines differently from the rain gauge C which records 1 mm less at the end of the event. As previously shown in the 6.32 graph, the interpolation methods are too consistent with the values given by the radar pixel in which the rain gauges are located, so that it is difficult to provide appreciable spatial variability; also, their features, to “smooth” the rainfall peaks, don’t help in this sense. The results indicate the only method, which provides little differences between the three points, is the Inverse distance weighting (Idw) and as a consequence also the Inverse squared distance weighting which gives the same results as Idw. On the contrary, the ordinary kriging doesn’t show any spatial variability for any rainfall events analysed. So, in the figures 6.36, 6.48,.6.40, 6.42, 6.44 the accumulations in the three points obtained with the Idw method are plotted. The graphs are located under the rain gauges accumulation so that a comparison in view can be done. Of course regading the 25/8/2012 no comparison can be done because the radar didn’t work properly. For the first and second events the interpolation methods provide values too close for the three points, even if the respective rain gauges show some differences. In the 7/7/2012 event the idw method shows appreciable differences and in particular in point C it has rained less than the other two. If the respective rain gauges accumulation are checked, exactly the contrary happens, so that in this case the idw method failed completely. This could be due to the feature of the interpolation method to ”smooth” the rainfall peaks, as mentioned before. In the last event 21/6/2012, the positions of the three lines obtained with the Idw method is consistent with those ones obtained with the rain gauges. Nevertheless, the differences of the interpolated values are small.

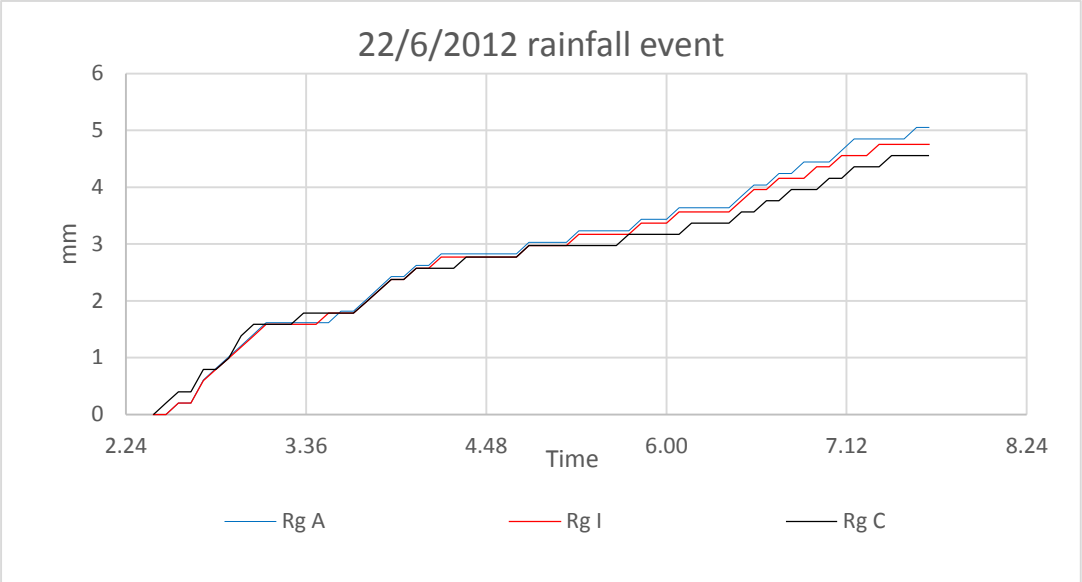

Figure 6.35 Rain gauges accumulations comparison for the 22/6/2012 event.

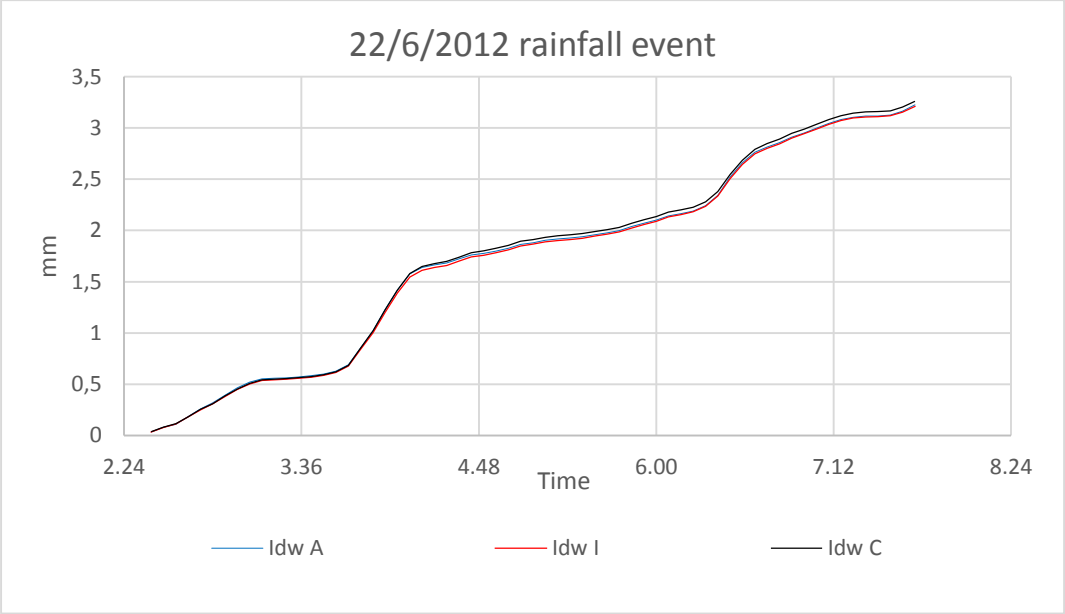

Figure 6.36 Accumulations comparison in the points A,I,C obtained with the Idw method for the 22/6/2012 event.

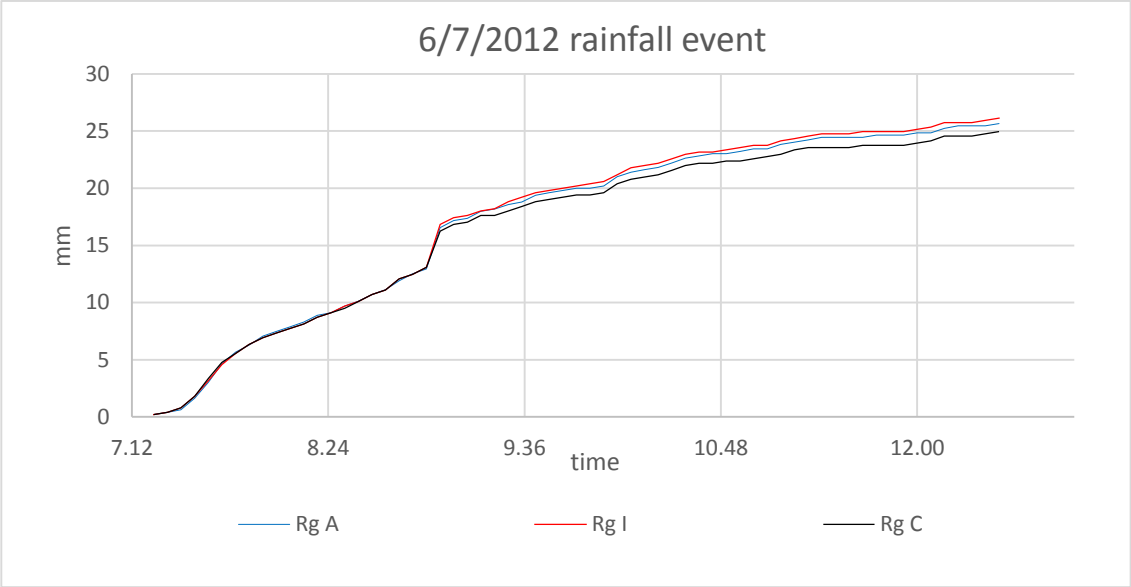

Figure 6.37 Rain gauges accumulations comparison for the 6/7/2012 event

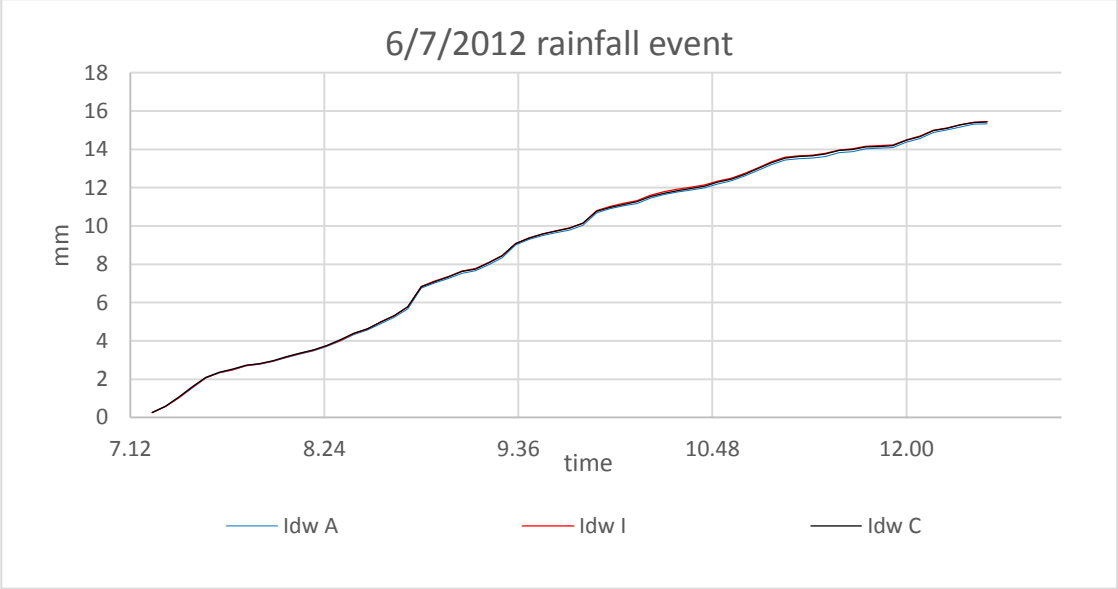

Figure 6.38 Accumulations comparison in the points A,I,C obtained with the Idw method for the 6/7/2012 event

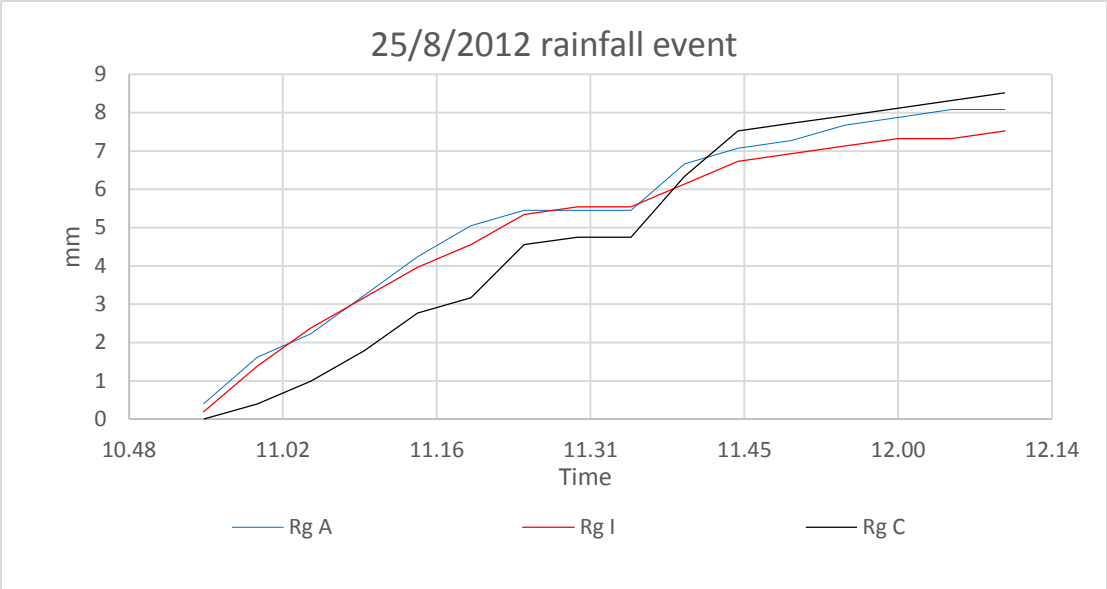

Figure 6.39 Rain gauges accumulations comparison for the 25/8/2012 event

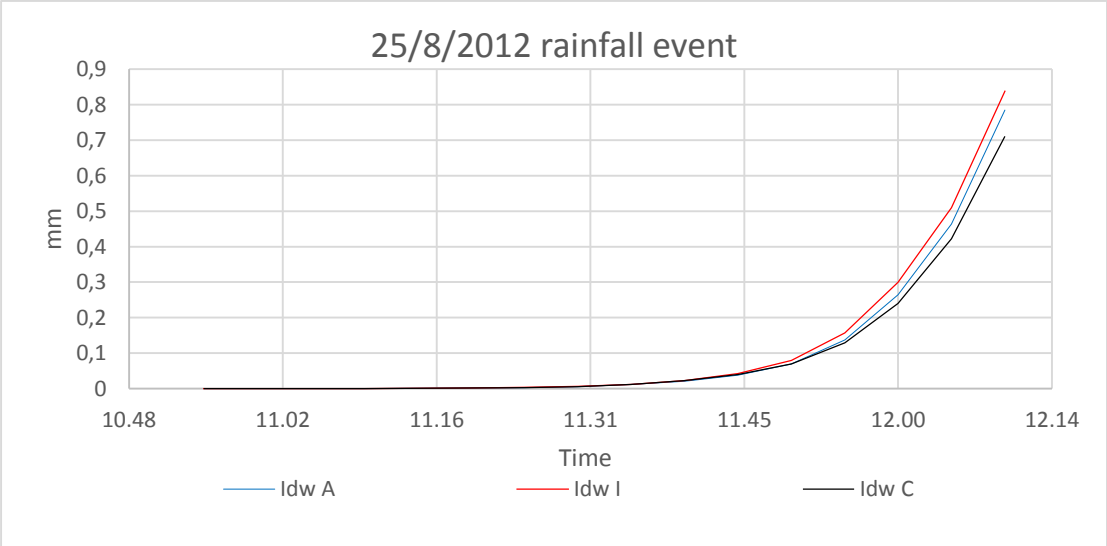

Figure 6.40 Accumulations comparison in the points A,I,C obtained with the Idw method for the 25/8/2012 event.

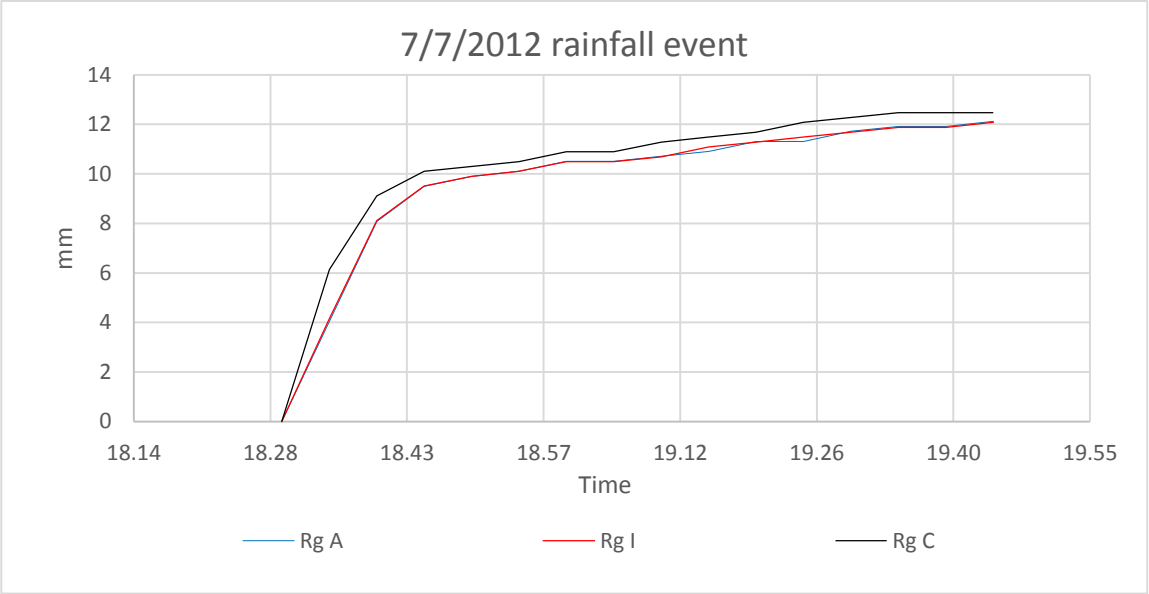

Figure 6.41 Rain gauges accumulations comparison for the 7/7/2012 event.

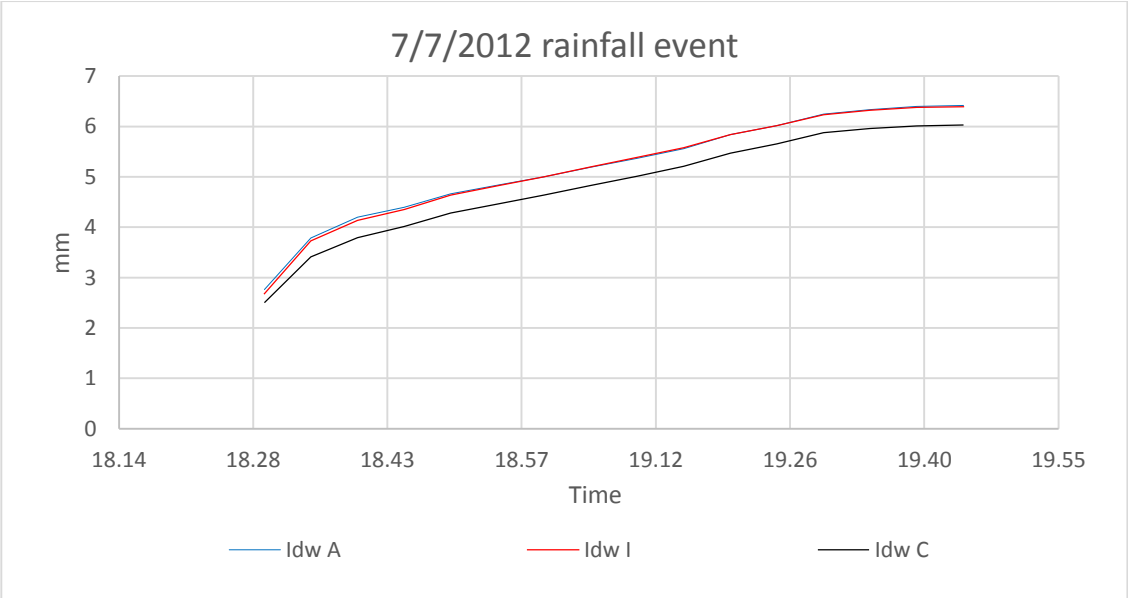

Figure 6.42 Accumulations comparison in the points A,I,C obtained with the Idw method for the 7/7/2012 event.

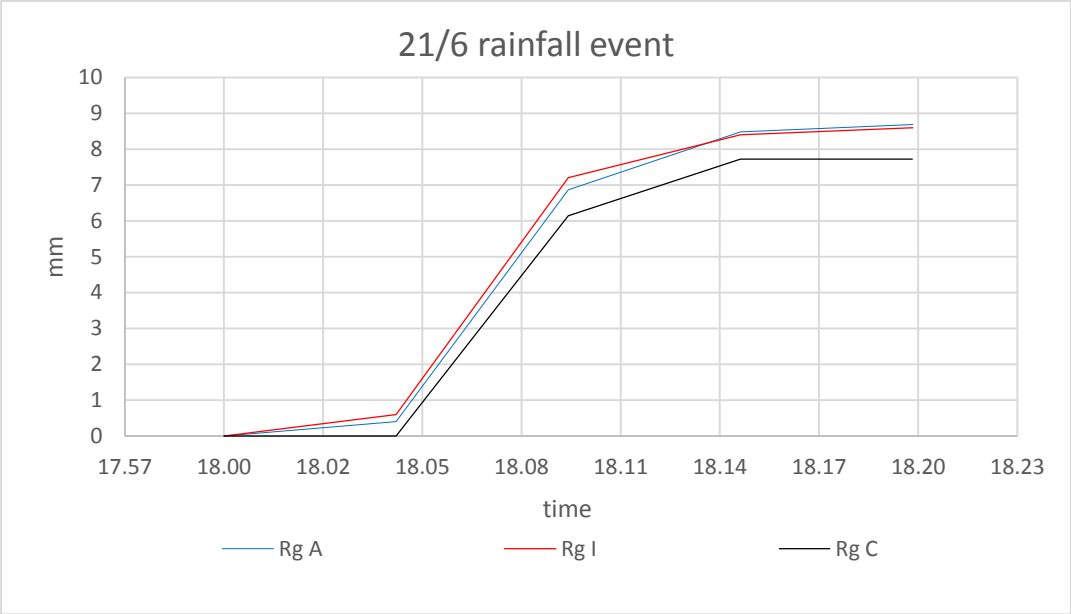

Figure 6.43 Rain gauges accumulations comparison for the 21/6/2012 event.

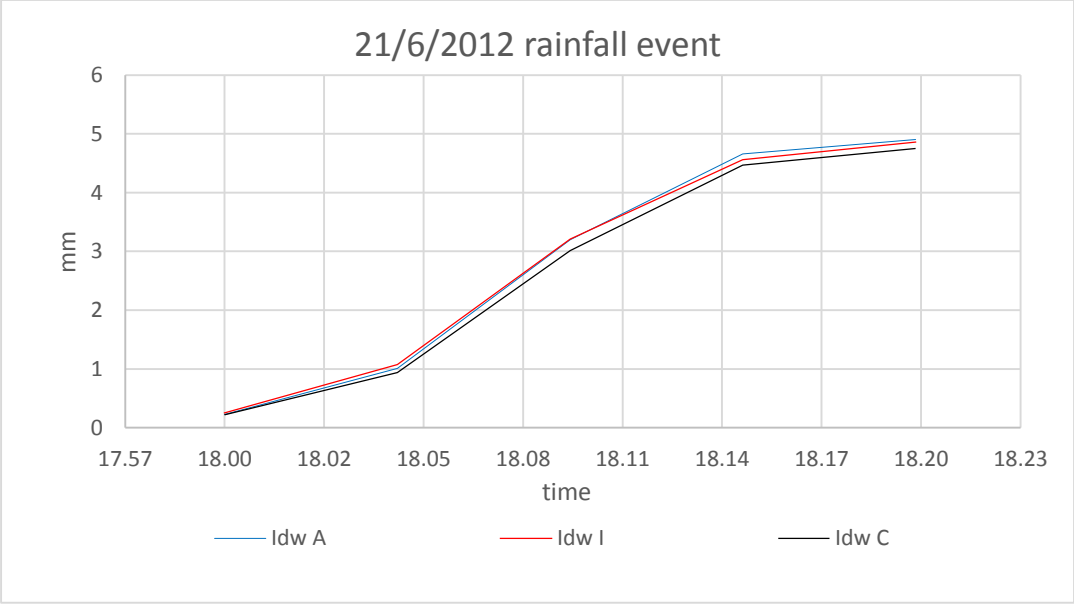

Figure 6.44 Accumulations comparison in the points A,I,C obtained with the Idw method for the 21/6/2012 event.

Chapter 7

Conclusions

The applicability of both the interpolation and downscaling methods is heavily affected by the radar working which systematically underestimates the rain gauge records. The percentage of error committed by the radar is around 40%; anyway this percentage is proved to change according to the rainfall intensity and accumulation changing (table 6.1 and 6.2 respectively). In particular the radar tends to worsen for high intensity rainfall events (figure 6.4) and for important accumulation (figure 6.6).

The downscaling method presents good performance for low rainfall intensities in which it is able to be really consistent with the radar values (figure 6.7 and figure 6.8). For these events, the wrong estimations with the rain gauge are due to the radar deficiency which for these rainfall intensities commits an error percentage around 35%. For higher rainfall intensities (figures 6.10 and 6.11), the downscaling method is also not consistent with the radar values; it entails that, in this case, the wrong estimations with the rain gauge are due to both the radar deficiency(which increases until 41% for higher intensities) and an intrinsic method limit. Considering all the rainfall events, at the end, the downscaling method always underestimates the rain gauge values; as shown in figure n°6.12 the order magnitude is respected for lower rainfall intensity events; the contrary happens for higher intensities. Further, the 25/8/2012 rainfall event (figure 6.9), shows the downscaling method is strictly dependent on the radar working.

A downscaling method adjustment is proposed in order to improve the estimations based on the application of an algorithm; this is able to provide an estimation of the best position of the downscaled realizations, which minimize the errors with the rain gauge records according to the radar intensity. The latter is the only possible parameter to obtain in advance, in order to improve the downscaled estimations for forecasting. The method provides really appreciable results (table 6.4); The percentage

of improvement of the adjusted downscaled value on the value of the 2nd quartile is almost about 50%.

The interpolation methods present values really close to the radar estimations of the pixel in which the rain gauges are located (figure 6.29). Little differences can be appreciated for higher rainfall intensity event. Nonetheless a “smoothing” process of the interpolation methods occurs so that the rainfall peaks are mitigated. This is the contrary effect that this research is looking to reach because even if the interpolated field is more variable, at the same time, it misses the high rainfall peaks. The ordinary Kriging provides the same estimation for all the three points considered so that no spatial variability is observed. On the contrary, the Inverse distance weighting (Idw) and the Inverse squared distance weighting interpolation methods, which give the same results, can provide small spatial variability in particular for higher rainfall intensities. Nevertheless, the “smoothing” process and the consistency with the value of the central pixel in which rain gauges are located, don’t permit appreciable results.

Finally, the comparison between the interpolated and downscaled values is not discussed in this thesis; as the first is too consistent with the radar and only little differences are appreciable, whereas the second is too variable according to all the realizations, which the stochastic downscaling method produces based upon the scale invariant properties of rainfall.

Bibliography

Wang, L., 2012, Improved Rainfall Downscaling for Real-Time Urban Pluvial Flood Forecasting, PhD Thesis, Imperial College London;

EA, 2007. Review of 2007 summer floods. Tech. rep., Environment Agency;

Parker, D. J., Priest, S. J., McCarthy, S. S., 2011. Surface water flood warnings require- ments and potential in England and Wales. Applied Geography;

Fabry, F., Bellon, A., Duncan, M. R., Austin, G. L., 1994. High resolution rainfall mea- surements by radar for very small basins: the sampling problem reexamined. Journal of Hydrology;

International association for hydro-environment engineering and research, Hidrolink, Number 2/2012;

A. Gires, I. Tchiguirinskaia, D. Schertzer, S. Lovejoy, A. Schellart, Definition and implementation of innovative comparison tools between radar and rain gauge rainfall measurements;

A. Schellart, W.J. Shepherdb, A.J. Saulb, Influence of rainfall estimation error and spatial variability on sewer flow prediction at a small urban scale;

Wang, L., Maksimovi´c, C., Onof, C., 2009b. A semi-deterministic multiplicative cascade method for sub-daily rainfall forecast. In: Molnar, P., Burlando, P., Einfalt, T. (Eds.), Proceedings of the 8th International Workshop on Precipitation in Urban Areas. St. Moritz, Switzerland;

Lovejoy, S., Mandelbrot, B. B., 1985. Fractal properties of rain, and a fractal model;

Lovejoy, S., Schertzer, D., 1990. Multifractals, universality classes and satellite and radar measurements of cloud and rain fields. Journal of Geophysical Research;

Mandelbrot, B. B., 1983. The Fractal Geometry of Nature. W. H. Freeman and Company, New York;

Mandelbrot, B. B., Evertsz, C. J. G., Hayakawa, Y., 1990. Exactly self-similar left-sided multifractal measures;

Olsson, J., 1995. Limits and characteristics of the multifractal behaviour of a high- resolution rainfall time series. Nonlinear Process in Geophysics;

Lovejoy, S., Mandelbrot, B. B., 1985. Fractal properties of rain, and a fractal model;

Wang, L., 2005. Applications of multifractals to rainfall forecast. Master's thesis, National Taiwan University;

Wang, L., Onof, C., Maksimovi´c, C., 2010. Analysis of high-resolution spatiotemporal structures of mesoscale rainfields based upon the theory of left-sided multifractals. In: American Geophysics Union (AGU) Fall Meeting 2010;

Todini, E., 2001a. Influence of parameter estimation uncertainty in kriging: Part 1 - theoretical development. Hydrol. Earth System;

Parker, D. J., Priest, S. J., McCarthy, S. S., 2011. Surface water flood warnings require- ments and potential in England and Wales. Applied Geography 31;

EA, 2009. Flooding in England: A national assessment of flood risk. Tech. rep., Environ- ment Agency;

Appendix

In this appendix are reported the data obtained with the rain gauges, radar, interpolation and downscaling methods. As explained in the chapter n°6, the Inverse squared distance weighting interpolation method is dismissed because it provides the same values given by the Inverse distance weighting. Firstly the values in the point A are reported and consequently in the points I and C for each event(the deployment of the three points is shown in the figure 2.1) . For each points two tables are reported: the first is the rainfall rate every 5 minutes and the second is the accumulation. The order of the rainfall events follow the table2.1.

21/6/2012 event

Rainfall rate(mm/5min) in point A , 21/6/2012 rainfall event

time	Rg	Pixel	Krig.	IDW	Dow. min.	Dow.1°q.	Dow.2°q.	Dow. Ave.	Dow.3°q.	Dow. max.
18.00	0,00E+00	3,13E-02	3,46E-02	2,25E-01	2,91E-08	1,65E-04	9,36E-03	2,74E-01	2,79E-02	2,82E+00
18.05	4,04E-01	1,51E-01	1,14E+00	7,80E-01	3,89E-06	7,04E-03	2,89E-01	3,17E+00	4,77E-01	1,90E+01
18.10	6,46E+00	2,82E+00	1,74E+00	2,19E+00	9,53E-07	8,01E-04	2,03E-02	1,43E-01	3,22E-02	8,27E-01
18.15	1,62E+00	1,98E+00	1,24E+00	1,46E+00	9,38E-09	6,22E-05	4,16E-03	1,33E-01	9,48E-03	1,44E+00
18.20	2,02E-01	9,38E-02	2,67E-01	2,44E-01	4,50E-09	3,66E-05	2,32E-03	7,87E-02	5,88E-02	1,08E+00

time	Rg	Pixel	Krig.	IDW	Dow. min.	Dow.1°q.	Dow.2°q.	Dow. Ave.	Dow.3°q.	Dow. max.
18.00	0,00E+00	3,13E-02	3,46E-02	2,25E-01	2,91E-08	1,65E-04	9,36E-03	2,74E-01	2,79E-02	2,82E+00
18.05	4,04E-01	1,82E-01	1,17E+00	1,01E+00	3,92E-06	7,21E-03	2,98E-01	3,45E+00	5,05E-01	2,18E+01
18.10	6,87E+00	3,00E+00	2,91E+00	3,20E+00	4,87E-06	8,01E-03	3,18E-01	3,59E+00	5,38E-01	2,26E+01
18.15	8,48E+00	4,98E+00	4,16E+00	4,66E+00	4,88E-06	8,07E-03	3,22E-01	3,72E+00	5,47E-01	2,41E+01
18.20	8,69E+00	5,07E+00	4,42E+00	4,90E+00	4,89E-06	8,11E-03	3,25E-01	3,80E+00	6,06E-01	2,52E+01

Rainfall accumulation(mm) in point A, 21/6/2012 rainfall event

Rainfall rate(mm/5min) in point I, 21/6/2012 rainfall event

time	Rg	Pixel	Krig.	IDW	Dow. min.	Dow.1°q.	Dow.2°q.	Dow. Ave.	Dow.3°q.	Dow. max.
18.00	0,00E+00	3,13E-02	3,46E-02	2,48E-01	2,94E-08	1,64E-04	1,61E-02	4,47E-01	9,15E-01	2,77E+00
18.05	6,00E-01	1,51E-01	1,14E+00	8,27E-01	1,01E-07	7,50E-03	2,71E-01	3,15E+00	3,70E-01	1,90E+01
18.10	6,60E+00	2,82E+00	1,74E+00	2,13E+00	1,19E-06	7,91E-04	1,63E-02	1,22E-01	2,58E-02	8,38E-01
18.15	1,20E+00	1,98E+00	1,24E+00	1,35E+00	5,98E-07	6,22E-05	4,92E-03	1,46E-01	3,49E-01	1,10E+00
18.20	2,00E-01	9,38E-02	2,67E-01	2,99E-01	8,66E-09	1,87E-05	1,19E-03	5,35E-02	4,50E-03	1,10E+00

Rainfall accumulation(mm) in point I (mm) , 21/6/2012 rainfall event

time	Rg	Pixel	Krig.	IDW	Dow. min.	Dow.1°q.	Dow.2°q.	Dow. Ave.	Dow.3°q.	Dow. max.
18.00	0,00E+00	3,13E-02	3,46E-02	2,48E-01	2,94E-08	1,64E-04	1,61E-02	4,47E-01	9,15E-01	2,77E+00
18.05	6,00E-01	1,82E-01	1,17E+00	1,08E+00	1,30E-07	7,66E-03	2,87E-01	3,60E+00	1,28E+00	2,18E+01
18.10	7,20E+00	3,00E+00	2,91E+00	3,21E+00	1,32E-06	8,45E-03	3,03E-01	3,72E+00	1,31E+00	2,26E+01
18.15	8,40E+00	4,98E+00	4,16E+00	4,56E+00	1,91E-06	8,52E-03	3,08E-01	3,87E+00	1,66E+00	2,37E+01
18.20	8,60E+00	5,07E+00	4,42E+00	4,86E+00	1,92E-06	8,53E-03	3,10E-01	3,92E+00	1,66E+00	2,48E+01

Rainfall rate(mm/5min) in point C , 21/6/2012 rainfall event

time	Rg	Pixel	Krig.	IDW	Dow. min.	Dow.1°q.	Dow.2°q.	Dow. Ave.	Dow.3°q.	Dow. max.
18.00	0,00E+00	3,13E-02	3,46E-02	2,18E-01	1,69E-08	1,65E-04	9,40E-03	4,47E-01	4,03E-01	2,79E+00
18.05	0,00E+00	1,51E-01	1,14E+00	7,21E-01	4,75E-06	7,50E-03	2,89E-01	3,15E+00	7,39E+00	1,76E+01
18.10	6,14E+00	2,82E+00	1,74E+00	2,07E+00	9,41E-07	7,91E-04	1,66E-02	1,22E-01	2,59E-02	1,04E+00
18.15	1,58E+00	1,98E+00	1,24E+00	1,46E+00	8,43E-09	6,40E-05	4,92E-03	1,46E-01	1,03E-02	1,10E+00
18.20	0,00E+00	9,38E-02	2,67E-01	2,83E-01	2,88E-07	3,62E-05	2,30E-03	5,35E-02	1,47E-01	5,71E-01

Rainfall accumulation(mm) in point C , 21/6/2012 rainfall event

time	Rg	Pixel	Krig.	IDW	Dow. min.	Dow.1°q.	Dow.2°q.	Dow. Ave.	Dow.3°q.	Dow. max.
18.00	0,00E+00	3,13E-02	3,46E-02	2,18E-01	1,69E-08	1,65E-04	9,40E-03	4,47E-01	4,03E-01	2,79E+00
18.05	0,00E+00	1,82E-01	1,17E+00	9,39E-01	4,77E-06	7,66E-03	2,98E-01	3,60E+00	7,80E+00	2,04E+01
18.10	6,14E+00	3,00E+00	2,91E+00	3,01E+00	5,71E-06	8,45E-03	3,15E-01	3,72E+00	7,82E+00	2,15E+01
18.15	7,72E+00	4,98E+00	4,16E+00	4,47E+00	5,72E-06	8,52E-03	3,20E-01	3,87E+00	7,83E+00	2,26E+01
18.20	7,72E+00	5,07E+00	4,42E+00	4,75E+00	6,00E-06	8,55E-03	3,22E-01	3,92E+00	7,98E+00	2,31E+01

7/7/2012 event

Rainfall rate(mm/5min) in point A, 7/7/2012 rainfall event

time	Rg	Pixel	Krig.	IDW	Dow. min.	Dow.1°q.	Dow.2°q.	Dow. Ave.	Dow.3°q.	Dow. max.
18.30	0,00E+00	3,60E+00	2,88E+00	2,76E+00	1,40E-06	1,36E-03	8,85E-03	6,66E-02	2,77E-02	9,08E-01
18.35	4,04E+00	9,53E-01	8,49E-01	1,03E+00	1,43E-04	7,18E-03	2,49E-02	9,48E-02	6,85E-02	1,08E+00
18.40	4,04E+00	4,14E-01	2,71E-01	4,12E-01	2,53E-03	2,78E-02	7,37E-02	1,89E-01	2,17E-01	1,25E+00
18.45	1,41E+00	1,09E-01	2,39E-01	1,97E-01	1,66E-03	1,25E-02	2,59E-02	5,20E-02	5,70E-02	3,29E-01
18.50	4,04E-01	2,34E-01	2,60E-01	2,66E-01	1,39E-02	2,71E-02	4,81E-02	7,21E-02	1,01E-01	5,24E-01
18.55	2,02E-01	1,02E-01	1,91E-01	1,70E-01	1,51E-02	4,88E-02	8,43E-02	1,22E-01	1,56E-01	7,07E-01
19.00	4,04E-01	1,38E-01	1,70E-01	1,65E-01	2,26E-02	4,44E-02	4,61E-02	6,69E-02	8,87E-02	3,28E-01
19.05	0,00E+00	1,88E-01	1,95E-01	1,89E-01	1,07E-02	2,80E-02	4,61E-02	5,63E-02	7,57E-02	1,87E-01
19.10	2,02E-01	1,64E-01	1,75E-01	1,83E-01	3,28E-03	1,58E-02	3,00E-02	4,37E-02	6,27E-02	1,72E-01
19.15	2,02E-01	1,80E-01	1,81E-01	1,86E-01	1,82E-03	2,73E-02	9,36E-02	1,49E-01	2,84E-01	8,80E-01
19.20	4,04E-01	3,54E-01	2,43E-01	2,84E-01	9,45E-03	8,18E-02	2,39E-01	3,09E-01	6,97E-01	7,27E-01
19.25	0,00E+00	1,46E-01	1,83E-01	1,75E-01	1,94E-03	3,35E-02	1,37E-01	1,98E-01	1,45E-01	6,08E-01
19.30	4,04E-01	2,89E-01	1,98E-01	2,30E-01	2,41E-03	5,95E-02	2,94E-01	4,71E-01	3,01E-01	1,51E+00
19.35	2,02E-01	8,59E-02	8,28E-02	8,90E-02	2,01E-04	1,15E-02	7,81E-02	1,81E-01	1,18E-01	1,21E+00
19.40	0,00E+00	7,81E-02	5,68E-02	6,25E-02	5,26E-09	5,78E-05	2,52E-03	2,11E-01	1,36E-01	5,05E+00
19.45	2,02E-01	7,81E-03	7,03E-03	1,75E-02	2,97E-10	3,29E-06	9,19E-05	3,79E-03	5,57E-04	8,03E-02

Rainfall accumulation(mm) in point A , 7/7/2012 rainfall event

time	Rg	Pixel	Krig.	IDW	Dow. min.	Dow.1°q.	Dow.2°q.	Dow. Ave.	Dow.3°q.	Dow. max.
18.30	0,00E+00	3,60E+00	2,88E+00	2,76E+00	1,40E-06	1,36E-03	8,85E-03	6,66E-02	2,77E-02	9,08E-01
18.35	4,04E+00	4,55E+00	3,73E+00	3,79E+00	1,45E-04	8,54E-03	3,38E-02	1,61E-01	9,62E-02	1,99E+00
18.40	8,08E+00	4,97E+00	4,00E+00	4,20E+00	2,67E-03	3,63E-02	1,08E-01	3,50E-01	3,13E-01	3,24E+00
18.45	9,49E+00	5,08E+00	4,24E+00	4,40E+00	4,33E-03	4,89E-02	1,33E-01	4,02E-01	3,70E-01	3,57E+00
18.50	9,90E+00	5,31E+00	4,50E+00	4,66E+00	1,82E-02	7,60E-02	1,82E-01	4,75E-01	4,71E-01	4,09E+00
18.55	1,01E+01	5,41E+00	4,69E+00	4,83E+00	3,33E-02	1,25E-01	2,66E-01	5,97E-01	6,27E-01	4,80E+00
19.00	1,05E+01	5,55E+00	4,86E+00	5,00E+00	5,60E-02	1,69E-01	3,12E-01	6,63E-01	7,16E-01	5,13E+00
19.05	1,05E+01	5,74E+00	5,05E+00	5,19E+00	6,67E-02	1,97E-01	3,58E-01	7,20E-01	7,91E-01	5,32E+00
19.10	1,07E+01	5,90E+00	5,23E+00	5,37E+00	7,00E-02	2,13E-01	3,88E-01	7,63E-01	8,54E-01	5,49E+00
19.15	1,09E+01	6,08E+00	5,41E+00	5,56E+00	7,18E-02	2,40E-01	4,82E-01	9,13E-01	1,14E+00	6,37E+00
19.20	1,13E+01	6,43E+00	5,65E+00	5,84E+00	8,12E-02	3,22E-01	7,21E-01	1,22E+00	1,83E+00	7,10E+00
19.25	1,13E+01	6,58E+00	5,83E+00	6,02E+00	8,32E-02	3,55E-01	8,58E-01	1,42E+00	1,98E+00	7,70E+00
19.30	1,17E+01	6,87E+00	6,03E+00	6,25E+00	8,56E-02	4,15E-01	1,15E+00	1,89E+00	2,28E+00	9,21E+00
19.35	1,19E+01	6,96E+00	6,12E+00	6,34E+00	8,58E-02	4,26E-01	1,23E+00	2,07E+00	2,40E+00	1,04E+01
19.40	1,19E+01	7,03E+00	6,17E+00	6,40E+00	8,58E-02	4,27E-01	1,23E+00	2,28E+00	2,53E+00	1,55E+01
19.45	1,21E+01	7,04E+00	6,18E+00	6,42E+00	8,58E-02	4,27E-01	1,23E+00	2,29E+00	2,54E+00	1,56E+01

Rainfall rate(mm/5min) in point I, 7/7/2012 rainfall event

time	Rg	Pixel	Krig.	IDW	Dow. min.	Dow.1°q.	Dow.2°q.	Dow. Ave.	Dow.3°q.	Dow. max.
18.30	0,00E+00	3,60E+00	2,88E+00	2,68E+00	1,40E-06	1,36E-03	1,27E-02	1,27E-01	9,61E-02	2,59E+00
18.35	4,16E+00	9,53E-01	8,49E-01	1,05E+00	8,00E-04	7,18E-03	2,46E-02	1,07E-01	1,24E-01	6,53E-01
18.40	3,96E+00	4,14E-01	2,71E-01	4,05E-01	5,43E-03	3,66E-02	1,27E-01	2,03E-01	2,53E-01	1,25E+00
18.45	1,39E+00	1,09E-01	2,39E-01	2,20E-01	2,86E-03	1,24E-02	2,13E-02	4,55E-02	5,79E-02	3,29E-01
18.50	3,96E-01	2,34E-01	2,60E-01	2,83E-01	1,64E-02	3,91E-02	4,81E-02	8,76E-02	1,16E-01	5,45E-01
18.55	1,98E-01	1,02E-01	1,91E-01	1,85E-01	2,13E-02	4,63E-02	8,43E-02	1,03E-01	1,25E-01	3,81E-01
19.00	3,96E-01	1,38E-01	1,70E-01	1,80E-01	2,31E-02	4,46E-02	4,61E-02	6,85E-02	8,87E-02	3,34E-01
19.05	0,00E+00	1,88E-01	1,95E-01	1,95E-01	3,94E-03	2,75E-02	4,58E-02	5,75E-02	7,67E-02	2,87E-01
19.10	1,98E-01	1,64E-01	1,75E-01	1,93E-01	1,43E-03	1,09E-02	2,74E-02	3,71E-02	6,23E-02	1,20E-01
19.15	3,96E-01	1,80E-01	1,81E-01	1,88E-01	1,87E-03	2,73E-02	9,36E-02	1,34E-01	2,19E-01	6,89E-01
19.20	1,98E-01	3,54E-01	2,43E-01	2,61E-01	9,45E-03	8,18E-02	2,39E-01	3,22E-01	6,97E-01	7,36E-01
19.25	1,98E-01	1,46E-01	1,83E-01	1,78E-01	1,94E-03	3,35E-02	1,34E-01	1,62E-01	1,41E-01	5,93E-01
19.30	1,98E-01	2,89E-01	1,98E-01	2,16E-01	1,18E-02	5,95E-02	2,94E-01	5,14E-01	1,45E+00	1,51E+00
19.35	1,98E-01	8,59E-02	8,28E-02	8,62E-02	2,06E-04	1,18E-02	8,02E-02	2,13E-01	4,79E-01	9,83E-01
19.40	0,00E+00	7,81E-02	5,68E-02	5,55E-02	5,26E-09	4,27E-05	1,01E-03	6,81E-02	5,98E-03	2,09E+00
19.45	1,98E-01	7,81E-03	7,03E-03	1,86E-02	2,97E-10	4,71E-06	2,02E-04	5,56E-03	2,12E-03	5,22E-02

Rainfall accumulation(mm) in point I , 7/7/2012 rainfall event

time	Rg	Pixel	Krig.	IDW	Dow. min.	Dow.1°q.	Dow.2°q.	Dow. Ave.	Dow.3°q.	Dow. max.
18.30	0,00E+00	3,60E+00	2,88E+00	2,68E+00	1,40E-06	1,36E-03	1,27E-02	1,27E-01	9,61E-02	2,59E+00
18.35	4,16E+00	4,55E+00	3,73E+00	3,73E+00	8,02E-04	8,54E-03	3,73E-02	2,33E-01	2,20E-01	3,24E+00
18.40	8,12E+00	4,97E+00	4,00E+00	4,13E+00	6,23E-03	4,51E-02	1,64E-01	4,37E-01	4,73E-01	4,49E+00
18.45	9,50E+00	5,08E+00	4,24E+00	4,35E+00	9,09E-03	5,75E-02	1,85E-01	4,82E-01	5,31E-01	4,82E+00
18.50	9,90E+00	5,31E+00	4,50E+00	4,64E+00	2,55E-02	9,67E-02	2,33E-01	5,70E-01	6,46E-01	5,36E+00
18.55	1,01E+01	5,41E+00	4,69E+00	4,82E+00	4,68E-02	1,43E-01	3,18E-01	6,73E-01	7,71E-01	5,75E+00
19.00	1,05E+01	5,55E+00	4,86E+00	5,00E+00	6,99E-02	1,88E-01	3,64E-01	7,41E-01	8,60E-01	6,08E+00
19.05	1,05E+01	5,74E+00	5,05E+00	5,20E+00	7,38E-02	2,15E-01	4,10E-01	7,99E-01	9,37E-01	6,37E+00
19.10	1,07E+01	5,90E+00	5,23E+00	5,39E+00	7,53E-02	2,26E-01	4,37E-01	8,36E-01	9,99E-01	6,49E+00
19.15	1,11E+01	6,08E+00	5,41E+00	5,58E+00	7,71E-02	2,53E-01	5,31E-01	9,70E-01	1,22E+00	7,18E+00
19.20	1,13E+01	6,43E+00	5,65E+00	5,84E+00	8,66E-02	3,35E-01	7,70E-01	1,29E+00	1,91E+00	7,91E+00
19.25	1,15E+01	6,58E+00	5,83E+00	6,02E+00	8,85E-02	3,68E-01	9,04E-01	1,45E+00	2,06E+00	8,51E+00
19.30	1,17E+01	6,87E+00	6,03E+00	6,23E+00	1,00E-01	4,28E-01	1,20E+00	1,97E+00	3,51E+00	1,00E+01
19.35	1,19E+01	6,96E+00	6,12E+00	6,32E+00	1,00E-01	4,40E-01	1,28E+00	2,18E+00	3,99E+00	1,10E+01
19.40	1,19E+01	7,03E+00	6,17E+00	6,38E+00	1,00E-01	4,40E-01	1,28E+00	2,25E+00	3,99E+00	1,31E+01
19.45	1,21E+01	7,04E+00	6,18E+00	6,40E+00	1,00E-01	4,40E-01	1,28E+00	2,25E+00	3,99E+00	1,31E+01

Rainfall rate(mm/5min) in point C, 7/7/2012 rainfall event

time	Rg	Pixel	Krig.	IDW	Dow. min.	Dow.1°q.	Dow.2°q.	Dow. Ave.	Dow.3°q.	Dow. max.
18.30	0,00E+00	3,60E+00	2,88E+00	2,50E+00	3,98E-06	7,70E-04	1,27E-02	1,27E-01	7,90E-02	1,46E+00
18.35	6,14E+00	9,53E-01	8,49E-01	9,14E-01	1,48E-04	7,24E-03	4,01E-02	1,07E-01	1,13E-01	1,08E+00
18.40	2,97E+00	4,14E-01	2,71E-01	3,82E-01	2,00E-03	4,50E-02	1,18E-01	2,03E-01	2,42E-01	8,58E-01
18.45	9,90E-01	1,09E-01	2,39E-01	2,21E-01	3,75E-03	1,62E-02	3,40E-02	4,55E-02	7,12E-02	3,51E-01
18.50	1,98E-01	2,34E-01	2,60E-01	2,67E-01	1,45E-02	2,61E-02	4,45E-02	8,76E-02	9,49E-02	2,50E-01
18.55	1,98E-01	1,02E-01	1,91E-01	1,79E-01	1,51E-02	5,67E-02	9,04E-02	1,03E-01	1,65E-01	7,58E-01
19.00	3,96E-01	1,38E-01	1,70E-01	1,75E-01	2,31E-02	4,52E-02	4,61E-02	6,85E-02	8,87E-02	1,74E-01
19.05	0,00E+00	1,88E-01	1,95E-01	1,93E-01	6,50E-03	2,93E-02	4,65E-02	5,75E-02	7,82E-02	2,87E-01
19.10	3,96E-01	1,64E-01	1,75E-01	1,85E-01	1,43E-03	1,09E-02	2,74E-02	3,71E-02	5,25E-02	1,72E-01
19.15	1,98E-01	1,80E-01	1,81E-01	1,94E-01	5,45E-04	2,73E-02	9,10E-02	1,34E-01	2,01E-01	5,39E-01
19.20	1,98E-01	3,54E-01	2,43E-01	2,62E-01	2,76E-02	8,18E-02	2,39E-01	3,22E-01	2,42E-01	7,27E-01
19.25	3,96E-01	1,46E-01	1,83E-01	1,86E-01	1,94E-03	3,35E-02	1,37E-01	1,62E-01	5,64E-01	6,08E-01
19.30	1,98E-01	2,89E-01	1,98E-01	2,19E-01	2,41E-03	6,03E-02	2,94E-01	5,14E-01	3,01E-01	1,51E+00
19.35	1,98E-01	8,59E-02	8,28E-02	8,41E-02	1,41E-03	1,21E-02	8,24E-02	2,13E-01	1,18E-01	9,83E-01
19.40	0,00E+00	7,81E-02	5,68E-02	5,33E-02	1,32E-08	1,03E-04	2,48E-03	6,81E-02	1,50E-02	8,68E-01
19.45	0,00E+00	7,81E-03	7,03E-03	1,90E-02	9,35E-10	2,30E-06	2,02E-04	5,56E-03	5,27E-03	1,15E-01

Rainfall accumulation(mm) in point C , 7/7/2012 rainfall event

time	Rg	Pixel	Krig.	IDW	Dow. min.	Dow.1°q.	Dow.2°q.	Dow. Ave.	Dow.3°q.	Dow. max.
18.30	0,00E+00	3,60E+00	2,88E+00	2,50E+00	3,98E-06	7,70E-04	1,27E-02	1,27E-01	7,90E-02	1,46E+00
18.35	6,14E+00	4,55E+00	3,73E+00	3,41E+00	1,52E-04	8,01E-03	5,28E-02	2,33E-01	1,92E-01	2,54E+00
18.40	9,11E+00	4,97E+00	4,00E+00	3,79E+00	2,15E-03	5,30E-02	1,70E-01	4,37E-01	4,34E-01	3,40E+00
18.45	1,01E+01	5,08E+00	4,24E+00	4,02E+00	5,91E-03	6,93E-02	2,04E-01	4,82E-01	5,05E-01	3,75E+00
18.50	1,03E+01	5,31E+00	4,50E+00	4,28E+00	2,04E-02	9,54E-02	2,49E-01	5,70E-01	6,00E-01	4,00E+00
18.55	1,05E+01	5,41E+00	4,69E+00	4,46E+00	3,55E-02	1,52E-01	3,39E-01	6,73E-01	7,65E-01	4,76E+00
19.00	1,09E+01	5,55E+00	4,86E+00	4,64E+00	5,85E-02	1,97E-01	3,85E-01	7,41E-01	8,54E-01	4,93E+00
19.05	1,09E+01	5,74E+00	5,05E+00	4,83E+00	6,50E-02	2,27E-01	4,32E-01	7,99E-01	9,32E-01	5,22E+00
19.10	1,13E+01	5,90E+00	5,23E+00	5,01E+00	6,65E-02	2,37E-01	4,59E-01	8,36E-01	9,85E-01	5,39E+00
19.15	1,15E+01	6,08E+00	5,41E+00	5,21E+00	6,70E-02	2,65E-01	5,50E-01	9,70E-01	1,19E+00	5,93E+00
19.20	1,17E+01	6,43E+00	5,65E+00	5,47E+00	9,46E-02	3,47E-01	7,89E-01	1,29E+00	1,43E+00	6,66E+00
19.25	1,21E+01	6,58E+00	5,83E+00	5,66E+00	9,66E-02	3,80E-01	9,27E-01	1,45E+00	1,99E+00	7,27E+00
19.30	1,23E+01	6,87E+00	6,03E+00	5,87E+00	9,90E-02	4,40E-01	1,22E+00	1,97E+00	2,29E+00	8,77E+00
19.35	1,25E+01	6,96E+00	6,12E+00	5,96E+00	1,00E-01	4,52E-01	1,30E+00	2,18E+00	2,41E+00	9,76E+00
19.40	1,25E+01	7,03E+00	6,17E+00	6,01E+00	1,00E-01	4,52E-01	1,31E+00	2,25E+00	2,43E+00	1,06E+01
19.45	1,25E+01	7,04E+00	6,18E+00	6,03E+00	1,00E-01	4,52E-01	1,31E+00	2,25E+00	2,43E+00	1,07E+01

25/8/2012 event

Rainfall rate(mm/5min) in point A , 25/8/2012 rainfall event

time	Rg	Pixel	Krig.	IDW	Dow. min.	Dow.1°q.	Dow.2°q.	Dow. Ave.	Dow.3°q.	Dow. max.
10.55	4,04E-01	0,00E+00	0,00E+00	0,00E+00	0,00E+00	0,00E+00	0,00E+00	0,00E+00	0,00E+00	0,00E+00
11.00	1,21E+00	0,00E+00	5,21E-04	1,35E-04	0,00E+00	0,00E+00	0,00E+00	0,00E+00	0,00E+00	0,00E+00
11.05	6,06E-01	0,00E+00	0,00E+00	0,00E+00	0,00E+00	0,00E+00	0,00E+00	0,00E+00	0,00E+00	0,00E+00
11.10	1,01E+00	0,00E+00	0,00E+00	2,51E-05	0,00E+00	0,00E+00	0,00E+00	0,00E+00	0,00E+00	0,00E+00
11.15	1,01E+00	0,00E+00	0,00E+00	9,37E-04	0,00E+00	0,00E+00	0,00E+00	0,00E+00	0,00E+00	0,00E+00
11.20	8,08E-01	0,00E+00	0,00E+00	7,43E-04	0,00E+00	0,00E+00	0,00E+00	0,00E+00	0,00E+00	0,00E+00
11.25	4,04E-01	0,00E+00	5,21E-04	1,54E-03	0,00E+00	0,00E+00	0,00E+00	2,03E-02	0,00E+00	9,71E-01
11.30	0,00E+00	0,00E+00	2,60E-03	2,32E-03	0,00E+00	0,00E+00	0,00E+00	6,72E-03	0,00E+00	1,67E-01
11.35	0,00E+00	5,21E-03	4,95E-03	6,26E-03	0,00E+00	0,00E+00	0,00E+00	5,16E-02	2,01E-02	6,63E-01
11.40	1,21E+00	0,00E+00	7,29E-03	9,38E-03	2,67E-07	8,01E-05	1,36E-03	3,91E-02	8,29E-03	1,58E+00
11.45	4,04E-01	0,00E+00	5,73E-03	1,72E-02	1,14E-09	1,39E-05	5,33E-04	1,87E-02	4,87E-03	1,93E-01
11.50	2,02E-01	0,00E+00	1,33E-02	3,14E-02	2,26E-07	1,02E-04	9,18E-04	4,44E-03	2,82E-03	5,66E-02
11.55	4,04E-01	5,21E-03	4,92E-02	6,75E-02	3,09E-07	5,77E-05	6,49E-04	2,52E-03	2,85E-03	1,67E-02
12.00	2,02E-01	4,69E-02	1,32E-01	1,27E-01	8,27E-04	1,25E-02	6,41E-02	1,18E-01	1,65E-01	6,27E-01
12.05	2,02E-01	1,41E-01	1,68E-01	1,99E-01	1,88E-03	3,02E-02	1,07E-01	1,83E-01	2,80E-01	7,31E-01
12.10	0,00E+00	2,99E-01	3,28E-01	3,20E-01	3,54E-03	4,20E-02	1,33E-01	1,60E-01	1,57E-01	6,91E-01

Rainfall accumulation(mm) in point A , 25/8/2012 rainfall event

time	Rg	Pixel	Krig.	IDW	Dow. min.	Dow.1°q.	Dow.2°q.	Dow. Ave.	Dow.3°q.	Dow. max.
10.55	4,04E-01	0,00E+00	0,00E+00	0,00E+00	0,00E+00	0,00E+00	0,00E+00	0,00E+00	0,00E+00	0,00E+00
11.00	1,62E+00	0,00E+00	5,21E-04	1,35E-04	0,00E+00	0,00E+00	0,00E+00	0,00E+00	0,00E+00	0,00E+00
11.05	2,22E+00	0,00E+00	5,21E-04	1,35E-04	0,00E+00	0,00E+00	0,00E+00	0,00E+00	0,00E+00	0,00E+00
11.10	3,23E+00	0,00E+00	5,21E-04	1,60E-04	0,00E+00	0,00E+00	0,00E+00	0,00E+00	0,00E+00	0,00E+00
11.15	4,24E+00	0,00E+00	5,21E-04	1,10E-03	0,00E+00	0,00E+00	0,00E+00	0,00E+00	0,00E+00	0,00E+00
11.20	5,05E+00	0,00E+00	5,21E-04	1,84E-03	0,00E+00	0,00E+00	0,00E+00	0,00E+00	0,00E+00	0,00E+00
11.25	5,45E+00	0,00E+00	1,04E-03	3,38E-03	0,00E+00	0,00E+00	0,00E+00	2,03E-02	0,00E+00	9,71E-01
11.30	5,45E+00	0,00E+00	3,65E-03	5,70E-03	0,00E+00	0,00E+00	0,00E+00	2,70E-02	0,00E+00	1,14E+00
11.35	5,45E+00	5,21E-03	8,59E-03	1,20E-02	0,00E+00	0,00E+00	0,00E+00	7,86E-02	2,01E-02	1,80E+00
11.40	6,67E+00	5,21E-03	1,59E-02	2,13E-02	2,67E-07	8,01E-05	1,36E-03	1,18E-01	2,84E-02	3,38E+00
11.45	7,07E+00	5,21E-03	2,16E-02	3,85E-02	2,68E-07	9,40E-05	1,90E-03	1,36E-01	3,33E-02	3,57E+00
11.50	7,27E+00	5,21E-03	3,49E-02	6,99E-02	4,94E-07	1,96E-04	2,81E-03	1,41E-01	3,61E-02	3,63E+00
11.55	7,68E+00	1,04E-02	8,41E-02	1,37E-01	8,02E-07	2,53E-04	3,46E-03	1,43E-01	3,90E-02	3,65E+00
12.00	7,88E+00	5,73E-02	2,16E-01	2,64E-01	8,28E-04	1,28E-02	6,76E-02	2,62E-01	2,04E-01	4,27E+00
12.05	8,08E+00	1,98E-01	3,84E-01	4,64E-01	2,71E-03	4,30E-02	1,74E-01	4,44E-01	4,84E-01	5,01E+00
12.10	8,08E+00	4,97E-01	7,12E-01	7,84E-01	6,24E-03	8,50E-02	3,07E-01	6,04E-01	6,41E-01	5,70E+00

Rainfall rate(mm/5min) in point I , 25/8/2012 rainfall event

time	Rg	Pixel	Krig.	IDW	Dow. min.	Dow.1°q.	Dow.2°q.	Dow. Ave.	Dow.3°q.	Dow. max.
10.55	1,98E-01	0,00E+00	0,00E+00	0,00E+00	0,00E+00	0,00E+00	0,00E+00	0,00E+00	0,00E+00	0,00E+00
11.00	1,19E+00	0,00E+00	5,21E-04	1,35E-04	0,00E+00	0,00E+00	0,00E+00	0,00E+00	0,00E+00	0,00E+00
11.05	9,90E-01	0,00E+00	0,00E+00	0,00E+00	0,00E+00	0,00E+00	0,00E+00	0,00E+00	0,00E+00	0,00E+00
11.10	7,92E-01	0,00E+00	0,00E+00	2,86E-05	0,00E+00	0,00E+00	0,00E+00	0,00E+00	0,00E+00	0,00E+00
11.15	7,92E-01	0,00E+00	0,00E+00	1,06E-03	0,00E+00	0,00E+00	0,00E+00	0,00E+00	0,00E+00	0,00E+00
11.20	5,94E-01	0,00E+00	0,00E+00	8,35E-04	0,00E+00	0,00E+00	0,00E+00	0,00E+00	0,00E+00	0,00E+00
11.25	7,92E-01	0,00E+00	5,21E-04	1,72E-03	0,00E+00	0,00E+00	0,00E+00	1,16E-02	5,28E-03	2,64E-01
11.30	1,98E-01	0,00E+00	2,60E-03	2,59E-03	0,00E+00	0,00E+00	0,00E+00	1,08E-02	2,83E-03	2,48E-01
11.35	0,00E+00	5,21E-03	4,95E-03	6,04E-03	0,00E+00	0,00E+00	0,00E+00	4,13E-02	0,00E+00	1,02E+00
11.40	5,94E-01	0,00E+00	7,29E-03	1,07E-02	5,41E-09	8,01E-05	1,36E-03	2,79E-02	8,87E-03	5,66E-01
11.45	5,94E-01	0,00E+00	5,73E-03	1,99E-02	5,23E-08	1,16E-05	5,33E-04	1,91E-02	2,44E-03	3,31E-01
11.50	1,98E-01	0,00E+00	1,33E-02	3,65E-02	2,26E-07	6,28E-05	5,99E-04	4,32E-03	1,48E-03	7,00E-02
11.55	1,98E-01	5,21E-03	4,92E-02	7,79E-02	4,16E-08	5,77E-05	5,19E-04	2,37E-03	1,52E-03	2,47E-02
12.00	1,98E-01	4,69E-02	1,32E-01	1,42E-01	2,29E-04	1,78E-02	3,89E-02	1,21E-01	1,74E-01	1,03E+00
12.05	0,00E+00	1,41E-01	1,68E-01	2,10E-01	1,88E-03	2,62E-02	7,11E-02	1,39E-01	1,54E-01	9,48E-01
12.10	1,98E-01	2,99E-01	3,28E-01	3,28E-01	4,17E-03	4,20E-02	1,33E-01	1,95E-01	3,63E-01	6,91E-01

Rainfall accumulation(mm) in point I, 25/8/2012 rainfall event

time	Rg	Pixel	Krig.	IDW	Dow. min.	Dow.1°q.	Dow.2°q.	Dow. Ave.	Dow.3°q.	Dow. max.
10.55	1,98E-01	0,00E+00	0,00E+00	0,00E+00	0,00E+00	0,00E+00	0,00E+00	0,00E+00	0,00E+00	0,00E+00
11.00	1,39E+00	0,00E+00	5,21E-04	1,35E-04	0,00E+00	0,00E+00	0,00E+00	0,00E+00	0,00E+00	0,00E+00
11.05	2,38E+00	0,00E+00	5,21E-04	1,35E-04	0,00E+00	0,00E+00	0,00E+00	0,00E+00	0,00E+00	0,00E+00
11.10	3,17E+00	0,00E+00	5,21E-04	1,64E-04	0,00E+00	0,00E+00	0,00E+00	0,00E+00	0,00E+00	0,00E+00
11.15	3,96E+00	0,00E+00	5,21E-04	1,23E-03	0,00E+00	0,00E+00	0,00E+00	0,00E+00	0,00E+00	0,00E+00
11.20	4,55E+00	0,00E+00	5,21E-04	2,06E-03	0,00E+00	0,00E+00	0,00E+00	0,00E+00	0,00E+00	0,00E+00
11.25	5,35E+00	0,00E+00	1,04E-03	3,78E-03	0,00E+00	0,00E+00	0,00E+00	1,16E-02	5,28E-03	2,64E-01
11.30	5,54E+00	0,00E+00	3,65E-03	6,38E-03	0,00E+00	0,00E+00	0,00E+00	2,24E-02	8,11E-03	5,12E-01
11.35	5,54E+00	5,21E-03	8,59E-03	1,24E-02	0,00E+00	0,00E+00	0,00E+00	6,36E-02	8,11E-03	1,53E+00
11.40	6,14E+00	5,21E-03	1,59E-02	2,32E-02	5,41E-09	8,01E-05	1,36E-03	9,15E-02	1,70E-02	2,09E+00
11.45	6,73E+00	5,21E-03	2,16E-02	4,30E-02	5,77E-08	9,17E-05	1,90E-03	1,11E-01	1,94E-02	2,42E+00
11.50	6,93E+00	5,21E-03	3,49E-02	7,95E-02	2,83E-07	1,55E-04	2,50E-03	1,15E-01	2,09E-02	2,49E+00
11.55	7,13E+00	1,04E-02	8,41E-02	1,57E-01	3,25E-07	2,12E-04	3,01E-03	1,17E-01	2,24E-02	2,52E+00
12.00	7,33E+00	5,73E-02	2,16E-01	2,99E-01	2,29E-04	1,80E-02	4,20E-02	2,38E-01	1,96E-01	3,55E+00
12.05	7,33E+00	1,98E-01	3,84E-01	5,10E-01	2,11E-03	4,41E-02	1,13E-01	3,77E-01	3,51E-01	4,50E+00
12.10	7,52E+00	4,97E-01	7,12E-01	8,38E-01	6,27E-03	8,61E-02	2,46E-01	5,72E-01	7,14E-01	5,19E+00

Rainfall rate(mm/5min) in point C , 25/8/2012 rainfall event

time	Rg	Pixel	Krig.	IDW	Dow. min.	Dow.1°q.	Dow.2°q.	Dow. Ave.	Dow.3°q.	Dow. max.
10.55	0,00E+00	0,00E+00	0,00E+00	0,00E+00	0,00E+00	0,00E+00	0,00E+00	0,00E+00	0,00E+00	0,00E+00
11.00	3,96E-01	0,00E+00	5,21E-04	1,44E-04	0,00E+00	0,00E+00	0,00E+00	0,00E+00	0,00E+00	0,00E+00
11.05	5,94E-01	0,00E+00	0,00E+00	0,00E+00	0,00E+00	0,00E+00	0,00E+00	0,00E+00	0,00E+00	0,00E+00
11.10	7,92E-01	0,00E+00	0,00E+00	2,61E-05	0,00E+00	0,00E+00	0,00E+00	0,00E+00	0,00E+00	0,00E+00
11.15	9,90E-01	0,00E+00	0,00E+00	9,24E-04	0,00E+00	0,00E+00	0,00E+00	0,00E+00	0,00E+00	0,00E+00
11.20	3,96E-01	0,00E+00	0,00E+00	6,97E-04	0,00E+00	0,00E+00	0,00E+00	0,00E+00	0,00E+00	0,00E+00
11.25	1,39E+00	0,00E+00	5,21E-04	1,55E-03	0,00E+00	0,00E+00	0,00E+00	1,16E-02	5,20E-03	4,05E-01
11.30	1,98E-01	0,00E+00	2,60E-03	2,61E-03	0,00E+00	0,00E+00	0,00E+00	1,08E-02	0,00E+00	2,48E-01
11.35	0,00E+00	5,21E-03	4,95E-03	6,19E-03	0,00E+00	0,00E+00	0,00E+00	4,13E-02	2,01E-02	4,33E-01
11.40	1,58E+00	0,00E+00	7,29E-03	1,04E-02	9,20E-08	8,01E-05	1,36E-03	2,79E-02	4,11E-03	5,66E-01
11.45	1,19E+00	0,00E+00	5,73E-03	1,74E-02	1,95E-09	1,16E-05	5,47E-04	1,91E-02	2,45E-02	3,31E-01
11.50	1,98E-01	0,00E+00	1,33E-02	2,96E-02	3,65E-07	7,78E-05	9,18E-04	4,32E-03	8,64E-03	4,33E-02
11.55	1,98E-01	5,21E-03	4,92E-02	5,93E-02	2,29E-06	8,92E-05	6,22E-04	2,37E-03	3,40E-03	2,47E-02
12.00	1,98E-01	4,69E-02	1,32E-01	1,12E-01	8,27E-04	1,78E-02	6,41E-02	1,21E-01	1,74E-01	6,27E-01
12.05	1,98E-01	1,41E-01	1,68E-01	1,82E-01	2,17E-03	4,54E-02	1,07E-01	1,39E-01	2,00E-01	1,23E+00
12.10	1,98E-01	2,99E-01	3,28E-01	2,88E-01	3,54E-03	4,20E-02	1,33E-01	1,95E-01	4,23E-01	6,91E-01

Rainfall accumulation(mm) in point C , 25/8/2012 rainfall event

time	Rg	Pixel	Krig.	IDW	Dow. min.	Dow.1°q.	Dow.2°q.	Dow. Ave.	Dow.3°q.	Dow. max.
10.55	0,00E+00	0,00E+00	0,00E+00	0,00E+00	0,00E+00	0,00E+00	0,00E+00	0,00E+00	0,00E+00	0,00E+00
11.00	3,96E-01	0,00E+00	5,21E-04	1,44E-04	0,00E+00	0,00E+00	0,00E+00	0,00E+00	0,00E+00	0,00E+00
11.05	9,90E-01	0,00E+00	5,21E-04	1,44E-04	0,00E+00	0,00E+00	0,00E+00	0,00E+00	0,00E+00	0,00E+00
11.10	1,78E+00	0,00E+00	5,21E-04	1,70E-04	0,00E+00	0,00E+00	0,00E+00	0,00E+00	0,00E+00	0,00E+00
11.15	2,77E+00	0,00E+00	5,21E-04	1,09E-03	0,00E+00	0,00E+00	0,00E+00	0,00E+00	0,00E+00	0,00E+00
11.20	3,17E+00	0,00E+00	5,21E-04	1,79E-03	0,00E+00	0,00E+00	0,00E+00	0,00E+00	0,00E+00	0,00E+00
11.25	4,55E+00	0,00E+00	1,04E-03	3,35E-03	0,00E+00	0,00E+00	0,00E+00	1,16E-02	5,20E-03	4,05E-01
11.30	4,75E+00	0,00E+00	3,65E-03	5,96E-03	0,00E+00	0,00E+00	0,00E+00	2,24E-02	5,20E-03	6,53E-01
11.35	4,75E+00	5,21E-03	8,59E-03	1,21E-02	0,00E+00	0,00E+00	0,00E+00	6,36E-02	2,53E-02	1,09E+00
11.40	6,34E+00	5,21E-03	1,59E-02	2,25E-02	9,20E-08	8,01E-05	1,36E-03	9,15E-02	2,94E-02	1,65E+00
11.45	7,52E+00	5,21E-03	2,16E-02	3,99E-02	9,39E-08	9,17E-05	1,91E-03	1,11E-01	5,40E-02	1,98E+00
11.50	7,72E+00	5,21E-03	3,49E-02	6,95E-02	4,59E-07	1,69E-04	2,83E-03	1,15E-01	6,26E-02	2,03E+00
11.55	7,92E+00	1,04E-02	8,41E-02	1,29E-01	2,75E-06	2,59E-04	3,45E-03	1,17E-01	6,60E-02	2,05E+00
12.00	8,12E+00	5,73E-02	2,16E-01	2,40E-01	8,30E-04	1,80E-02	6,75E-02	2,38E-01	2,40E-01	2,68E+00
12.05	8,32E+00	1,98E-01	3,84E-01	4,22E-01	3,00E-03	6,34E-02	1,74E-01	3,77E-01	4,40E-01	3,91E+00
12.10	8,51E+00	4,97E-01	7,12E-01	7,11E-01	6,54E-03	1,05E-01	3,07E-01	5,72E-01	8,63E-01	4,60E+00

6/7/2012 event

Rainfall rate(mm/5min) in point A , 6/7/2012 rainfall event

time	Rg	Pixel	Krig.	IDW	Dow. min.	Dow.1°q.	Dow.2°q.	Dow. Ave.	Dow.3°q.	Dow. max.
7.20	2,02E-01	2,89E-01	2,48E-01	2,62E-01	5,59E-02	1,60E-01	2,67E-01	3,48E-01	4,09E-01	2,07E+00
7.25	2,02E-01	2,92E-01	3,21E-01	3,22E-01	1,60E-01	1,97E-01	3,28E-01	4,05E-01	5,70E-01	1,93E+00
7.30	2,02E-01	3,88E-01	4,51E-01	4,43E-01	2,07E-01	3,12E-01	3,96E-01	4,95E-01	5,98E-01	1,66E+00
7.35	1,01E+00	4,38E-01	5,22E-01	5,14E-01	2,30E-01	3,88E-01	5,07E-01	5,94E-01	7,23E-01	2,92E+00
7.40	1,41E+00	5,21E-01	5,33E-01	5,18E-01	2,17E-01	3,94E-01	5,28E-01	6,26E-01	7,80E-01	2,34E+00
7.45	1,62E+00	2,94E-01	2,58E-01	2,70E-01	9,10E-02	1,49E-01	2,11E-01	2,29E-01	2,99E-01	4,77E-01
7.50	1,01E+00	1,30E-01	1,56E-01	1,52E-01	5,29E-02	1,17E-01	1,30E-01	1,55E-01	2,06E-01	5,13E-01
7.55	6,06E-01	2,29E-01	2,00E-01	2,12E-01	7,66E-02	1,21E-01	1,50E-01	1,74E-01	2,17E-01	4,81E-01
8.00	8,08E-01	6,77E-02	7,94E-02	8,94E-02	4,89E-02	8,61E-02	1,13E-01	1,19E-01	1,42E-01	2,63E-01
8.05	4,04E-01	1,41E-01	1,41E-01	1,47E-01	4,42E-02	6,38E-02	9,60E-02	1,23E-01	1,58E-01	4,72E-01
8.10	4,04E-01	1,98E-01	2,06E-01	2,12E-01	1,04E-01	1,78E-01	2,15E-01	2,63E-01	3,09E-01	9,06E-01
8.15	4,04E-01	1,67E-01	1,76E-01	1,82E-01	5,67E-02	6,96E-02	9,91E-02	1,21E-01	1,63E-01	4,57E-01
8.20	6,06E-01	1,35E-01	1,58E-01	1,57E-01	5,10E-02	8,26E-02	8,56E-02	9,59E-02	1,34E-01	3,50E-01
8.25	2,02E-01	2,66E-01	2,29E-01	2,43E-01	5,43E-02	1,06E-01	1,49E-01	1,42E-01	1,54E-01	2,17E-01
8.30	6,06E-01	2,79E-01	2,81E-01	2,83E-01	1,21E-01	2,09E-01	2,50E-01	2,62E-01	2,95E-01	4,03E-01
8.35	4,04E-01	3,33E-01	3,23E-01	3,37E-01	9,70E-02	1,57E-01	2,17E-01	2,27E-01	2,88E-01	3,91E-01
8.40	6,06E-01	1,64E-01	2,30E-01	2,23E-01	5,10E-02	1,03E-01	1,47E-01	1,73E-01	2,09E-01	5,61E-01
8.45	4,04E-01	2,40E-01	4,38E-01	3,45E-01	2,14E-01	5,53E-01	9,27E-01	1,15E+00	1,58E+00	4,00E+00
8.50	8,08E-01	3,02E-01	2,81E-01	3,20E-01	5,71E-02	1,19E-01	1,34E-01	2,01E-01	2,63E-01	1,01E+00
8.55	6,06E-01	4,40E-01	4,07E-01	4,41E-01	8,70E-02	2,00E-01	3,19E-01	3,77E-01	4,69E-01	1,30E+00
9.00	4,04E-01	1,22E+00	1,14E+00	1,08E+00	6,75E-02	1,35E-01	1,96E-01	2,55E-01	2,83E-01	9,09E-01
9.05	3,64E+00	2,06E-01	2,64E-01	2,66E-01	8,99E-02	2,02E-01	2,46E-01	4,05E-01	4,96E-01	2,28E+00
9.10	6,06E-01	2,01E-01	2,34E-01	2,35E-01	8,61E-02	1,63E-01	1,96E-01	2,55E-01	3,04E-01	1,11E+00
9.15	2,02E-01	2,79E-01	2,68E-01	2,79E-01	1,08E-01	1,80E-01	2,19E-01	2,32E-01	2,68E-01	4,37E-01
9.20	6,06E-01	1,02E-01	1,11E-01	1,29E-01	5,11E-02	1,16E-01	1,70E-01	1,92E-01	2,49E-01	5,57E-01
9.25	2,02E-01	2,94E-01	3,61E-01	3,13E-01	1,03E-01	1,12E-01	1,83E-01	2,32E-01	3,06E-01	8,71E-01
9.30	4,04E-01	3,28E-01	3,54E-01	3,70E-01	1,26E-01	2,14E-01	3,06E-01	3,48E-01	4,36E-01	1,65E+00
9.35	2,02E-01	8,88E-01	5,20E-01	6,62E-01	1,30E-01	2,34E-01	2,57E-01	3,52E-01	4,32E-01	1,38E+00
9.40	6,06E-01	2,03E-01	2,84E-01	2,87E-01	1,84E-01	2,96E-01	3,66E-01	4,58E-01	5,31E-01	1,38E+00
9.45	2,02E-01	1,82E-01	2,04E-01	2,03E-01	9,19E-02	1,18E-01	1,72E-01	1,97E-01	2,39E-01	6,08E-01
9.50	2,02E-01	1,25E-01	1,51E-01	1,52E-01	9,02E-02	1,72E-01	2,30E-01	2,26E-01	2,52E-01	4,73E-01
9.55	2,02E-01	1,09E-01	1,40E-01	1,42E-01	2,96E-02	6,33E-02	9,90E-02	1,07E-01	1,35E-01	2,74E-01
10.00	0,00E+00	2,37E-01	2,10E-01	2,42E-01	3,86E-02	9,91E-02	1,61E-01	1,84E-01	2,36E-01	8,38E-01
10.05	2,02E-01	7,63E-01	6,19E-01	6,58E-01	3,78E-02	1,48E-01	2,91E-01	3,03E-01	3,11E-01	6,06E-01
10.10	8,08E-01	1,74E-01	1,94E-01	2,16E-01	8,91E-04	4,88E-03	1,02E-02	1,28E-02	1,57E-02	4,00E-02
10.15	4,04E-01	9,64E-02	1,73E-01	1,40E-01	2,63E-03	5,32E-03	8,35E-03	9,78E-03	1,24E-02	3,93E-02
10.20	2,02E-01	1,09E-01	1,35E-01	1,22E-01	1,72E-03	7,59E-03	1,60E-02	2,00E-02	3,02E-02	5,86E-02
10.25	2,02E-01	2,89E-01	3,05E-01	2,87E-01	2,35E-02	5,26E-02	7,82E-02	8,98E-02	1,07E-01	3,74E-01
10.30	4,04E-01	1,56E-01	1,79E-01	1,75E-01	1,61E-02	4,52E-02	7,66E-02	1,02E-01	1,36E-01	6,75E-01
10.35	4,04E-01	1,54E-01	1,21E-01	1,35E-01	2,40E-02	7,19E-02	1,10E-01	1,47E-01	1,87E-01	5,66E-01
10.40	2,02E-01	1,07E-01	1,07E-01	1,10E-01	1,80E-02	5,05E-02	7,34E-02	8,07E-02	9,89E-02	2,19E-01
10.45	2,02E-01	9,90E-02	1,05E-01	1,12E-01	4,19E-02	1,08E-01	1,54E-01	1,92E-01	2,41E-01	6,81E-01
10.50	0,00E+00	2,32E-01	2,11E-01	2,04E-01	5,69E-02	1,59E-01	2,51E-01	2,91E-01	3,68E-01	7,35E-01
10.55	2,02E-01	1,51E-01	1,52E-01	1,57E-01	9,86E-03	2,90E-02	6,66E-02	7,42E-02	8,51E-02	2,21E-01
11.00	2,02E-01	2,79E-01	2,42E-01	2,51E-01	1,47E-02	1,22E-01	2,20E-01	2,39E-01	3,68E-01	5,09E-01

11.05	0,00E+00	3,26E-01	3,00E-01	3,12E-01	7,02E-02	1,99E-01	3,09E-01	3,08E-01	4,14E-01	7,61E-01
11.10	4,04E-01	2,40E-01	2,80E-01	2,93E-01	7,02E-02	1,99E-01	3,09E-01	3,08E-01	4,14E-01	7,61E-01
11.15	2,02E-01	1,98E-01	2,58E-01	2,35E-01	1,14E-01	2,86E-01	4,93E-01	5,06E-01	6,90E-01	1,47E+00
11.20	2,02E-01	4,17E-02	6,93E-02	7,47E-02	2,83E-02	7,46E-02	1,56E-01	1,77E-01	2,60E-01	4,34E-01
11.25	2,02E-01	2,60E-02	3,23E-02	3,34E-02	2,03E-03	8,82E-03	2,20E-02	4,17E-02	5,64E-02	2,44E-01
11.30	0,00E+00	7,55E-02	7,92E-02	8,45E-02	9,91E-03	3,82E-02	6,48E-02	7,31E-02	9,17E-02	2,15E-01
11.35	0,00E+00	2,34E-01	1,88E-01	1,90E-01	9,20E-03	4,61E-02	8,17E-02	1,05E-01	1,45E-01	5,52E-01
11.40	0,00E+00	4,17E-02	5,57E-02	6,18E-02	7,05E-03	2,35E-02	3,66E-02	4,71E-02	5,79E-02	1,88E-01
11.45	2,02E-01	1,85E-01	1,20E-01	1,39E-01	2,19E-02	6,96E-02	1,19E-01	1,63E-01	2,22E-01	7,49E-01
11.50	0,00E+00	2,08E-02	2,21E-02	2,95E-02	9,18E-04	6,15E-03	1,42E-02	1,79E-02	2,23E-02	6,46E-02
11.55	0,00E+00	2,86E-02	3,80E-02	4,34E-02	1,85E-03	1,25E-02	2,84E-02	3,70E-02	5,82E-02	1,25E-01
12.00	2,02E-01	3,41E-01	2,97E-01	2,79E-01	2,76E-02	8,08E-02	1,85E-01	2,28E-01	3,11E-01	8,74E-01
12.05	0,00E+00	1,56E-01	2,05E-01	1,85E-01	2,49E-03	3,84E-02	9,11E-02	1,40E-01	1,94E-01	6,16E-01
12.10	4,04E-01	4,35E-01	2,82E-01	3,20E-01	1,40E-02	6,17E-02	2,00E-01	2,98E-01	5,00E-01	1,06E+00
12.15	2,02E-01	1,46E-01	1,41E-01	1,35E-01	8,52E-03	6,75E-02	1,77E-01	2,22E-01	3,63E-01	6,47E-01
12.20	0,00E+00	1,46E-01	1,64E-01	1,56E-01	1,92E-02	4,06E-02	8,42E-02	8,06E-02	8,59E-02	1,84E-01
12.25	0,00E+00	1,09E-01	1,40E-01	1,39E-01	3,43E-03	5,30E-02	1,22E-01	1,52E-01	2,77E-01	4,62E-01
12.30	2,02E-01	1,56E-02	1,67E-02	2,51E-02	7,83E-03	3,66E-02	7,96E-02	8,47E-02	8,07E-02	1,76E-01

Rainfall accumulation(mm) in point A , 6/7/2012 rainfall event

time	Rg	Pixel	Krig.	IDW	Dow. min.	Dow.1°q.	Dow.2°q.	Dow. Ave.	Dow.3°q.	Dow. max.
7.20	2,02E-01	2,89E-01	2,48E-01	2,62E-01	5,59E-02	1,60E-01	2,67E-01	3,48E-01	4,09E-01	2,07E+00
7.25	4,04E-01	5,81E-01	5,69E-01	5,84E-01	2,16E-01	3,58E-01	5,95E-01	7,53E-01	9,79E-01	4,00E+00
7.30	6,06E-01	9,69E-01	1,02E+00	1,03E+00	4,23E-01	6,69E-01	9,91E-01	1,25E+00	1,58E+00	5,65E+00
7.35	1,62E+00	1,41E+00	1,54E+00	1,54E+00	6,53E-01	1,06E+00	1,50E+00	1,84E+00	2,30E+00	8,58E+00
7.40	3,03E+00	1,93E+00	2,08E+00	2,06E+00	8,71E-01	1,45E+00	2,03E+00	2,47E+00	3,08E+00	1,09E+01
7.45	4,65E+00	2,22E+00	2,33E+00	2,33E+00	9,62E-01	1,60E+00	2,24E+00	2,70E+00	3,38E+00	1,14E+01
7.50	5,66E+00	2,35E+00	2,49E+00	2,48E+00	1,01E+00	1,72E+00	2,37E+00	2,85E+00	3,58E+00	1,19E+01
7.55	6,26E+00	2,58E+00	2,69E+00	2,69E+00	1,09E+00	1,84E+00	2,52E+00	3,03E+00	3,80E+00	1,24E+01
8.00	7,07E+00	2,65E+00	2,77E+00	2,78E+00	1,14E+00	1,92E+00	2,63E+00	3,15E+00	3,94E+00	1,26E+01
8.05	7,47E+00	2,79E+00	2,91E+00	2,93E+00	1,18E+00	1,99E+00	2,73E+00	3,27E+00	4,10E+00	1,31E+01
8.10	7,88E+00	2,99E+00	3,12E+00	3,14E+00	1,29E+00	2,17E+00	2,94E+00	3,53E+00	4,41E+00	1,40E+01
8.15	8,28E+00	3,15E+00	3,29E+00	3,32E+00	1,35E+00	2,24E+00	3,04E+00	3,65E+00	4,57E+00	1,45E+01
8.20	8,89E+00	3,29E+00	3,45E+00	3,48E+00	1,40E+00	2,32E+00	3,13E+00	3,75E+00	4,71E+00	1,48E+01
8.25	9,09E+00	3,55E+00	3,68E+00	3,72E+00	1,45E+00	2,43E+00	3,28E+00	3,89E+00	4,86E+00	1,50E+01
8.30	9,70E+00	3,83E+00	3,96E+00	4,01E+00	1,57E+00	2,63E+00	3,53E+00	4,15E+00	5,16E+00	1,55E+01
8.35	1,01E+01	4,17E+00	4,28E+00	4,34E+00	1,67E+00	2,79E+00	3,75E+00	4,38E+00	5,44E+00	1,58E+01
8.40	1,07E+01	4,33E+00	4,51E+00	4,57E+00	1,72E+00	2,89E+00	3,89E+00	4,55E+00	5,65E+00	1,64E+01
8.45	1,11E+01	4,57E+00	4,95E+00	4,91E+00	1,93E+00	3,45E+00	4,82E+00	5,70E+00	7,23E+00	2,04E+01
8.50	1,19E+01	4,87E+00	5,23E+00	5,23E+00	1,99E+00	3,57E+00	4,95E+00	5,91E+00	7,50E+00	2,14E+01
8.55	1,25E+01	5,31E+00	5,64E+00	5,67E+00	2,08E+00	3,77E+00	5,27E+00	6,28E+00	7,97E+00	2,27E+01
9.00	1,29E+01	6,53E+00	6,78E+00	6,75E+00	2,14E+00	3,90E+00	5,47E+00	6,54E+00	8,25E+00	2,36E+01
9.05	1,66E+01	6,74E+00	7,05E+00	7,02E+00	2,23E+00	4,10E+00	5,71E+00	6,94E+00	8,75E+00	2,59E+01
9.10	1,72E+01	6,94E+00	7,28E+00	7,25E+00	2,32E+00	4,27E+00	5,91E+00	7,20E+00	9,05E+00	2,70E+01
9.15	1,74E+01	7,22E+00	7,55E+00	7,53E+00	2,43E+00	4,45E+00	6,13E+00	7,43E+00	9,32E+00	2,75E+01
9.20	1,80E+01	7,32E+00	7,66E+00	7,66E+00	2,48E+00	4,56E+00	6,30E+00	7,62E+00	9,57E+00	2,80E+01

9.25	1,82E+01	7,61E+00	8,02E+00	7,98E+00	2,58E+00	4,67E+00	6,48E+00	7,85E+00	9,87E+00	2,89E+01
9.30	1,86E+01	7,94E+00	8,38E+00	8,35E+00	2,71E+00	4,89E+00	6,79E+00	8,20E+00	1,03E+01	3,05E+01
9.35	1,88E+01	8,83E+00	8,90E+00	9,01E+00	2,84E+00	5,12E+00	7,04E+00	8,55E+00	1,07E+01	3,19E+01
9.40	1,94E+01	9,03E+00	9,18E+00	9,29E+00	3,02E+00	5,42E+00	7,41E+00	9,01E+00	1,13E+01	3,33E+01
9.45	1,96E+01	9,22E+00	9,38E+00	9,50E+00	3,12E+00	5,54E+00	7,58E+00	9,21E+00	1,15E+01	3,39E+01
9.50	1,98E+01	9,34E+00	9,53E+00	9,65E+00	3,21E+00	5,71E+00	7,81E+00	9,43E+00	1,18E+01	3,44E+01
9.55	2,00E+01	9,45E+00	9,67E+00	9,79E+00	3,24E+00	5,77E+00	7,91E+00	9,54E+00	1,19E+01	3,47E+01
10.00	2,00E+01	9,69E+00	9,88E+00	1,00E+01	3,27E+00	5,87E+00	8,07E+00	9,72E+00	1,21E+01	3,55E+01
10.05	2,02E+01	1,05E+01	1,05E+01	1,07E+01	3,31E+00	6,02E+00	8,36E+00	1,00E+01	1,24E+01	3,61E+01
10.10	2,10E+01	1,06E+01	1,07E+01	1,09E+01	3,31E+00	6,03E+00	8,37E+00	1,00E+01	1,25E+01	3,61E+01
10.15	2,14E+01	1,07E+01	1,09E+01	1,10E+01	3,31E+00	6,03E+00	8,38E+00	1,01E+01	1,25E+01	3,62E+01
10.20	2,16E+01	1,08E+01	1,10E+01	1,12E+01	3,32E+00	6,04E+00	8,40E+00	1,01E+01	1,25E+01	3,62E+01
10.25	2,18E+01	1,11E+01	1,13E+01	1,15E+01	3,34E+00	6,09E+00	8,48E+00	1,02E+01	1,26E+01	3,66E+01
10.30	2,22E+01	1,13E+01	1,15E+01	1,16E+01	3,36E+00	6,14E+00	8,55E+00	1,03E+01	1,27E+01	3,73E+01
10.35	2,26E+01	1,14E+01	1,16E+01	1,18E+01	3,38E+00	6,21E+00	8,66E+00	1,04E+01	1,29E+01	3,79E+01
10.40	2,28E+01	1,15E+01	1,17E+01	1,19E+01	3,40E+00	6,26E+00	8,74E+00	1,05E+01	1,30E+01	3,81E+01
10.45	2,30E+01	1,16E+01	1,18E+01	1,20E+01	3,44E+00	6,37E+00	8,89E+00	1,07E+01	1,33E+01	3,88E+01
10.50	2,30E+01	1,19E+01	1,20E+01	1,22E+01	3,50E+00	6,53E+00	9,14E+00	1,10E+01	1,36E+01	3,95E+01
10.55	2,32E+01	1,20E+01	1,22E+01	1,24E+01	3,51E+00	6,55E+00	9,21E+00	1,10E+01	1,37E+01	3,97E+01
11.00	2,34E+01	1,23E+01	1,24E+01	1,26E+01	3,52E+00	6,68E+00	9,43E+00	1,13E+01	1,41E+01	4,02E+01
11.05	2,34E+01	1,26E+01	1,27E+01	1,29E+01	3,59E+00	6,88E+00	9,74E+00	1,16E+01	1,45E+01	4,10E+01
11.10	2,38E+01	1,29E+01	1,30E+01	1,32E+01	3,66E+00	7,07E+00	1,00E+01	1,19E+01	1,49E+01	4,17E+01
11.15	2,40E+01	1,31E+01	1,33E+01	1,34E+01	3,78E+00	7,36E+00	1,05E+01	1,24E+01	1,56E+01	4,32E+01
11.20	2,42E+01	1,31E+01	1,33E+01	1,35E+01	3,80E+00	7,43E+00	1,07E+01	1,26E+01	1,59E+01	4,36E+01
11.25	2,44E+01	1,31E+01	1,34E+01	1,35E+01	3,81E+00	7,44E+00	1,07E+01	1,26E+01	1,59E+01	4,39E+01
11.30	2,44E+01	1,32E+01	1,34E+01	1,36E+01	3,82E+00	7,48E+00	1,08E+01	1,27E+01	1,60E+01	4,41E+01
11.35	2,44E+01	1,34E+01	1,36E+01	1,38E+01	3,83E+00	7,53E+00	1,09E+01	1,28E+01	1,62E+01	4,47E+01
11.40	2,44E+01	1,35E+01	1,37E+01	1,39E+01	3,83E+00	7,55E+00	1,09E+01	1,29E+01	1,62E+01	4,48E+01
11.45	2,46E+01	1,37E+01	1,38E+01	1,40E+01	3,85E+00	7,62E+00	1,10E+01	1,30E+01	1,64E+01	4,56E+01
11.50	2,46E+01	1,37E+01	1,38E+01	1,41E+01	3,86E+00	7,63E+00	1,10E+01	1,30E+01	1,65E+01	4,57E+01
11.55	2,46E+01	1,37E+01	1,39E+01	1,41E+01	3,86E+00	7,64E+00	1,11E+01	1,31E+01	1,65E+01	4,58E+01
12.00	2,48E+01	1,41E+01	1,42E+01	1,44E+01	3,89E+00	7,72E+00	1,12E+01	1,33E+01	1,68E+01	4,67E+01
12.05	2,48E+01	1,42E+01	1,44E+01	1,46E+01	3,89E+00	7,76E+00	1,13E+01	1,34E+01	1,70E+01	4,73E+01
12.10	2,53E+01	1,46E+01	1,47E+01	1,49E+01	3,90E+00	7,82E+00	1,15E+01	1,37E+01	1,75E+01	4,83E+01
12.15	2,55E+01	1,48E+01	1,48E+01	1,50E+01	3,91E+00	7,89E+00	1,17E+01	1,40E+01	1,79E+01	4,90E+01
12.20	2,55E+01	1,49E+01	1,50E+01	1,52E+01	3,93E+00	7,93E+00	1,18E+01	1,40E+01	1,80E+01	4,92E+01
12.25	2,55E+01	1,50E+01	1,51E+01	1,53E+01	3,93E+00	7,98E+00	1,19E+01	1,42E+01	1,83E+01	4,96E+01
12.30	2,57E+01	1,51E+01	1,51E+01	1,53E+01	3,94E+00	8,02E+00	1,20E+01	1,43E+01	1,83E+01	4,98E+01

Rainfall rate(mm/5min) in point I , 6/7/2012 rainfall event

time	Rg	Pixel	Krig.	IDW	Dow. min.	Dow.1°q.	Dow.2°q.	Dow. Ave.	Dow.3°q.	Dow. max.
7.20	1,98E-01	2,89E-01	2,48E-01	2,53E-01	4,87E-02	1,51E-01	2,19E-01	3,07E-01	3,69E-01	1,51E+00
7.25	1,98E-01	2,92E-01	3,21E-01	3,28E-01	1,48E-01	2,23E-01	3,41E-01	4,45E-01	5,88E-01	1,93E+00
7.30	3,96E-01	3,88E-01	4,51E-01	4,58E-01	1,79E-01	2,74E-01	3,86E-01	4,19E-01	5,16E-01	1,04E+00
7.35	9,90E-01	4,38E-01	5,22E-01	5,32E-01	2,30E-01	3,78E-01	5,37E-01	6,02E-01	7,35E-01	1,86E+00
7.40	1,39E+00	5,21E-01	5,33E-01	5,08E-01	2,17E-01	3,58E-01	4,59E-01	5,87E-01	7,50E-01	2,03E+00

7.45	1,39E+00	2,94E-01	2,58E-01	2,63E-01	9,16E-02	1,66E-01	2,24E-01	2,26E-01	2,72E-01	4,28E-01
7.50	9,90E-01	1,30E-01	1,56E-01	1,60E-01	5,91E-02	1,04E-01	1,46E-01	1,66E-01	2,06E-01	5,13E-01
7.55	7,92E-01	2,29E-01	2,00E-01	2,06E-01	6,62E-02	1,02E-01	1,45E-01	1,62E-01	1,92E-01	4,81E-01
8.00	5,94E-01	6,77E-02	7,94E-02	9,32E-02	4,04E-02	7,13E-02	1,10E-01	1,12E-01	1,42E-01	2,33E-01
8.05	3,96E-01	1,41E-01	1,41E-01	1,48E-01	4,42E-02	6,36E-02	9,60E-02	1,35E-01	1,58E-01	5,17E-01
8.10	3,96E-01	1,98E-01	2,06E-01	2,16E-01	9,85E-02	1,52E-01	2,02E-01	2,54E-01	3,27E-01	1,37E+00
8.15	3,96E-01	1,67E-01	1,76E-01	1,88E-01	5,67E-02	5,99E-02	9,91E-02	1,14E-01	1,61E-01	2,76E-01
8.20	5,94E-01	1,35E-01	1,58E-01	1,63E-01	5,10E-02	8,26E-02	8,56E-02	1,07E-01	1,36E-01	2,24E-01
8.25	3,96E-01	2,66E-01	2,29E-01	2,40E-01	5,51E-02	1,08E-01	1,49E-01	1,48E-01	2,04E-01	2,17E-01
8.30	5,94E-01	2,79E-01	2,81E-01	2,85E-01	1,12E-01	2,14E-01	2,50E-01	2,58E-01	2,91E-01	3,97E-01
8.35	3,96E-01	3,33E-01	3,23E-01	3,43E-01	9,00E-02	1,51E-01	2,24E-01	2,25E-01	2,88E-01	4,08E-01
8.40	5,94E-01	1,64E-01	2,30E-01	2,42E-01	5,10E-02	9,23E-02	1,47E-01	1,66E-01	2,21E-01	3,93E-01
8.45	3,96E-01	2,40E-01	4,38E-01	3,72E-01	2,18E-01	5,96E-01	1,02E+00	1,38E+00	1,62E+00	5,49E+00
8.50	9,90E-01	3,02E-01	2,81E-01	3,29E-01	5,71E-02	7,24E-02	1,26E-01	1,83E-01	2,63E-01	5,46E-01
8.55	3,96E-01	4,40E-01	4,07E-01	4,46E-01	8,52E-02	1,91E-01	3,23E-01	3,95E-01	4,66E-01	1,72E+00
9.00	5,94E-01	1,22E+00	1,14E+00	1,07E+00	6,75E-02	1,46E-01	2,18E-01	2,57E-01	3,36E-01	9,09E-01
9.05	3,76E+00	2,06E-01	2,64E-01	2,72E-01	8,99E-02	2,22E-01	2,72E-01	4,11E-01	5,04E-01	1,13E+00
9.10	5,94E-01	2,01E-01	2,34E-01	2,43E-01	8,77E-02	1,60E-01	1,96E-01	2,81E-01	3,52E-01	1,11E+00
9.15	1,98E-01	2,79E-01	2,68E-01	2,78E-01	1,20E-01	1,97E-01	2,46E-01	2,48E-01	2,94E-01	4,44E-01
9.20	3,96E-01	1,02E-01	1,11E-01	1,32E-01	5,75E-02	1,07E-01	1,52E-01	1,74E-01	2,15E-01	4,21E-01
9.25	1,98E-01	2,94E-01	3,61E-01	3,20E-01	1,03E-01	1,09E-01	1,79E-01	2,46E-01	3,06E-01	8,71E-01
9.30	5,94E-01	3,28E-01	3,54E-01	3,78E-01	1,18E-01	2,22E-01	3,06E-01	3,49E-01	4,36E-01	1,16E+00
9.35	3,96E-01	8,88E-01	5,20E-01	6,13E-01	1,23E-01	2,23E-01	2,52E-01	3,53E-01	4,30E-01	2,32E+00
9.40	3,96E-01	2,03E-01	2,84E-01	2,98E-01	1,84E-01	2,96E-01	3,29E-01	4,15E-01	5,31E-01	1,24E+00
9.45	1,98E-01	1,82E-01	2,04E-01	2,07E-01	9,02E-02	1,18E-01	1,62E-01	1,89E-01	2,39E-01	5,97E-01
9.50	1,98E-01	1,25E-01	1,51E-01	1,58E-01	9,02E-02	1,63E-01	2,20E-01	2,26E-01	2,87E-01	4,99E-01
9.55	1,98E-01	1,09E-01	1,40E-01	1,51E-01	2,96E-02	6,63E-02	9,18E-02	1,04E-01	1,36E-01	2,74E-01
10.00	1,98E-01	2,37E-01	2,10E-01	2,47E-01	3,86E-02	1,18E-01	2,28E-01	2,38E-01	3,35E-01	7,78E-01
10.05	1,98E-01	7,63E-01	6,19E-01	6,54E-01	3,78E-02	1,51E-01	2,89E-01	3,03E-01	3,10E-01	6,14E-01
10.10	5,94E-01	1,74E-01	1,94E-01	2,31E-01	1,56E-03	4,88E-03	1,02E-02	1,32E-02	1,59E-02	4,15E-02
10.15	5,94E-01	9,64E-02	1,73E-01	1,58E-01	1,97E-03	5,32E-03	9,14E-03	1,11E-02	1,43E-02	6,17E-02
10.20	1,98E-01	1,09E-01	1,35E-01	1,32E-01	1,40E-03	7,54E-03	1,60E-02	1,99E-02	3,18E-02	5,86E-02
10.25	1,98E-01	2,89E-01	3,05E-01	2,87E-01	2,35E-02	4,78E-02	7,53E-02	8,17E-02	1,08E-01	2,98E-01
10.30	3,96E-01	1,56E-01	1,79E-01	1,82E-01	1,61E-02	4,84E-02	7,75E-02	1,06E-01	1,29E-01	6,31E-01
10.35	3,96E-01	1,54E-01	1,21E-01	1,30E-01	2,29E-02	7,77E-02	1,19E-01	1,39E-01	1,87E-01	4,10E-01
10.40	1,98E-01	1,07E-01	1,07E-01	1,12E-01	1,55E-02	5,25E-02	7,34E-02	8,22E-02	9,89E-02	2,19E-01
10.45	0,00E+00	9,90E-02	1,05E-01	1,14E-01	3,69E-02	9,55E-02	1,29E-01	1,86E-01	2,41E-01	7,91E-01
10.50	1,98E-01	2,32E-01	2,11E-01	1,96E-01	6,97E-02	1,59E-01	2,82E-01	3,00E-01	3,84E-01	8,39E-01
10.55	1,98E-01	1,51E-01	1,52E-01	1,59E-01	4,84E-03	2,99E-02	6,66E-02	8,25E-02	8,51E-02	2,21E-01
11.00	1,98E-01	2,79E-01	2,42E-01	2,43E-01	2,75E-02	1,11E-01	2,07E-01	2,19E-01	2,58E-01	5,09E-01
11.05	0,00E+00	3,26E-01	3,00E-01	3,05E-01	7,02E-02	1,99E-01	3,09E-01	3,40E-01	4,82E-01	7,61E-01
11.10	3,96E-01	2,40E-01	2,80E-01	3,07E-01	7,02E-02	1,99E-01	3,09E-01	3,40E-01	4,82E-01	7,61E-01
11.15	1,98E-01	1,98E-01	2,58E-01	2,36E-01	7,24E-02	2,75E-01	4,17E-01	4,45E-01	5,95E-01	1,19E+00
11.20	1,98E-01	4,17E-02	6,93E-02	7,82E-02	1,56E-02	7,24E-02	1,49E-01	1,72E-01	2,46E-01	4,47E-01
11.25	1,98E-01	2,60E-02	3,23E-02	3,52E-02	8,82E-04	8,14E-03	2,03E-02	2,98E-02	3,82E-02	2,44E-01
11.30	0,00E+00	7,55E-02	7,92E-02	8,76E-02	9,91E-03	2,77E-02	5,45E-02	6,79E-02	9,11E-02	3,59E-01
11.35	0,00E+00	2,34E-01	1,88E-01	1,79E-01	9,20E-03	5,14E-02	8,17E-02	1,08E-01	1,60E-01	3,32E-01
11.40	1,98E-01	4,17E-02	5,57E-02	6,66E-02	8,07E-03	2,65E-02	5,06E-02	6,18E-02	8,00E-02	2,15E-01
11.45	0,00E+00	1,85E-01	1,20E-01	1,23E-01	8,05E-03	6,96E-02	1,15E-01	1,44E-01	2,05E-01	7,49E-01
11.50	0,00E+00	2,08E-02	2,21E-02	3,12E-02	3,55E-04	6,15E-03	1,42E-02	1,72E-02	1,99E-02	6,46E-02
11.55	0,00E+00	2,86E-02	3,80E-02	4,72E-02	1,77E-03	1,15E-02	2,61E-02	3,17E-02	4,99E-02	1,03E-01
12.00	1,98E-01	3,41E-01	2,97E-01	2,67E-01	1,18E-02	6,43E-02	1,37E-01	2,04E-01	2,48E-01	9,14E-01

12.05	1,98E-01	1,56E-01	2,05E-01	1,92E-01	2,49E-03	3,24E-02	8,07E-02	1,12E-01	1,53E-01	4,76E-01
12.10	3,96E-01	4,35E-01	2,82E-01	2,98E-01	4,13E-03	5,92E-02	2,08E-01	3,06E-01	3,14E-01	1,33E+00
12.15	0,00E+00	1,46E-01	1,41E-01	1,25E-01	7,99E-03	6,30E-02	1,61E-01	1,99E-01	2,16E-01	5,70E-01
12.20	0,00E+00	1,46E-01	1,64E-01	1,60E-01	9,34E-03	4,06E-02	8,47E-02	9,13E-02	1,74E-01	1,84E-01
12.25	1,98E-01	1,09E-01	1,40E-01	1,40E-01	7,88E-03	5,30E-02	1,22E-01	1,47E-01	2,40E-01	4,30E-01
12.30	1,98E-01	1,56E-02	1,67E-02	2,63E-02	7,83E-03	3,66E-02	7,96E-02	8,47E-02	8,07E-02	1,76E-01

Rainfall accumulation(mm) in point I , 6/7/2012 rainfall event

time	Rg	Pixel	Krig.	IDW	Dow. min.	Dow.1°q.	Dow.2°q.	Dow. Ave.	Dow.3°q.	Dow. max.
7.20	1,98E-01	2,89E-01	2,48E-01	2,53E-01	4,87E-02	1,51E-01	2,19E-01	3,07E-01	3,69E-01	1,51E+00
7.25	3,96E-01	5,81E-01	5,69E-01	5,81E-01	1,97E-01	3,74E-01	5,60E-01	7,53E-01	9,57E-01	3,44E+00
7.30	7,92E-01	9,69E-01	1,02E+00	1,04E+00	3,76E-01	6,49E-01	9,46E-01	1,17E+00	1,47E+00	4,48E+00
7.35	1,78E+00	1,41E+00	1,54E+00	1,57E+00	6,06E-01	1,03E+00	1,48E+00	1,77E+00	2,21E+00	6,34E+00
7.40	3,17E+00	1,93E+00	2,08E+00	2,08E+00	8,24E-01	1,39E+00	1,94E+00	2,36E+00	2,96E+00	8,37E+00
7.45	4,55E+00	2,22E+00	2,33E+00	2,34E+00	9,15E-01	1,55E+00	2,17E+00	2,59E+00	3,23E+00	8,80E+00
7.50	5,54E+00	2,35E+00	2,49E+00	2,50E+00	9,75E-01	1,66E+00	2,31E+00	2,75E+00	3,44E+00	9,31E+00
7.55	6,34E+00	2,58E+00	2,69E+00	2,71E+00	1,04E+00	1,76E+00	2,46E+00	2,91E+00	3,63E+00	9,80E+00
8.00	6,93E+00	2,65E+00	2,77E+00	2,80E+00	1,08E+00	1,83E+00	2,57E+00	3,03E+00	3,77E+00	1,00E+01
8.05	7,33E+00	2,79E+00	2,91E+00	2,95E+00	1,13E+00	1,89E+00	2,66E+00	3,16E+00	3,93E+00	1,05E+01
8.10	7,72E+00	2,99E+00	3,12E+00	3,16E+00	1,22E+00	2,04E+00	2,86E+00	3,42E+00	4,26E+00	1,19E+01
8.15	8,12E+00	3,15E+00	3,29E+00	3,35E+00	1,28E+00	2,10E+00	2,96E+00	3,53E+00	4,42E+00	1,22E+01
8.20	8,71E+00	3,29E+00	3,45E+00	3,52E+00	1,33E+00	2,19E+00	3,05E+00	3,64E+00	4,55E+00	1,24E+01
8.25	9,11E+00	3,55E+00	3,68E+00	3,76E+00	1,39E+00	2,29E+00	3,20E+00	3,78E+00	4,76E+00	1,26E+01
8.30	9,70E+00	3,83E+00	3,96E+00	4,04E+00	1,50E+00	2,51E+00	3,45E+00	4,04E+00	5,05E+00	1,30E+01
8.35	1,01E+01	4,17E+00	4,28E+00	4,38E+00	1,59E+00	2,66E+00	3,67E+00	4,27E+00	5,34E+00	1,34E+01
8.40	1,07E+01	4,33E+00	4,51E+00	4,63E+00	1,64E+00	2,75E+00	3,82E+00	4,43E+00	5,56E+00	1,38E+01
8.45	1,11E+01	4,57E+00	4,95E+00	5,00E+00	1,86E+00	3,35E+00	4,84E+00	5,81E+00	7,17E+00	1,93E+01
8.50	1,21E+01	4,87E+00	5,23E+00	5,33E+00	1,92E+00	3,42E+00	4,96E+00	6,00E+00	7,44E+00	1,99E+01
8.55	1,25E+01	5,31E+00	5,64E+00	5,77E+00	2,00E+00	3,61E+00	5,28E+00	6,39E+00	7,90E+00	2,16E+01
9.00	1,31E+01	6,53E+00	6,78E+00	6,85E+00	2,07E+00	3,76E+00	5,50E+00	6,65E+00	8,24E+00	2,25E+01
9.05	1,68E+01	6,74E+00	7,05E+00	7,12E+00	2,16E+00	3,98E+00	5,77E+00	7,06E+00	8,74E+00	2,36E+01
9.10	1,74E+01	6,94E+00	7,28E+00	7,36E+00	2,25E+00	4,14E+00	5,97E+00	7,34E+00	9,10E+00	2,47E+01
9.15	1,76E+01	7,22E+00	7,55E+00	7,64E+00	2,37E+00	4,34E+00	6,22E+00	7,59E+00	9,39E+00	2,52E+01
9.20	1,80E+01	7,32E+00	7,66E+00	7,77E+00	2,42E+00	4,44E+00	6,37E+00	7,76E+00	9,60E+00	2,56E+01
9.25	1,82E+01	7,61E+00	8,02E+00	8,09E+00	2,53E+00	4,55E+00	6,55E+00	8,01E+00	9,91E+00	2,65E+01
9.30	1,88E+01	7,94E+00	8,38E+00	8,47E+00	2,65E+00	4,78E+00	6,85E+00	8,36E+00	1,03E+01	2,76E+01
9.35	1,92E+01	8,83E+00	8,90E+00	9,08E+00	2,77E+00	5,00E+00	7,11E+00	8,71E+00	1,08E+01	3,00E+01
9.40	1,96E+01	9,03E+00	9,18E+00	9,38E+00	2,95E+00	5,29E+00	7,44E+00	9,13E+00	1,13E+01	3,12E+01
9.45	1,98E+01	9,22E+00	9,38E+00	9,59E+00	3,04E+00	5,41E+00	7,60E+00	9,32E+00	1,15E+01	3,18E+01
9.50	2,00E+01	9,34E+00	9,53E+00	9,75E+00	3,13E+00	5,58E+00	7,82E+00	9,54E+00	1,18E+01	3,23E+01
9.55	2,02E+01	9,45E+00	9,67E+00	9,90E+00	3,16E+00	5,64E+00	7,91E+00	9,65E+00	1,20E+01	3,26E+01
10.00	2,04E+01	9,69E+00	9,88E+00	1,01E+01	3,20E+00	5,76E+00	8,14E+00	9,88E+00	1,23E+01	3,33E+01
10.05	2,06E+01	1,05E+01	1,05E+01	1,08E+01	3,24E+00	5,91E+00	8,43E+00	1,02E+01	1,26E+01	3,40E+01

10.10	2,12E+01	1,06E+01	1,07E+01	1,10E+01	3,24E+00	5,92E+00	8,44E+00	1,02E+01	1,26E+01	3,40E+01
10.15	2,18E+01	1,07E+01	1,09E+01	1,12E+01	3,24E+00	5,92E+00	8,44E+00	1,02E+01	1,26E+01	3,41E+01
10.20	2,20E+01	1,08E+01	1,10E+01	1,13E+01	3,24E+00	5,93E+00	8,46E+00	1,02E+01	1,27E+01	3,41E+01
10.25	2,22E+01	1,11E+01	1,13E+01	1,16E+01	3,27E+00	5,98E+00	8,54E+00	1,03E+01	1,28E+01	3,44E+01
10.30	2,26E+01	1,13E+01	1,15E+01	1,18E+01	3,28E+00	6,03E+00	8,61E+00	1,04E+01	1,29E+01	3,50E+01
10.35	2,30E+01	1,14E+01	1,16E+01	1,19E+01	3,31E+00	6,10E+00	8,73E+00	1,06E+01	1,31E+01	3,55E+01
10.40	2,32E+01	1,15E+01	1,17E+01	1,20E+01	3,32E+00	6,16E+00	8,81E+00	1,06E+01	1,32E+01	3,57E+01
10.45	2,32E+01	1,16E+01	1,18E+01	1,21E+01	3,36E+00	6,25E+00	8,94E+00	1,08E+01	1,34E+01	3,65E+01
10.50	2,34E+01	1,19E+01	1,20E+01	1,23E+01	3,43E+00	6,41E+00	9,22E+00	1,11E+01	1,38E+01	3,73E+01
10.55	2,36E+01	1,20E+01	1,22E+01	1,25E+01	3,43E+00	6,44E+00	9,28E+00	1,12E+01	1,39E+01	3,75E+01
11.00	2,38E+01	1,23E+01	1,24E+01	1,27E+01	3,46E+00	6,55E+00	9,49E+00	1,14E+01	1,42E+01	3,80E+01
11.05	2,38E+01	1,26E+01	1,27E+01	1,30E+01	3,53E+00	6,75E+00	9,80E+00	1,18E+01	1,46E+01	3,88E+01
11.10	2,42E+01	1,29E+01	1,30E+01	1,34E+01	3,60E+00	6,95E+00	1,01E+01	1,21E+01	1,51E+01	3,96E+01
11.15	2,44E+01	1,31E+01	1,33E+01	1,36E+01	3,67E+00	7,22E+00	1,05E+01	1,26E+01	1,57E+01	4,07E+01
11.20	2,46E+01	1,31E+01	1,33E+01	1,37E+01	3,69E+00	7,30E+00	1,07E+01	1,27E+01	1,60E+01	4,12E+01
11.25	2,48E+01	1,31E+01	1,34E+01	1,37E+01	3,69E+00	7,30E+00	1,07E+01	1,28E+01	1,60E+01	4,14E+01
11.30	2,48E+01	1,32E+01	1,34E+01	1,38E+01	3,70E+00	7,33E+00	1,08E+01	1,28E+01	1,61E+01	4,18E+01
11.35	2,48E+01	1,34E+01	1,36E+01	1,40E+01	3,71E+00	7,38E+00	1,08E+01	1,29E+01	1,63E+01	4,21E+01
11.40	2,49E+01	1,35E+01	1,37E+01	1,40E+01	3,72E+00	7,41E+00	1,09E+01	1,30E+01	1,63E+01	4,23E+01
11.45	2,49E+01	1,37E+01	1,38E+01	1,42E+01	3,72E+00	7,48E+00	1,10E+01	1,31E+01	1,65E+01	4,31E+01
11.50	2,49E+01	1,37E+01	1,38E+01	1,42E+01	3,73E+00	7,49E+00	1,10E+01	1,32E+01	1,66E+01	4,32E+01
11.55	2,49E+01	1,37E+01	1,39E+01	1,42E+01	3,73E+00	7,50E+00	1,10E+01	1,32E+01	1,66E+01	4,33E+01
12.00	2,51E+01	1,41E+01	1,42E+01	1,45E+01	3,74E+00	7,56E+00	1,12E+01	1,34E+01	1,69E+01	4,42E+01
12.05	2,53E+01	1,42E+01	1,44E+01	1,47E+01	3,74E+00	7,59E+00	1,13E+01	1,35E+01	1,70E+01	4,47E+01
12.10	2,57E+01	1,46E+01	1,47E+01	1,50E+01	3,75E+00	7,65E+00	1,15E+01	1,38E+01	1,73E+01	4,60E+01
12.15	2,57E+01	1,48E+01	1,48E+01	1,51E+01	3,75E+00	7,72E+00	1,16E+01	1,40E+01	1,75E+01	4,66E+01
12.20	2,57E+01	1,49E+01	1,50E+01	1,53E+01	3,76E+00	7,76E+00	1,17E+01	1,41E+01	1,77E+01	4,67E+01
12.25	2,59E+01	1,50E+01	1,51E+01	1,54E+01	3,77E+00	7,81E+00	1,18E+01	1,42E+01	1,80E+01	4,72E+01
12.30	2,61E+01	1,51E+01	1,51E+01	1,54E+01	3,78E+00	7,85E+00	1,19E+01	1,43E+01	1,80E+01	4,73E+01

Rainfall rate(mm/5min) in point C , 6/7/2012 rainfall event

time	Rg	Pixel	Krig.	IDW	Dow. min.	Dow.1°q.	Dow.2°q.	Dow. Ave.	Dow.3°q.	Dow. max.
7.20	1,98E-01	2,89E-01	2,48E-01	2,66E-01	5,59E-02	1,27E-01	2,83E-01	3,07E-01	5,28E-01	1,11E+00
7.25	1,98E-01	2,92E-01	3,21E-01	3,34E-01	1,70E-01	3,01E-01	3,34E-01	4,45E-01	5,78E-01	1,79E+00
7.30	3,96E-01	3,88E-01	4,51E-01	4,72E-01	1,70E-01	3,12E-01	3,96E-01	4,19E-01	5,61E-01	1,43E+00
7.35	9,90E-01	4,38E-01	5,22E-01	5,40E-01	2,25E-01	3,31E-01	4,37E-01	6,02E-01	6,60E-01	1,69E+00
7.40	1,58E+00	5,21E-01	5,33E-01	4,90E-01	2,09E-01	3,84E-01	5,08E-01	5,87E-01	6,97E-01	2,34E+00
7.45	1,39E+00	2,94E-01	2,58E-01	2,60E-01	7,21E-02	1,66E-01	2,11E-01	2,26E-01	2,98E-01	5,40E-01
7.50	7,92E-01	1,30E-01	1,56E-01	1,62E-01	6,61E-02	1,04E-01	1,38E-01	1,66E-01	2,06E-01	5,13E-01
7.55	7,92E-01	2,29E-01	2,00E-01	2,04E-01	7,12E-02	1,09E-01	1,49E-01	1,62E-01	2,06E-01	4,18E-01
8.00	5,94E-01	6,77E-02	7,94E-02	9,29E-02	4,04E-02	7,23E-02	1,10E-01	1,12E-01	1,39E-01	2,63E-01
8.05	3,96E-01	1,41E-01	1,41E-01	1,47E-01	4,42E-02	7,99E-02	9,60E-02	1,35E-01	1,58E-01	4,72E-01
8.10	3,96E-01	1,98E-01	2,06E-01	2,19E-01	1,04E-01	1,81E-01	2,17E-01	2,54E-01	3,27E-01	8,45E-01

8.15	3,96E-01	1,67E-01	1,76E-01	1,83E-01	5,67E-02	9,73E-02	1,01E-01	1,14E-01	1,64E-01	4,57E-01
8.20	5,94E-01	1,35E-01	1,58E-01	1,62E-01	5,10E-02	5,48E-02	8,56E-02	1,07E-01	1,36E-01	2,24E-01
8.25	3,96E-01	2,66E-01	2,29E-01	2,40E-01	7,65E-02	1,09E-01	1,49E-01	1,48E-01	1,54E-01	2,17E-01
8.30	3,96E-01	2,79E-01	2,81E-01	2,89E-01	1,21E-01	2,01E-01	2,66E-01	2,58E-01	3,03E-01	3,92E-01
8.35	5,94E-01	3,33E-01	3,23E-01	3,37E-01	9,70E-02	1,69E-01	2,24E-01	2,25E-01	2,88E-01	4,08E-01
8.40	5,94E-01	1,64E-01	2,30E-01	2,38E-01	5,10E-02	9,90E-02	1,26E-01	1,66E-01	1,86E-01	4,58E-01
8.45	3,96E-01	2,40E-01	4,38E-01	3,58E-01	2,09E-01	4,90E-01	1,04E+00	1,38E+00	1,83E+00	5,49E+00
8.50	9,90E-01	3,02E-01	2,81E-01	3,31E-01	5,71E-02	1,21E-01	1,34E-01	1,83E-01	2,63E-01	1,07E+00
8.55	3,96E-01	4,40E-01	4,07E-01	4,62E-01	8,34E-02	1,81E-01	2,64E-01	3,95E-01	4,69E-01	1,72E+00
9.00	5,94E-01	1,22E+00	1,14E+00	1,04E+00	6,21E-02	1,29E-01	2,18E-01	2,57E-01	3,50E-01	1,46E+00
9.05	3,17E+00	2,06E-01	2,64E-01	2,77E-01	8,99E-02	1,28E-01	2,46E-01	4,11E-01	4,96E-01	2,24E+00
9.10	5,94E-01	2,01E-01	2,34E-01	2,47E-01	8,61E-02	1,60E-01	1,96E-01	2,81E-01	3,17E-01	9,97E-01
9.15	1,98E-01	2,79E-01	2,68E-01	2,74E-01	1,08E-01	1,80E-01	2,34E-01	2,48E-01	2,68E-01	4,50E-01
9.20	5,94E-01	1,02E-01	1,11E-01	1,28E-01	5,11E-02	1,07E-01	1,52E-01	1,74E-01	2,25E-01	5,57E-01
9.25	0,00E+00	2,94E-01	3,61E-01	3,23E-01	1,03E-01	1,09E-01	1,79E-01	2,46E-01	3,00E-01	8,71E-01
9.30	3,96E-01	3,28E-01	3,54E-01	3,75E-01	1,26E-01	2,28E-01	2,86E-01	3,49E-01	3,73E-01	7,59E-01
9.35	3,96E-01	8,88E-01	5,20E-01	6,38E-01	1,23E-01	2,34E-01	2,57E-01	3,53E-01	4,32E-01	1,38E+00
9.40	3,96E-01	2,03E-01	2,84E-01	2,88E-01	1,84E-01	2,96E-01	3,66E-01	4,15E-01	5,31E-01	1,24E+00
9.45	1,98E-01	1,82E-01	2,04E-01	2,08E-01	9,86E-02	1,49E-01	1,70E-01	1,89E-01	2,56E-01	9,62E-01
9.50	1,98E-01	1,25E-01	1,51E-01	1,59E-01	8,69E-02	1,61E-01	1,82E-01	2,26E-01	2,47E-01	4,48E-01
9.55	1,98E-01	1,09E-01	1,40E-01	1,51E-01	3,39E-02	6,30E-02	8,45E-02	1,04E-01	1,23E-01	3,21E-01
10.00	0,00E+00	2,37E-01	2,10E-01	2,53E-01	3,86E-02	1,05E-01	1,84E-01	2,38E-01	2,87E-01	7,22E-01
10.05	1,98E-01	7,63E-01	6,19E-01	6,20E-01	7,26E-02	1,48E-01	2,83E-01	3,03E-01	3,07E-01	6,06E-01
10.10	7,92E-01	1,74E-01	1,94E-01	2,08E-01	7,42E-04	5,21E-03	1,18E-02	1,32E-02	2,06E-02	3,71E-02
10.15	3,96E-01	9,64E-02	1,73E-01	1,48E-01	1,53E-03	5,45E-03	9,14E-03	1,11E-02	1,43E-02	6,17E-02
10.20	1,98E-01	1,09E-01	1,35E-01	1,42E-01	1,44E-03	7,54E-03	1,55E-02	1,99E-02	2,30E-02	4,88E-02
10.25	1,98E-01	2,89E-01	3,05E-01	2,68E-01	2,21E-02	4,78E-02	7,31E-02	8,17E-02	1,01E-01	3,74E-01
10.30	3,96E-01	1,56E-01	1,79E-01	1,79E-01	1,02E-02	2,96E-02	7,93E-02	1,06E-01	1,36E-01	3,98E-01
10.35	3,96E-01	1,54E-01	1,21E-01	1,32E-01	2,29E-02	8,63E-02	1,19E-01	1,39E-01	2,10E-01	5,66E-01
10.40	1,98E-01	1,07E-01	1,07E-01	1,14E-01	1,55E-02	5,05E-02	7,41E-02	8,22E-02	1,13E-01	2,19E-01
10.45	0,00E+00	9,90E-02	1,05E-01	1,16E-01	3,69E-02	1,02E-01	1,37E-01	1,86E-01	2,07E-01	5,04E-01
10.50	1,98E-01	2,32E-01	2,11E-01	2,14E-01	4,99E-02	1,82E-01	2,82E-01	3,00E-01	4,45E-01	7,35E-01
10.55	0,00E+00	1,51E-01	1,52E-01	1,53E-01	1,86E-03	2,90E-02	7,10E-02	8,25E-02	8,51E-02	2,21E-01
11.00	1,98E-01	2,79E-01	2,42E-01	2,60E-01	1,47E-02	1,14E-01	2,07E-01	2,19E-01	2,63E-01	5,09E-01
11.05	1,98E-01	3,26E-01	3,00E-01	3,10E-01	7,02E-02	1,99E-01	3,09E-01	3,40E-01	4,19E-01	6,53E-01
11.10	1,98E-01	2,40E-01	2,80E-01	3,04E-01	7,02E-02	1,99E-01	3,09E-01	3,40E-01	4,19E-01	6,53E-01
11.15	3,96E-01	1,98E-01	2,58E-01	2,35E-01	1,14E-01	3,11E-01	4,93E-01	4,45E-01	6,91E-01	1,67E+00
11.20	1,98E-01	4,17E-02	6,93E-02	7,62E-02	1,35E-02	7,03E-02	1,47E-01	1,72E-01	2,70E-01	5,16E-01
11.25	0,00E+00	2,60E-02	3,23E-02	3,64E-02	8,82E-04	9,00E-03	2,20E-02	2,98E-02	5,40E-02	1,53E-01
11.30	0,00E+00	7,55E-02	7,92E-02	9,53E-02	7,11E-03	3,29E-02	5,95E-02	6,79E-02	8,72E-02	2,55E-01
11.35	0,00E+00	2,34E-01	1,88E-01	1,83E-01	9,20E-03	4,61E-02	8,17E-02	1,08E-01	1,23E-01	4,28E-01
11.40	1,98E-01	4,17E-02	5,57E-02	6,23E-02	7,05E-03	2,46E-02	3,90E-02	6,18E-02	6,63E-02	2,47E-01
11.45	0,00E+00	1,85E-01	1,20E-01	1,22E-01	2,56E-02	6,96E-02	1,29E-01	1,44E-01	2,40E-01	5,55E-01
11.50	0,00E+00	2,08E-02	2,21E-02	3,03E-02	8,20E-04	5,49E-03	1,42E-02	1,72E-02	2,23E-02	5,16E-02
11.55	0,00E+00	2,86E-02	3,80E-02	4,98E-02	1,77E-03	1,30E-02	2,72E-02	3,17E-02	5,28E-02	1,20E-01
12.00	1,98E-01	3,41E-01	2,97E-01	2,74E-01	1,18E-02	8,08E-02	1,81E-01	2,04E-01	3,11E-01	5,78E-01
12.05	1,98E-01	1,56E-01	2,05E-01	1,79E-01	1,17E-02	4,19E-02	1,09E-01	1,12E-01	2,51E-01	6,16E-01
12.10	3,96E-01	4,35E-01	2,82E-01	3,21E-01	4,13E-03	5,68E-02	1,79E-01	3,06E-01	2,61E-01	1,33E+00
12.15	0,00E+00	1,46E-01	1,41E-01	1,26E-01	7,99E-03	5,92E-02	1,55E-01	1,99E-01	2,16E-01	6,07E-01
12.20	0,00E+00	1,46E-01	1,64E-01	1,73E-01	9,21E-03	4,06E-02	8,47E-02	9,13E-02	8,68E-02	1,82E-01
12.25	1,98E-01	1,09E-01	1,40E-01	1,29E-01	7,88E-03	5,30E-02	1,22E-01	1,47E-01	1,77E-01	4,88E-01
12.30	1,98E-01	1,56E-02	1,67E-02	2,61E-02	7,72E-03	3,66E-02	7,85E-02	8,47E-02	8,07E-02	1,76E-01

Rainfall accumulation(mm) in point C , 6/7/2012 rainfall event

time	Rg	Pixel	Krig.	IDW	Dow. min.	Dow.1°q.	Dow.2°q.	Dow. Ave.	Dow.3°q.	Dow. max.
7.20	1,98E-01	2,89E-01	2,48E-01	2,66E-01	5,59E-02	1,27E-01	2,83E-01	3,07E-01	5,28E-01	1,11E+00
7.25	3,96E-01	5,81E-01	5,69E-01	6,00E-01	2,25E-01	4,28E-01	6,17E-01	7,53E-01	1,11E+00	2,90E+00
7.30	7,92E-01	9,69E-01	1,02E+00	1,07E+00	3,95E-01	7,40E-01	1,01E+00	1,17E+00	1,67E+00	4,33E+00
7.35	1,78E+00	1,41E+00	1,54E+00	1,61E+00	6,20E-01	1,07E+00	1,45E+00	1,77E+00	2,33E+00	6,02E+00
7.40	3,37E+00	1,93E+00	2,08E+00	2,10E+00	8,29E-01	1,45E+00	1,96E+00	2,36E+00	3,02E+00	8,36E+00
7.45	4,75E+00	2,22E+00	2,33E+00	2,36E+00	9,01E-01	1,62E+00	2,17E+00	2,59E+00	3,32E+00	8,90E+00
7.50	5,54E+00	2,35E+00	2,49E+00	2,52E+00	9,67E-01	1,72E+00	2,31E+00	2,75E+00	3,53E+00	9,41E+00
7.55	6,34E+00	2,58E+00	2,69E+00	2,73E+00	1,04E+00	1,83E+00	2,46E+00	2,91E+00	3,73E+00	9,83E+00
8.00	6,93E+00	2,65E+00	2,77E+00	2,82E+00	1,08E+00	1,91E+00	2,57E+00	3,03E+00	3,87E+00	1,01E+01
8.05	7,33E+00	2,79E+00	2,91E+00	2,97E+00	1,12E+00	1,99E+00	2,66E+00	3,16E+00	4,03E+00	1,06E+01
8.10	7,72E+00	2,99E+00	3,12E+00	3,19E+00	1,23E+00	2,17E+00	2,88E+00	3,42E+00	4,36E+00	1,14E+01
8.15	8,12E+00	3,15E+00	3,29E+00	3,37E+00	1,28E+00	2,26E+00	2,98E+00	3,53E+00	4,52E+00	1,19E+01
8.20	8,71E+00	3,29E+00	3,45E+00	3,53E+00	1,34E+00	2,32E+00	3,07E+00	3,64E+00	4,66E+00	1,21E+01
8.25	9,11E+00	3,55E+00	3,68E+00	3,77E+00	1,41E+00	2,43E+00	3,22E+00	3,78E+00	4,81E+00	1,23E+01
8.30	9,50E+00	3,83E+00	3,96E+00	4,06E+00	1,53E+00	2,63E+00	3,48E+00	4,04E+00	5,11E+00	1,27E+01
8.35	1,01E+01	4,17E+00	4,28E+00	4,40E+00	1,63E+00	2,80E+00	3,71E+00	4,27E+00	5,40E+00	1,31E+01
8.40	1,07E+01	4,33E+00	4,51E+00	4,64E+00	1,68E+00	2,90E+00	3,83E+00	4,43E+00	5,59E+00	1,36E+01
8.45	1,11E+01	4,57E+00	4,95E+00	4,99E+00	1,89E+00	3,39E+00	4,87E+00	5,81E+00	7,42E+00	1,91E+01
8.50	1,21E+01	4,87E+00	5,23E+00	5,32E+00	1,95E+00	3,51E+00	5,00E+00	6,00E+00	7,69E+00	2,01E+01
8.55	1,25E+01	5,31E+00	5,64E+00	5,79E+00	2,03E+00	3,69E+00	5,27E+00	6,39E+00	8,15E+00	2,18E+01
9.00	1,31E+01	6,53E+00	6,78E+00	6,82E+00	2,09E+00	3,82E+00	5,49E+00	6,65E+00	8,50E+00	2,33E+01
9.05	1,62E+01	6,74E+00	7,05E+00	7,10E+00	2,18E+00	3,95E+00	5,73E+00	7,06E+00	9,00E+00	2,55E+01
9.10	1,68E+01	6,94E+00	7,28E+00	7,35E+00	2,27E+00	4,11E+00	5,93E+00	7,34E+00	9,32E+00	2,65E+01
9.15	1,70E+01	7,22E+00	7,55E+00	7,62E+00	2,38E+00	4,29E+00	6,16E+00	7,59E+00	9,59E+00	2,70E+01
9.20	1,76E+01	7,32E+00	7,66E+00	7,75E+00	2,43E+00	4,39E+00	6,31E+00	7,76E+00	9,81E+00	2,75E+01
9.25	1,76E+01	7,61E+00	8,02E+00	8,07E+00	2,53E+00	4,50E+00	6,49E+00	8,01E+00	1,01E+01	2,84E+01
9.30	1,80E+01	7,94E+00	8,38E+00	8,45E+00	2,66E+00	4,73E+00	6,78E+00	8,36E+00	1,05E+01	2,92E+01
9.35	1,84E+01	8,83E+00	8,90E+00	9,09E+00	2,78E+00	4,97E+00	7,04E+00	8,71E+00	1,09E+01	3,06E+01
9.40	1,88E+01	9,03E+00	9,18E+00	9,37E+00	2,96E+00	5,26E+00	7,40E+00	9,13E+00	1,14E+01	3,18E+01
9.45	1,90E+01	9,22E+00	9,38E+00	9,58E+00	3,06E+00	5,41E+00	7,57E+00	9,32E+00	1,17E+01	3,28E+01
9.50	1,92E+01	9,34E+00	9,53E+00	9,74E+00	3,15E+00	5,57E+00	7,76E+00	9,54E+00	1,19E+01	3,32E+01
9.55	1,94E+01	9,45E+00	9,67E+00	9,89E+00	3,18E+00	5,63E+00	7,84E+00	9,65E+00	1,21E+01	3,35E+01
10.00	1,94E+01	9,69E+00	9,88E+00	1,01E+01	3,22E+00	5,74E+00	8,02E+00	9,88E+00	1,24E+01	3,43E+01
10.05	1,96E+01	1,05E+01	1,05E+01	1,08E+01	3,29E+00	5,89E+00	8,31E+00	1,02E+01	1,27E+01	3,49E+01
10.10	2,04E+01	1,06E+01	1,07E+01	1,10E+01	3,29E+00	5,89E+00	8,32E+00	1,02E+01	1,27E+01	3,49E+01
10.15	2,08E+01	1,07E+01	1,09E+01	1,11E+01	3,30E+00	5,90E+00	8,33E+00	1,02E+01	1,27E+01	3,50E+01
10.20	2,10E+01	1,08E+01	1,10E+01	1,13E+01	3,30E+00	5,91E+00	8,34E+00	1,02E+01	1,27E+01	3,50E+01
10.25	2,12E+01	1,11E+01	1,13E+01	1,15E+01	3,32E+00	5,95E+00	8,42E+00	1,03E+01	1,28E+01	3,54E+01
10.30	2,16E+01	1,13E+01	1,15E+01	1,17E+01	3,33E+00	5,98E+00	8,50E+00	1,04E+01	1,30E+01	3,58E+01
10.35	2,20E+01	1,14E+01	1,16E+01	1,18E+01	3,35E+00	6,07E+00	8,61E+00	1,06E+01	1,32E+01	3,63E+01
10.40	2,22E+01	1,15E+01	1,17E+01	1,20E+01	3,37E+00	6,12E+00	8,69E+00	1,06E+01	1,33E+01	3,66E+01
10.45	2,22E+01	1,16E+01	1,18E+01	1,21E+01	3,41E+00	6,22E+00	8,83E+00	1,08E+01	1,35E+01	3,71E+01
10.50	2,24E+01	1,19E+01	1,20E+01	1,23E+01	3,46E+00	6,40E+00	9,11E+00	1,11E+01	1,39E+01	3,78E+01
10.55	2,24E+01	1,20E+01	1,22E+01	1,24E+01	3,46E+00	6,43E+00	9,18E+00	1,12E+01	1,40E+01	3,80E+01
11.00	2,26E+01	1,23E+01	1,24E+01	1,27E+01	3,47E+00	6,55E+00	9,39E+00	1,14E+01	1,43E+01	3,85E+01
11.05	2,28E+01	1,26E+01	1,27E+01	1,30E+01	3,54E+00	6,74E+00	9,70E+00	1,18E+01	1,47E+01	3,92E+01
11.10	2,30E+01	1,29E+01	1,30E+01	1,33E+01	3,61E+00	6,94E+00	1,00E+01	1,21E+01	1,51E+01	3,98E+01
11.15	2,34E+01	1,31E+01	1,33E+01	1,35E+01	3,73E+00	7,25E+00	1,05E+01	1,26E+01	1,58E+01	4,15E+01

11.20	2,36E+01	1,31E+01	1,33E+01	1,36E+01	3,74E+00	7,32E+00	1,06E+01	1,27E+01	1,61E+01	4,20E+01
11.25	2,36E+01	1,31E+01	1,34E+01	1,37E+01	3,74E+00	7,33E+00	1,07E+01	1,28E+01	1,61E+01	4,22E+01
11.30	2,36E+01	1,32E+01	1,34E+01	1,38E+01	3,75E+00	7,37E+00	1,07E+01	1,28E+01	1,62E+01	4,24E+01
11.35	2,36E+01	1,34E+01	1,36E+01	1,39E+01	3,76E+00	7,41E+00	1,08E+01	1,29E+01	1,63E+01	4,29E+01
11.40	2,38E+01	1,35E+01	1,37E+01	1,40E+01	3,76E+00	7,44E+00	1,08E+01	1,30E+01	1,64E+01	4,31E+01
11.45	2,38E+01	1,37E+01	1,38E+01	1,41E+01	3,79E+00	7,51E+00	1,10E+01	1,31E+01	1,67E+01	4,37E+01
11.50	2,38E+01	1,37E+01	1,38E+01	1,42E+01	3,79E+00	7,51E+00	1,10E+01	1,32E+01	1,67E+01	4,37E+01
11.55	2,38E+01	1,37E+01	1,39E+01	1,42E+01	3,79E+00	7,53E+00	1,10E+01	1,32E+01	1,67E+01	4,38E+01
12.00	2,40E+01	1,41E+01	1,42E+01	1,45E+01	3,80E+00	7,61E+00	1,12E+01	1,34E+01	1,70E+01	4,44E+01
12.05	2,42E+01	1,42E+01	1,44E+01	1,47E+01	3,82E+00	7,65E+00	1,13E+01	1,35E+01	1,73E+01	4,50E+01
12.10	2,46E+01	1,46E+01	1,47E+01	1,50E+01	3,82E+00	7,70E+00	1,15E+01	1,38E+01	1,76E+01	4,64E+01
12.15	2,46E+01	1,48E+01	1,48E+01	1,51E+01	3,83E+00	7,76E+00	1,16E+01	1,40E+01	1,78E+01	4,70E+01
12.20	2,46E+01	1,49E+01	1,50E+01	1,53E+01	3,84E+00	7,80E+00	1,17E+01	1,41E+01	1,79E+01	4,71E+01
12.25	2,48E+01	1,50E+01	1,51E+01	1,54E+01	3,85E+00	7,86E+00	1,18E+01	1,42E+01	1,80E+01	4,76E+01
12.30	2,49E+01	1,51E+01	1,51E+01	1,54E+01	3,85E+00	7,89E+00	1,19E+01	1,43E+01	1,81E+01	4,78E+01

22/6/2012 event

Rainfall rate(mm/5min) in point A , 22/6/2012 rainfall event

time	Rg	Pixel	Krig.	IDW	Dow. min.	Dow.1°q.	Dow.2°q.	Dow. Ave.	Dow.3°q.	Dow. max.
02.35	0,00E+00	3,39E-02	2,89E-02	3,49E-02	1,42E-05	1,58E-03	1,37E-02	5,09E-02	9,69E-02	3,20E-01
02.40	0,00E+00	4,69E-02	5,78E-02	4,57E-02	9,15E-07	1,35E-03	1,06E-02	4,80E-02	3,21E-02	6,29E-01
02.45	2,02E-01	1,56E-02	3,88E-02	2,94E-02	1,73E-03	1,42E-02	4,12E-02	8,96E-02	1,61E-01	4,88E-01
02.50	0,00E+00	1,02E-01	7,06E-02	7,45E-02	1,98E-04	4,38E-03	2,03E-02	4,41E-02	3,80E-02	2,70E-01
02.55	4,04E-01	9,90E-02	7,45E-02	7,56E-02	5,59E-05	2,50E-03	1,27E-02	2,35E-02	2,58E-02	1,12E-01
03.00	2,02E-01	6,25E-02	5,76E-02	5,77E-02	9,15E-06	2,32E-03	2,16E-02	9,64E-02	1,46E-01	6,97E-01
03.05	2,02E-01	8,85E-02	8,65E-02	7,67E-02	2,34E-06	1,64E-03	1,16E-02	3,66E-02	2,13E-02	3,69E-01
03.10	2,02E-01	8,07E-02	6,56E-02	6,90E-02	5,16E-04	2,19E-03	6,97E-03	1,16E-02	2,07E-02	5,03E-02
03.15	2,02E-01	7,03E-02	5,16E-02	5,67E-02	8,82E-04	2,89E-03	5,06E-03	6,54E-03	9,11E-03	2,65E-02
03.20	2,02E-01	3,39E-02	3,36E-02	3,15E-02	1,50E-04	9,39E-04	2,35E-03	2,53E-03	2,35E-03	5,87E-03
03.25	0,00E+00	2,60E-03	6,77E-03	6,85E-03	6,95E-05	1,12E-03	3,60E-03	5,11E-03	5,98E-03	4,47E-02
03.30	0,00E+00	0,00E+00	4,69E-03	4,13E-03	5,13E-06	4,39E-04	1,73E-03	5,71E-03	5,45E-03	6,16E-02
03.35	0,00E+00	1,04E-02	8,85E-03	9,49E-03	2,84E-05	1,42E-03	6,61E-03	1,57E-02	2,41E-02	7,96E-02
03.40	0,00E+00	7,81E-03	1,07E-02	1,03E-02	6,85E-04	3,96E-03	9,45E-03	9,90E-03	9,70E-03	2,35E-02
03.45	0,00E+00	1,04E-02	8,07E-03	1,73E-02	2,45E-03	7,36E-03	1,14E-02	1,44E-02	1,81E-02	5,47E-02
03.50	2,02E-01	1,56E-02	2,73E-02	2,82E-02	2,30E-02	5,96E-02	7,97E-02	8,02E-02	9,24E-02	1,57E-01
03.55	0,00E+00	5,73E-02	5,63E-02	6,16E-02	3,25E-02	6,46E-02	8,62E-02	8,60E-02	1,00E-01	1,43E-01
04.00	2,02E-01	1,67E-01	1,89E-01	1,62E-01	3,19E-02	9,93E-02	1,60E-01	1,70E-01	2,49E-01	3,08E-01
04.05	2,02E-01	2,01E-01	1,59E-01	1,70E-01	5,84E-02	1,41E-01	2,08E-01	2,16E-01	2,51E-01	5,34E-01
04.10	2,02E-01	2,42E-01	1,98E-01	2,09E-01	6,04E-02	1,40E-01	2,05E-01	2,17E-01	2,69E-01	5,83E-01
04.15	0,00E+00	1,77E-01	2,14E-01	1,88E-01	2,50E-02	1,62E-01	2,36E-01	2,92E-01	4,11E-01	8,19E-01
04.20	2,02E-01	1,77E-01	1,64E-01	1,58E-01	2,22E-02	8,10E-02	1,40E-01	1,46E-01	1,81E-01	3,63E-01
04.25	0,00E+00	4,95E-02	6,43E-02	6,16E-02	5,71E-03	2,09E-02	3,98E-02	4,19E-02	6,96E-02	9,60E-02
04.30	2,02E-01	1,82E-02	2,27E-02	2,55E-02	2,41E-04	1,89E-03	4,38E-03	6,41E-03	7,88E-03	3,28E-02
04.35	0,00E+00	1,30E-02	1,54E-02	1,89E-02	1,49E-03	1,88E-02	4,25E-02	6,69E-02	9,64E-02	2,59E-01
04.40	0,00E+00	3,65E-02	5,13E-02	4,19E-02	9,04E-04	9,10E-03	2,59E-02	3,44E-02	6,75E-02	1,27E-01
04.45	0,00E+00	2,34E-02	4,58E-02	3,54E-02	1,36E-03	1,67E-02	2,57E-02	3,52E-02	4,02E-02	2,68E-01
04.50	0,00E+00	7,81E-03	7,55E-03	1,53E-02	1,23E-03	8,41E-03	1,87E-02	2,22E-02	3,15E-02	7,90E-02
04.55	0,00E+00	1,56E-02	3,12E-02	2,19E-02	2,09E-03	2,02E-02	5,69E-02	7,23E-02	7,73E-02	2,66E-01
05.00	0,00E+00	2,08E-02	3,10E-02	2,91E-02	1,18E-02	4,07E-02	7,41E-02	7,80E-02	1,33E-01	1,45E-01
05.05	2,02E-01	4,17E-02	3,65E-02	3,84E-02	2,95E-03	1,25E-02	2,46E-02	2,45E-02	2,67E-02	5,27E-02
05.10	0,00E+00	1,04E-02	1,41E-02	1,61E-02	1,88E-03	6,96E-03	1,21E-02	1,31E-02	1,88E-02	3,01E-02
05.15	0,00E+00	2,60E-02	2,21E-02	2,25E-02	3,79E-03	9,42E-03	1,43E-02	2,01E-02	2,58E-02	6,33E-02
05.20	0,00E+00	1,30E-02	1,43E-02	1,44E-02	3,33E-04	4,79E-03	1,56E-02	2,05E-02	2,85E-02	8,77E-02
05.25	2,02E-01	5,21E-03	1,09E-02	9,56E-03	2,16E-04	2,62E-03	5,87E-03	1,01E-02	1,41E-02	4,81E-02
05.30	0,00E+00	7,81E-03	1,20E-02	1,21E-02	8,41E-04	6,33E-03	1,63E-02	1,86E-02	2,50E-02	7,00E-02
05.35	0,00E+00	1,56E-02	2,11E-02	1,85E-02	1,77E-03	8,75E-03	1,85E-02	2,36E-02	2,88E-02	1,53E-01
05.40	0,00E+00	1,82E-02	1,69E-02	1,93E-02	4,31E-03	1,09E-02	1,76E-02	2,47E-02	2,98E-02	1,48E-01
05.45	0,00E+00	1,56E-02	2,06E-02	2,17E-02	3,96E-03	1,31E-02	1,82E-02	2,42E-02	2,89E-02	8,35E-02
05.50	2,02E-01	4,17E-02	3,75E-02	3,96E-02	9,31E-03	3,51E-02	5,57E-02	7,25E-02	1,01E-01	2,47E-01
05.55	0,00E+00	2,60E-02	3,98E-02	3,22E-02	8,03E-03	2,65E-02	5,49E-02	6,93E-02	7,30E-02	2,18E-01
06.00	0,00E+00	2,86E-02	3,31E-02	3,18E-02	4,59E-03	1,94E-02	3,71E-02	3,76E-02	4,20E-02	9,26E-02
06.05	2,02E-01	3,91E-02	4,17E-02	4,09E-02	1,75E-03	9,33E-03	2,10E-02	2,46E-02	4,42E-02	5,94E-02

06.10	0,00E+00	1,30E-02	1,93E-02	2,04E-02	2,81E-04	1,12E-03	3,71E-03	4,67E-03	4,45E-03	1,83E-02
06.15	0,00E+00	2,60E-02	2,14E-02	2,64E-02	4,13E-04	3,17E-03	7,02E-03	1,10E-02	1,56E-02	5,96E-02
06.20	0,00E+00	3,91E-02	5,83E-02	5,23E-02	2,28E-02	6,94E-02	1,20E-01	1,22E-01	1,85E-01	2,17E-01
06.25	0,00E+00	9,38E-02	9,58E-02	9,85E-02	2,81E-02	1,18E-01	2,33E-01	2,46E-01	4,62E-01	5,09E-01
06.30	2,02E-01	2,27E-01	1,63E-01	1,83E-01	2,37E-02	9,03E-02	1,46E-01	1,68E-01	2,36E-01	5,10E-01
06.35	2,02E-01	1,43E-01	1,42E-01	1,36E-01	2,07E-02	5,31E-02	6,96E-02	8,38E-02	1,05E-01	2,41E-01
06.40	0,00E+00	9,64E-02	1,13E-01	1,03E-01	1,13E-02	7,03E-02	1,44E-01	1,78E-01	2,33E-01	4,96E-01
06.45	2,02E-01	3,39E-02	4,97E-02	4,93E-02	1,12E-02	5,53E-02	1,07E-01	1,35E-01	2,14E-01	3,89E-01
06.50	0,00E+00	2,60E-02	4,37E-02	4,38E-02	1,76E-02	8,44E-02	1,51E-01	1,85E-01	2,47E-01	5,54E-01
06.55	2,02E-01	4,95E-02	5,00E-02	5,37E-02	3,61E-03	1,70E-02	2,95E-02	3,42E-02	4,72E-02	1,05E-01
07.00	0,00E+00	3,91E-02	3,85E-02	4,26E-02	6,18E-03	2,45E-02	3,57E-02	4,32E-02	5,79E-02	1,19E-01
07.05	0,00E+00	4,43E-02	4,53E-02	4,56E-02	3,03E-03	3,26E-02	6,32E-02	7,05E-02	8,05E-02	2,19E-01
07.10	2,02E-01	4,17E-02	5,08E-02	4,55E-02	1,77E-03	1,27E-02	2,64E-02	3,22E-02	4,34E-02	1,50E-01
07.15	2,02E-01	3,39E-02	4,24E-02	3,75E-02	2,49E-03	5,94E-03	1,42E-02	1,55E-02	1,49E-02	3,66E-02
07.20	0,00E+00	2,08E-02	3,49E-02	2,41E-02	1,74E-03	1,94E-02	3,77E-02	5,94E-02	7,42E-02	3,27E-01
07.25	0,00E+00	1,04E-02	1,33E-02	1,02E-02	2,48E-05	4,34E-04	1,75E-03	2,29E-03	1,91E-03	7,89E-03
07.30	0,00E+00	0,00E+00	5,21E-04	1,47E-03	0,00E+00	0,00E+00	0,00E+00	0,00E+00	0,00E+00	0,00E+00
07.35	0,00E+00	1,04E-02	4,17E-03	8,89E-03	1,72E-07	1,05E-05	3,52E-04	5,80E-03	1,02E-02	6,77E-02
07.40	2,02E-01	4,69E-02	3,96E-02	3,88E-02	1,85E-06	2,73E-04	3,69E-03	7,23E-02	1,57E-02	1,21E+00
07.45	0,00E+00	8,85E-02	4,32E-02	6,11E-02	3,36E-07	1,10E-04	2,14E-03	1,29E-02	5,83E-03	1,05E-01

Rainfall accumulation(mm) in point A , 22/6/2012 rainfall event

time	Rg	Pixel	Krig.	IDW	Dow. min.	Dow.1°q.	Dow.2°q.	Dow. Ave.	Dow.3°q.	Dow. max.
02.35	0,00E+00	3,39E-02	2,89E-02	3,49E-02	1,42E-05	1,58E-03	1,37E-02	5,09E-02	9,69E-02	3,20E-01
02.40	0,00E+00	8,07E-02	8,67E-02	8,06E-02	1,51E-05	2,93E-03	2,43E-02	9,89E-02	1,29E-01	9,50E-01
02.45	2,02E-01	9,64E-02	1,26E-01	1,10E-01	1,74E-03	1,71E-02	6,55E-02	1,89E-01	2,90E-01	1,44E+00
02.50	2,02E-01	1,98E-01	1,96E-01	1,84E-01	1,94E-03	2,15E-02	8,58E-02	2,33E-01	3,28E-01	1,71E+00
02.55	6,06E-01	2,97E-01	2,71E-01	2,60E-01	2,00E-03	2,40E-02	9,85E-02	2,56E-01	3,54E-01	1,82E+00
03.00	8,08E-01	3,59E-01	3,28E-01	3,18E-01	2,01E-03	2,63E-02	1,20E-01	3,52E-01	5,00E-01	2,52E+00
03.05	1,01E+00	4,48E-01	4,15E-01	3,95E-01	2,01E-03	2,80E-02	1,32E-01	3,89E-01	5,22E-01	2,88E+00
03.10	1,21E+00	5,29E-01	4,80E-01	4,64E-01	2,52E-03	3,02E-02	1,39E-01	4,01E-01	5,43E-01	2,93E+00
03.15	1,41E+00	5,99E-01	5,32E-01	5,20E-01	3,41E-03	3,31E-02	1,44E-01	4,07E-01	5,52E-01	2,96E+00
03.20	1,62E+00	6,33E-01	5,65E-01	5,52E-01	3,56E-03	3,40E-02	1,46E-01	4,10E-01	5,54E-01	2,97E+00
03.25	1,62E+00	6,35E-01	5,72E-01	5,59E-01	3,63E-03	3,51E-02	1,50E-01	4,15E-01	5,60E-01	3,01E+00
03.30	1,62E+00	6,35E-01	5,77E-01	5,63E-01	3,63E-03	3,56E-02	1,51E-01	4,21E-01	5,65E-01	3,07E+00
03.35	1,62E+00	6,46E-01	5,86E-01	5,72E-01	3,66E-03	3,70E-02	1,58E-01	4,36E-01	5,89E-01	3,15E+00
03.40	1,62E+00	6,54E-01	5,96E-01	5,83E-01	4,34E-03	4,09E-02	1,67E-01	4,46E-01	5,99E-01	3,18E+00
03.45	1,62E+00	6,64E-01	6,04E-01	6,00E-01	6,79E-03	4,83E-02	1,79E-01	4,61E-01	6,17E-01	3,23E+00
03.50	1,82E+00	6,80E-01	6,32E-01	6,28E-01	2,98E-02	1,08E-01	2,58E-01	5,41E-01	7,10E-01	3,39E+00
03.55	1,82E+00	7,37E-01	6,88E-01	6,90E-01	6,23E-02	1,72E-01	3,45E-01	6,27E-01	8,10E-01	3,53E+00
04.00	2,02E+00	9,04E-01	8,77E-01	8,52E-01	9,42E-02	2,72E-01	5,05E-01	7,97E-01	1,06E+00	3,84E+00
04.05	2,22E+00	1,10E+00	1,04E+00	1,02E+00	1,53E-01	4,12E-01	7,13E-01	1,01E+00	1,31E+00	4,37E+00
04.10	2,42E+00	1,35E+00	1,23E+00	1,23E+00	2,13E-01	5,53E-01	9,19E-01	1,23E+00	1,58E+00	4,96E+00
04.15	2,42E+00	1,52E+00	1,45E+00	1,42E+00	2,38E-01	7,15E-01	1,16E+00	1,52E+00	1,99E+00	5,78E+00
04.20	2,63E+00	1,70E+00	1,61E+00	1,58E+00	2,60E-01	7,96E-01	1,29E+00	1,67E+00	2,17E+00	6,14E+00
04.25	2,63E+00	1,75E+00	1,68E+00	1,64E+00	2,66E-01	8,17E-01	1,33E+00	1,71E+00	2,24E+00	6,23E+00

04.30	2,83E+00	1,77E+00	1,70E+00	1,66E+00	2,66E-01	8,19E-01	1,34E+00	1,72E+00	2,25E+00	6,27E+00
04.35	2,83E+00	1,78E+00	1,71E+00	1,68E+00	2,68E-01	8,37E-01	1,38E+00	1,78E+00	2,35E+00	6,53E+00
04.40	2,83E+00	1,82E+00	1,77E+00	1,72E+00	2,69E-01	8,46E-01	1,41E+00	1,82E+00	2,41E+00	6,65E+00
04.45	2,83E+00	1,84E+00	1,81E+00	1,76E+00	2,70E-01	8,63E-01	1,43E+00	1,85E+00	2,45E+00	6,92E+00
04.50	2,83E+00	1,85E+00	1,82E+00	1,78E+00	2,71E-01	8,72E-01	1,45E+00	1,87E+00	2,48E+00	7,00E+00
04.55	2,83E+00	1,86E+00	1,85E+00	1,80E+00	2,73E-01	8,92E-01	1,51E+00	1,95E+00	2,56E+00	7,27E+00
05.00	2,83E+00	1,89E+00	1,88E+00	1,83E+00	2,85E-01	9,32E-01	1,58E+00	2,03E+00	2,70E+00	7,41E+00
05.05	3,03E+00	1,93E+00	1,92E+00	1,86E+00	2,88E-01	9,45E-01	1,61E+00	2,05E+00	2,72E+00	7,46E+00
05.10	3,03E+00	1,94E+00	1,93E+00	1,88E+00	2,90E-01	9,52E-01	1,62E+00	2,06E+00	2,74E+00	7,49E+00
05.15	3,03E+00	1,96E+00	1,95E+00	1,90E+00	2,94E-01	9,61E-01	1,63E+00	2,08E+00	2,77E+00	7,56E+00
05.20	3,03E+00	1,98E+00	1,97E+00	1,92E+00	2,94E-01	9,66E-01	1,65E+00	2,10E+00	2,80E+00	7,64E+00
05.25	3,23E+00	1,98E+00	1,98E+00	1,93E+00	2,94E-01	9,69E-01	1,66E+00	2,11E+00	2,81E+00	7,69E+00
05.30	3,23E+00	1,99E+00	1,99E+00	1,94E+00	2,95E-01	9,75E-01	1,67E+00	2,13E+00	2,83E+00	7,76E+00
05.35	3,23E+00	2,01E+00	2,01E+00	1,96E+00	2,97E-01	9,84E-01	1,69E+00	2,16E+00	2,86E+00	7,91E+00
05.40	3,23E+00	2,02E+00	2,03E+00	1,98E+00	3,01E-01	9,95E-01	1,71E+00	2,18E+00	2,89E+00	8,06E+00
05.45	3,23E+00	2,04E+00	2,05E+00	2,00E+00	3,05E-01	1,01E+00	1,73E+00	2,20E+00	2,92E+00	8,15E+00
05.50	3,43E+00	2,08E+00	2,09E+00	2,04E+00	3,14E-01	1,04E+00	1,78E+00	2,28E+00	3,02E+00	8,39E+00
05.55	3,43E+00	2,11E+00	2,13E+00	2,07E+00	3,22E-01	1,07E+00	1,84E+00	2,35E+00	3,10E+00	8,61E+00
06.00	3,43E+00	2,14E+00	2,16E+00	2,10E+00	3,27E-01	1,09E+00	1,87E+00	2,38E+00	3,14E+00	8,70E+00
06.05	3,64E+00	2,17E+00	2,20E+00	2,14E+00	3,29E-01	1,10E+00	1,89E+00	2,41E+00	3,18E+00	8,76E+00
06.10	3,64E+00	2,19E+00	2,22E+00	2,16E+00	3,29E-01	1,10E+00	1,90E+00	2,41E+00	3,19E+00	8,78E+00
06.15	3,64E+00	2,21E+00	2,24E+00	2,19E+00	3,29E-01	1,10E+00	1,91E+00	2,42E+00	3,20E+00	8,84E+00
06.20	3,64E+00	2,25E+00	2,30E+00	2,24E+00	3,52E-01	1,17E+00	2,03E+00	2,55E+00	3,39E+00	9,06E+00
06.25	3,64E+00	2,35E+00	2,40E+00	2,34E+00	3,80E-01	1,29E+00	2,26E+00	2,79E+00	3,85E+00	9,57E+00
06.30	3,84E+00	2,57E+00	2,56E+00	2,52E+00	4,04E-01	1,38E+00	2,40E+00	2,96E+00	4,08E+00	1,01E+01
06.35	4,04E+00	2,72E+00	2,70E+00	2,66E+00	4,25E-01	1,43E+00	2,47E+00	3,04E+00	4,19E+00	1,03E+01
06.40	4,04E+00	2,81E+00	2,81E+00	2,76E+00	4,36E-01	1,50E+00	2,62E+00	3,22E+00	4,42E+00	1,08E+01
06.45	4,24E+00	2,85E+00	2,86E+00	2,81E+00	4,47E-01	1,56E+00	2,72E+00	3,36E+00	4,64E+00	1,12E+01
06.50	4,24E+00	2,87E+00	2,91E+00	2,86E+00	4,65E-01	1,64E+00	2,88E+00	3,54E+00	4,88E+00	1,18E+01
06.55	4,44E+00	2,92E+00	2,96E+00	2,91E+00	4,68E-01	1,66E+00	2,90E+00	3,58E+00	4,93E+00	1,19E+01
07.00	4,44E+00	2,96E+00	3,00E+00	2,95E+00	4,75E-01	1,68E+00	2,94E+00	3,62E+00	4,99E+00	1,20E+01
07.05	4,44E+00	3,01E+00	3,04E+00	3,00E+00	4,78E-01	1,72E+00	3,00E+00	3,69E+00	5,07E+00	1,22E+01
07.10	4,65E+00	3,05E+00	3,09E+00	3,04E+00	4,79E-01	1,73E+00	3,03E+00	3,72E+00	5,11E+00	1,24E+01
07.15	4,85E+00	3,08E+00	3,13E+00	3,08E+00	4,82E-01	1,74E+00	3,04E+00	3,74E+00	5,13E+00	1,24E+01
07.20	4,85E+00	3,10E+00	3,17E+00	3,10E+00	4,84E-01	1,75E+00	3,08E+00	3,80E+00	5,20E+00	1,27E+01
07.25	4,85E+00	3,11E+00	3,18E+00	3,12E+00	4,84E-01	1,76E+00	3,08E+00	3,80E+00	5,20E+00	1,27E+01
07.30	4,85E+00	3,11E+00	3,18E+00	3,12E+00	4,84E-01	1,76E+00	3,08E+00	3,80E+00	5,20E+00	1,27E+01
07.35	4,85E+00	3,12E+00	3,19E+00	3,13E+00	4,84E-01	1,76E+00	3,08E+00	3,80E+00	5,21E+00	1,28E+01
07.40	5,05E+00	3,17E+00	3,23E+00	3,16E+00	4,84E-01	1,76E+00	3,09E+00	3,88E+00	5,23E+00	1,40E+01
07.45	5,05E+00	3,26E+00	3,27E+00	3,23E+00	4,84E-01	1,76E+00	3,09E+00	3,89E+00	5,23E+00	1,41E+01

Rainfall rate(mm/5min) in point I , 22/6/2012 rainfall event

time	Rg	Pixel	Krig.	IDW	Dow. min.	Dow.1°q.	Dow.2°q.	Dow. Ave.	Dow.3°q.	Dow. max.
02.35	0,00E+00	3,39E-02	2,89E-02	3,55E-02	1,29E-05	1,55E-03	1,37E-02	5,29E-02	1,21E-01	2,32E-01
02.40	0,00E+00	4,69E-02	5,78E-02	4,37E-02	1,41E-05	2,64E-03	1,63E-02	7,04E-02	1,01E-01	7,99E-01

02.45	1,98E-01	1,56E-02	3,88E-02	3,28E-02	1,68E-03	9,58E-03	3,83E-02	6,91E-02	7,71E-02	4,88E-01
02.50	0,00E+00	1,02E-01	7,06E-02	6,73E-02	1,98E-04	4,32E-03	2,04E-02	3,89E-02	4,09E-02	1,94E-01
02.55	3,96E-01	9,90E-02	7,45E-02	7,17E-02	5,59E-05	3,07E-03	1,59E-02	4,07E-02	6,14E-02	2,12E-01
03.00	1,98E-01	6,25E-02	5,76E-02	5,65E-02	1,04E-04	1,99E-03	2,25E-02	1,12E-01	1,70E-01	1,08E+00
03.05	1,98E-01	8,85E-02	8,65E-02	7,36E-02	2,83E-05	1,76E-03	1,25E-02	3,95E-02	5,56E-02	3,97E-01
03.10	1,98E-01	8,07E-02	6,56E-02	6,77E-02	5,10E-05	2,16E-03	5,45E-03	8,69E-03	9,25E-03	5,03E-02
03.15	1,98E-01	7,03E-02	5,16E-02	5,44E-02	9,82E-04	2,81E-03	6,17E-03	8,03E-03	9,11E-03	4,78E-02
03.20	1,98E-01	3,39E-02	3,36E-02	3,31E-02	6,01E-05	9,39E-04	2,35E-03	2,58E-03	2,35E-03	5,87E-03
03.25	0,00E+00	2,60E-03	6,77E-03	7,82E-03	2,55E-05	1,32E-03	3,60E-03	5,76E-03	7,64E-03	3,42E-02
03.30	0,00E+00	0,00E+00	4,69E-03	5,01E-03	3,50E-05	6,36E-04	2,02E-03	7,12E-03	9,23E-03	6,16E-02
03.35	0,00E+00	1,04E-02	8,85E-03	8,99E-03	5,51E-06	1,28E-03	6,61E-03	1,44E-02	1,25E-02	7,96E-02
03.40	0,00E+00	7,81E-03	1,07E-02	1,08E-02	6,85E-04	3,96E-03	9,45E-03	1,09E-02	2,26E-02	2,35E-02
03.45	1,98E-01	1,04E-02	8,07E-03	1,82E-02	3,55E-03	8,34E-03	1,14E-02	1,44E-02	1,81E-02	4,24E-02
03.50	0,00E+00	1,56E-02	2,73E-02	2,89E-02	2,48E-02	5,64E-02	8,58E-02	8,69E-02	1,10E-01	1,66E-01
03.55	0,00E+00	5,73E-02	5,63E-02	6,12E-02	4,51E-02	6,53E-02	8,93E-02	8,86E-02	1,05E-01	1,37E-01
04.00	1,98E-01	1,67E-01	1,89E-01	1,62E-01	3,19E-02	9,51E-02	1,61E-01	1,61E-01	2,39E-01	3,21E-01
04.05	1,98E-01	2,01E-01	1,59E-01	1,62E-01	6,16E-02	1,41E-01	2,31E-01	2,37E-01	3,19E-01	5,20E-01
04.10	1,98E-01	2,42E-01	1,98E-01	2,00E-01	5,14E-02	1,52E-01	2,09E-01	2,21E-01	2,72E-01	5,83E-01
04.15	0,00E+00	1,77E-01	2,14E-01	1,88E-01	3,84E-02	1,54E-01	2,49E-01	2,86E-01	3,82E-01	8,19E-01
04.20	1,98E-01	1,77E-01	1,64E-01	1,56E-01	3,82E-02	8,10E-02	1,21E-01	1,34E-01	1,61E-01	3,63E-01
04.25	0,00E+00	4,95E-02	6,43E-02	6,56E-02	9,54E-03	2,07E-02	3,82E-02	4,05E-02	4,76E-02	1,00E-01
04.30	1,98E-01	1,82E-02	2,27E-02	2,81E-02	3,71E-04	2,26E-03	6,12E-03	7,46E-03	9,97E-03	4,23E-02
04.35	0,00E+00	1,30E-02	1,54E-02	1,98E-02	3,02E-03	1,44E-02	3,73E-02	6,26E-02	1,05E-01	2,03E-01
04.40	0,00E+00	3,65E-02	5,13E-02	4,37E-02	9,04E-04	9,01E-03	2,59E-02	3,49E-02	6,68E-02	9,93E-02
04.45	0,00E+00	2,34E-02	4,58E-02	4,03E-02	1,45E-03	1,57E-02	2,57E-02	3,61E-02	4,67E-02	1,80E-01
04.50	0,00E+00	7,81E-03	7,55E-03	1,64E-02	1,23E-03	8,55E-03	1,73E-02	2,54E-02	3,62E-02	1,09E-01
04.55	0,00E+00	1,56E-02	3,13E-02	2,21E-02	2,43E-03	2,09E-02	5,98E-02	7,78E-02	8,08E-02	2,34E-01
05.00	0,00E+00	2,08E-02	3,10E-02	2,93E-02	1,18E-02	4,07E-02	7,31E-02	7,06E-02	7,73E-02	1,47E-01
05.05	1,98E-01	4,17E-02	3,65E-02	3,82E-02	3,07E-03	1,30E-02	2,51E-02	2,83E-02	5,05E-02	5,49E-02
05.10	0,00E+00	1,04E-02	1,41E-02	1,71E-02	1,88E-03	6,28E-03	1,21E-02	1,29E-02	2,24E-02	3,01E-02
05.15	0,00E+00	2,60E-02	2,21E-02	2,17E-02	4,27E-03	1,27E-02	1,89E-02	2,46E-02	3,40E-02	6,33E-02
05.20	0,00E+00	1,30E-02	1,43E-02	1,43E-02	1,14E-03	4,79E-03	1,04E-02	1,70E-02	1,82E-02	9,74E-02
05.25	1,98E-01	5,21E-03	1,09E-02	1,03E-02	7,36E-04	2,74E-03	6,14E-03	9,34E-03	1,37E-02	3,32E-02
05.30	0,00E+00	7,81E-03	1,20E-02	1,26E-02	4,21E-04	8,26E-03	1,27E-02	1,77E-02	2,09E-02	7,00E-02
05.35	0,00E+00	1,56E-02	2,11E-02	1,98E-02	1,56E-03	8,47E-03	1,48E-02	2,40E-02	2,64E-02	1,31E-01
05.40	0,00E+00	1,82E-02	1,69E-02	1,94E-02	4,63E-03	9,32E-03	1,66E-02	2,20E-02	2,98E-02	1,07E-01
05.45	0,00E+00	1,56E-02	2,06E-02	2,26E-02	3,96E-03	1,27E-02	1,82E-02	2,60E-02	3,58E-02	1,04E-01
05.50	1,98E-01	4,17E-02	3,75E-02	3,81E-02	4,04E-03	3,25E-02	5,24E-02	6,43E-02	7,85E-02	2,32E-01
05.55	0,00E+00	2,60E-02	3,98E-02	3,34E-02	3,54E-03	2,42E-02	5,49E-02	6,25E-02	7,14E-02	1,99E-01
06.00	0,00E+00	2,86E-02	3,31E-02	3,17E-02	2,39E-03	1,95E-02	3,81E-02	4,09E-02	6,17E-02	9,51E-02
06.05	1,98E-01	3,91E-02	4,17E-02	4,35E-02	7,47E-04	9,40E-03	2,04E-02	2,42E-02	4,39E-02	5,94E-02
06.10	0,00E+00	1,30E-02	1,93E-02	2,27E-02	9,04E-05	1,18E-03	3,90E-03	5,46E-03	4,68E-03	1,66E-02
06.15	0,00E+00	2,60E-02	2,14E-02	2,67E-02	3,77E-04	2,89E-03	7,02E-03	1,01E-02	1,20E-02	5,43E-02
06.20	0,00E+00	3,91E-02	5,83E-02	5,41E-02	2,28E-02	6,84E-02	1,20E-01	1,13E-01	1,23E-01	2,17E-01
06.25	0,00E+00	9,38E-02	9,58E-02	9,73E-02	2,81E-02	1,19E-01	2,38E-01	2,52E-01	2,49E-01	5,02E-01
06.30	1,98E-01	2,27E-01	1,63E-01	1,72E-01	2,37E-02	9,27E-02	1,46E-01	1,78E-01	2,37E-01	6,21E-01
06.35	1,98E-01	1,43E-01	1,42E-01	1,37E-01	2,55E-02	5,64E-02	8,11E-02	9,63E-02	1,17E-01	3,54E-01
06.40	0,00E+00	9,64E-02	1,13E-01	1,05E-01	1,25E-02	8,73E-02	1,72E-01	2,20E-01	3,66E-01	6,39E-01
06.45	1,98E-01	3,39E-02	4,97E-02	5,18E-02	1,12E-02	4,99E-02	1,01E-01	1,24E-01	1,85E-01	4,31E-01
06.50	0,00E+00	2,60E-02	4,37E-02	4,58E-02	3,18E-02	8,60E-02	1,76E-01	2,00E-01	2,84E-01	5,54E-01
06.55	0,00E+00	4,95E-02	5,00E-02	5,52E-02	6,21E-03	1,71E-02	3,69E-02	3,73E-02	5,02E-02	1,04E-01
07.00	1,98E-01	3,91E-02	3,85E-02	4,26E-02	6,18E-03	2,27E-02	3,51E-02	4,13E-02	5,39E-02	1,39E-01

07.05	0,00E+00	4,43E-02	4,53E-02	4,51E-02	5,89E-03	2,87E-02	6,54E-02	6,52E-02	8,17E-02	2,19E-01
07.10	1,98E-01	4,17E-02	5,08E-02	4,61E-02	2,55E-03	1,43E-02	3,00E-02	3,90E-02	5,56E-02	1,69E-01
07.15	0,00E+00	3,39E-02	4,24E-02	3,87E-02	1,01E-03	5,78E-03	1,38E-02	1,34E-02	1,46E-02	3,66E-02
07.20	0,00E+00	2,08E-02	3,49E-02	2,40E-02	1,74E-03	1,27E-02	3,56E-02	4,78E-02	6,60E-02	2,06E-01
07.25	1,98E-01	1,04E-02	1,33E-02	1,01E-02	2,61E-05	4,34E-04	1,72E-03	2,22E-03	1,85E-03	8,00E-03
07.30	0,00E+00	0,00E+00	5,21E-04	1,79E-03	0,00E+00	0,00E+00	0,00E+00	0,00E+00	0,00E+00	0,00E+00
07.35	0,00E+00	1,04E-02	4,17E-03	8,39E-03	5,22E-09	1,05E-05	3,49E-04	8,05E-03	1,20E-02	6,77E-02
07.40	0,00E+00	4,69E-02	3,96E-02	3,60E-02	2,06E-09	1,23E-04	3,69E-03	3,00E-02	8,19E-03	5,45E-01
07.45	0,00E+00	8,85E-02	4,32E-02	5,46E-02	4,14E-06	1,73E-04	1,84E-03	1,53E-02	2,96E-02	1,22E-01

Rainfall accumulation(mm) in point I , 22/6/2012 rainfall event

time	Rg	Pixel	Krig.	IDW	Dow. min.	Dow.1°q.	Dow.2°q.	Dow. Ave.	Dow.3°q.	Dow. max.
02.35	0,00E+00	3,39E-02	2,89E-02	3,55E-02	1,29E-05	1,55E-03	1,37E-02	5,29E-02	1,21E-01	2,32E-01
02.40	0,00E+00	8,07E-02	8,67E-02	7,92E-02	2,71E-05	4,19E-03	3,01E-02	1,23E-01	2,22E-01	1,03E+00
02.45	1,98E-01	9,64E-02	1,26E-01	1,12E-01	1,70E-03	1,38E-02	6,84E-02	1,92E-01	2,99E-01	1,52E+00
02.50	1,98E-01	1,98E-01	1,96E-01	1,79E-01	1,90E-03	1,81E-02	8,89E-02	2,31E-01	3,40E-01	1,71E+00
02.55	5,94E-01	2,97E-01	2,71E-01	2,51E-01	1,96E-03	2,12E-02	1,05E-01	2,72E-01	4,01E-01	1,92E+00
03.00	7,92E-01	3,59E-01	3,28E-01	3,07E-01	2,06E-03	2,31E-02	1,27E-01	3,84E-01	5,71E-01	3,00E+00
03.05	9,90E-01	4,48E-01	4,15E-01	3,81E-01	2,09E-03	2,49E-02	1,40E-01	4,24E-01	6,27E-01	3,40E+00
03.10	1,19E+00	5,29E-01	4,80E-01	4,49E-01	2,14E-03	2,71E-02	1,45E-01	4,33E-01	6,36E-01	3,45E+00
03.15	1,39E+00	5,99E-01	5,32E-01	5,03E-01	3,12E-03	2,99E-02	1,51E-01	4,41E-01	6,45E-01	3,50E+00
03.20	1,58E+00	6,33E-01	5,65E-01	5,36E-01	3,18E-03	3,08E-02	1,54E-01	4,43E-01	6,47E-01	3,51E+00
03.25	1,58E+00	6,35E-01	5,72E-01	5,44E-01	3,21E-03	3,21E-02	1,57E-01	4,49E-01	6,55E-01	3,54E+00
03.30	1,58E+00	6,35E-01	5,77E-01	5,49E-01	3,24E-03	3,28E-02	1,59E-01	4,56E-01	6,64E-01	3,60E+00
03.35	1,58E+00	6,46E-01	5,86E-01	5,58E-01	3,25E-03	3,41E-02	1,66E-01	4,71E-01	6,77E-01	3,68E+00
03.40	1,58E+00	6,54E-01	5,96E-01	5,69E-01	3,93E-03	3,80E-02	1,75E-01	4,81E-01	6,99E-01	3,70E+00
03.45	1,78E+00	6,64E-01	6,04E-01	5,87E-01	7,49E-03	4,64E-02	1,87E-01	4,96E-01	7,17E-01	3,75E+00
03.50	1,78E+00	6,80E-01	6,32E-01	6,16E-01	3,23E-02	1,03E-01	2,73E-01	5,83E-01	8,28E-01	3,91E+00
03.55	1,78E+00	7,37E-01	6,88E-01	6,77E-01	7,74E-02	1,68E-01	3,62E-01	6,71E-01	9,32E-01	4,05E+00
04.00	1,98E+00	9,04E-01	8,77E-01	8,39E-01	1,09E-01	2,63E-01	5,23E-01	8,32E-01	1,17E+00	4,37E+00
04.05	2,18E+00	1,10E+00	1,04E+00	1,00E+00	1,71E-01	4,04E-01	7,53E-01	1,07E+00	1,49E+00	4,89E+00
04.10	2,38E+00	1,35E+00	1,23E+00	1,20E+00	2,22E-01	5,56E-01	9,62E-01	1,29E+00	1,76E+00	5,47E+00
04.15	2,38E+00	1,52E+00	1,45E+00	1,39E+00	2,61E-01	7,09E-01	1,21E+00	1,58E+00	2,15E+00	6,29E+00
04.20	2,57E+00	1,70E+00	1,61E+00	1,55E+00	2,99E-01	7,90E-01	1,33E+00	1,71E+00	2,31E+00	6,66E+00
04.25	2,57E+00	1,75E+00	1,68E+00	1,61E+00	3,09E-01	8,11E-01	1,37E+00	1,75E+00	2,35E+00	6,76E+00
04.30	2,77E+00	1,77E+00	1,70E+00	1,64E+00	3,09E-01	8,13E-01	1,38E+00	1,76E+00	2,36E+00	6,80E+00
04.35	2,77E+00	1,78E+00	1,71E+00	1,66E+00	3,12E-01	8,28E-01	1,41E+00	1,82E+00	2,47E+00	7,00E+00
04.40	2,77E+00	1,82E+00	1,77E+00	1,70E+00	3,13E-01	8,37E-01	1,44E+00	1,86E+00	2,54E+00	7,10E+00
04.45	2,77E+00	1,84E+00	1,81E+00	1,74E+00	3,14E-01	8,52E-01	1,47E+00	1,89E+00	2,58E+00	7,28E+00
04.50	2,77E+00	1,85E+00	1,82E+00	1,76E+00	3,15E-01	8,61E-01	1,48E+00	1,92E+00	2,62E+00	7,39E+00
04.55	2,77E+00	1,86E+00	1,85E+00	1,78E+00	3,18E-01	8,82E-01	1,54E+00	2,00E+00	2,70E+00	7,62E+00
05.00	2,77E+00	1,89E+00	1,88E+00	1,81E+00	3,30E-01	9,23E-01	1,62E+00	2,07E+00	2,78E+00	7,77E+00
05.05	2,97E+00	1,93E+00	1,92E+00	1,85E+00	3,33E-01	9,36E-01	1,64E+00	2,09E+00	2,83E+00	7,83E+00
05.10	2,97E+00	1,94E+00	1,93E+00	1,87E+00	3,35E-01	9,42E-01	1,65E+00	2,11E+00	2,85E+00	7,86E+00
05.15	2,97E+00	1,96E+00	1,95E+00	1,89E+00	3,39E-01	9,55E-01	1,67E+00	2,13E+00	2,88E+00	7,92E+00
05.20	2,97E+00	1,98E+00	1,97E+00	1,90E+00	3,40E-01	9,59E-01	1,68E+00	2,15E+00	2,90E+00	8,02E+00

05.25	3,17E+00	1,98E+00	1,98E+00	1,91E+00	3,41E-01	9,62E-01	1,69E+00	2,16E+00	2,92E+00	8,05E+00
05.30	3,17E+00	1,99E+00	1,99E+00	1,92E+00	3,41E-01	9,70E-01	1,70E+00	2,18E+00	2,94E+00	8,12E+00
05.35	3,17E+00	2,01E+00	2,01E+00	1,94E+00	3,43E-01	9,79E-01	1,72E+00	2,20E+00	2,96E+00	8,25E+00
05.40	3,17E+00	2,02E+00	2,03E+00	1,96E+00	3,47E-01	9,88E-01	1,73E+00	2,22E+00	2,99E+00	8,36E+00
05.45	3,17E+00	2,04E+00	2,05E+00	1,99E+00	3,51E-01	1,00E+00	1,75E+00	2,25E+00	3,03E+00	8,46E+00
05.50	3,37E+00	2,08E+00	2,09E+00	2,02E+00	3,55E-01	1,03E+00	1,80E+00	2,31E+00	3,11E+00	8,69E+00
05.55	3,37E+00	2,11E+00	2,13E+00	2,06E+00	3,59E-01	1,06E+00	1,86E+00	2,37E+00	3,18E+00	8,89E+00
06.00	3,37E+00	2,14E+00	2,16E+00	2,09E+00	3,61E-01	1,08E+00	1,90E+00	2,42E+00	3,24E+00	8,99E+00
06.05	3,56E+00	2,17E+00	2,20E+00	2,13E+00	3,62E-01	1,09E+00	1,92E+00	2,44E+00	3,28E+00	9,05E+00
06.10	3,56E+00	2,19E+00	2,22E+00	2,16E+00	3,62E-01	1,09E+00	1,92E+00	2,45E+00	3,29E+00	9,06E+00
06.15	3,56E+00	2,21E+00	2,24E+00	2,18E+00	3,63E-01	1,09E+00	1,93E+00	2,46E+00	3,30E+00	9,12E+00
06.20	3,56E+00	2,25E+00	2,30E+00	2,24E+00	3,85E-01	1,16E+00	2,05E+00	2,57E+00	3,42E+00	9,34E+00
06.25	3,56E+00	2,35E+00	2,40E+00	2,33E+00	4,13E-01	1,28E+00	2,28E+00	2,82E+00	3,67E+00	9,84E+00
06.30	3,76E+00	2,57E+00	2,56E+00	2,51E+00	4,37E-01	1,37E+00	2,43E+00	3,00E+00	3,91E+00	1,05E+01
06.35	3,96E+00	2,72E+00	2,70E+00	2,64E+00	4,63E-01	1,43E+00	2,51E+00	3,09E+00	4,03E+00	1,08E+01
06.40	3,96E+00	2,81E+00	2,81E+00	2,75E+00	4,75E-01	1,51E+00	2,68E+00	3,31E+00	4,39E+00	1,15E+01
06.45	4,16E+00	2,85E+00	2,86E+00	2,80E+00	4,86E-01	1,56E+00	2,78E+00	3,44E+00	4,58E+00	1,19E+01
06.50	4,16E+00	2,87E+00	2,91E+00	2,85E+00	5,18E-01	1,65E+00	2,96E+00	3,64E+00	4,86E+00	1,24E+01
06.55	4,16E+00	2,92E+00	2,96E+00	2,90E+00	5,24E-01	1,67E+00	3,00E+00	3,67E+00	4,91E+00	1,25E+01
07.00	4,36E+00	2,96E+00	3,00E+00	2,94E+00	5,31E-01	1,69E+00	3,03E+00	3,72E+00	4,97E+00	1,27E+01
07.05	4,36E+00	3,01E+00	3,04E+00	2,99E+00	5,36E-01	1,72E+00	3,10E+00	3,78E+00	5,05E+00	1,29E+01
07.10	4,55E+00	3,05E+00	3,09E+00	3,04E+00	5,39E-01	1,73E+00	3,13E+00	3,82E+00	5,10E+00	1,31E+01
07.15	4,55E+00	3,08E+00	3,13E+00	3,07E+00	5,40E-01	1,74E+00	3,14E+00	3,83E+00	5,12E+00	1,31E+01
07.20	4,55E+00	3,10E+00	3,17E+00	3,10E+00	5,42E-01	1,75E+00	3,18E+00	3,88E+00	5,18E+00	1,33E+01
07.25	4,75E+00	3,11E+00	3,18E+00	3,11E+00	5,42E-01	1,75E+00	3,18E+00	3,88E+00	5,18E+00	1,33E+01
07.30	4,75E+00	3,11E+00	3,18E+00	3,11E+00	5,42E-01	1,75E+00	3,18E+00	3,88E+00	5,18E+00	1,33E+01
07.35	4,75E+00	3,12E+00	3,19E+00	3,12E+00	5,42E-01	1,75E+00	3,18E+00	3,89E+00	5,20E+00	1,34E+01
07.40	4,75E+00	3,17E+00	3,23E+00	3,15E+00	5,42E-01	1,75E+00	3,18E+00	3,92E+00	5,20E+00	1,39E+01
07.45	4,75E+00	3,26E+00	3,27E+00	3,21E+00	5,42E-01	1,75E+00	3,19E+00	3,94E+00	5,23E+00	1,41E+01

Rainfall rate(mm/5min) in point C , 22/6/2012 rainfall event

time	Rg	Pixel	Krig.	IDW	Dow. min.	Dow.1°q.	Dow.2°q.	Dow. Ave.	Dow.3°q.	Dow. max.
02.35	0,00E+00	3,39E-02	2,89E-02	3,57E-02	1,15E-04	1,55E-03	1,25E-02	5,29E-02	2,56E-02	2,03E-01
02.40	1,98E-01	4,69E-02	5,78E-02	4,56E-02	1,41E-05	1,35E-03	8,32E-03	7,04E-02	4,08E-02	4,95E-01
02.45	1,98E-01	1,56E-02	3,88E-02	3,30E-02	4,07E-04	1,42E-02	4,06E-02	6,91E-02	5,97E-02	5,02E-01
02.50	0,00E+00	1,02E-01	7,06E-02	6,74E-02	1,40E-04	6,11E-03	2,04E-02	3,89E-02	4,03E-02	2,70E-01
02.55	3,96E-01	9,90E-02	7,45E-02	7,27E-02	8,65E-05	2,80E-03	1,42E-02	4,07E-02	2,20E-02	1,25E-01
03.00	0,00E+00	6,25E-02	5,76E-02	5,59E-02	9,56E-06	1,99E-03	2,20E-02	1,12E-01	3,80E-02	6,68E-01
03.05	1,98E-01	8,85E-02	8,65E-02	7,51E-02	1,84E-05	1,52E-03	8,44E-03	3,95E-02	2,82E-02	2,58E-01
03.10	3,96E-01	8,07E-02	6,56E-02	6,75E-02	2,13E-04	2,84E-03	7,07E-03	8,69E-03	1,76E-02	5,03E-02
03.15	1,98E-01	7,03E-02	5,16E-02	5,48E-02	8,82E-04	3,43E-03	5,63E-03	8,03E-03	9,97E-03	4,78E-02
03.20	0,00E+00	3,39E-02	3,36E-02	3,38E-02	1,50E-04	9,39E-04	2,35E-03	2,58E-03	2,35E-03	5,87E-03
03.25	0,00E+00	2,60E-03	6,77E-03	8,08E-03	1,14E-04	1,06E-03	2,75E-03	5,76E-03	4,70E-03	2,74E-02
03.30	0,00E+00	0,00E+00	4,69E-03	4,71E-03	5,13E-06	3,71E-04	9,86E-04	7,12E-03	3,79E-03	6,16E-02
03.35	1,98E-01	1,04E-02	8,85E-03	9,16E-03	1,46E-04	1,47E-03	6,61E-03	1,44E-02	3,41E-02	7,18E-02

03.40	0,00E+00	7,81E-03	1,07E-02	1,10E-02	1,64E-03	3,96E-03	9,45E-03	1,09E-02	9,67E-03	2,35E-02
03.45	0,00E+00	1,04E-02	8,07E-03	1,79E-02	4,28E-03	9,06E-03	1,31E-02	1,44E-02	1,81E-02	5,47E-02
03.50	0,00E+00	1,56E-02	2,73E-02	2,88E-02	2,30E-02	5,41E-02	8,58E-02	8,69E-02	1,24E-01	1,66E-01
03.55	0,00E+00	5,73E-02	5,63E-02	6,18E-02	4,44E-02	6,53E-02	9,00E-02	8,86E-02	1,17E-01	1,39E-01
04.00	1,98E-01	1,67E-01	1,89E-01	1,69E-01	3,33E-02	9,93E-02	1,54E-01	1,61E-01	2,39E-01	3,35E-01
04.05	1,98E-01	2,01E-01	1,59E-01	1,69E-01	4,59E-02	1,37E-01	1,89E-01	2,37E-01	2,45E-01	5,20E-01
04.10	1,98E-01	2,42E-01	1,98E-01	2,06E-01	5,14E-02	1,47E-01	2,22E-01	2,21E-01	3,03E-01	6,30E-01
04.15	0,00E+00	1,77E-01	2,14E-01	1,90E-01	4,87E-02	1,85E-01	2,36E-01	2,86E-01	3,64E-01	8,19E-01
04.20	1,98E-01	1,77E-01	1,64E-01	1,63E-01	2,39E-02	8,10E-02	1,44E-01	1,34E-01	2,39E-01	3,63E-01
04.25	0,00E+00	4,95E-02	6,43E-02	7,01E-02	5,12E-03	2,07E-02	3,95E-02	4,05E-02	7,16E-02	9,37E-02
04.30	0,00E+00	1,82E-02	2,27E-02	2,88E-02	2,41E-04	2,14E-03	4,38E-03	7,46E-03	7,88E-03	3,53E-02
04.35	0,00E+00	1,30E-02	1,54E-02	1,93E-02	1,49E-03	1,27E-02	3,73E-02	6,26E-02	6,90E-02	2,59E-01
04.40	1,98E-01	3,65E-02	5,13E-02	4,28E-02	9,04E-04	1,07E-02	2,70E-02	3,49E-02	7,36E-02	1,27E-01
04.45	0,00E+00	2,34E-02	4,58E-02	4,33E-02	1,36E-03	1,19E-02	2,73E-02	3,61E-02	4,05E-02	2,68E-01
04.50	0,00E+00	7,81E-03	7,55E-03	1,71E-02	1,42E-03	9,83E-03	1,87E-02	2,54E-02	3,45E-02	1,25E-01
04.55	0,00E+00	1,56E-02	3,13E-02	2,47E-02	2,43E-03	2,03E-02	5,98E-02	7,78E-02	7,17E-02	2,66E-01
05.00	0,00E+00	2,08E-02	3,10E-02	2,85E-02	1,21E-02	4,07E-02	7,46E-02	7,06E-02	7,73E-02	1,49E-01
05.05	1,98E-01	4,17E-02	3,65E-02	4,00E-02	3,07E-03	1,25E-02	2,46E-02	2,83E-02	4,60E-02	5,49E-02
05.10	0,00E+00	1,04E-02	1,41E-02	1,76E-02	1,75E-03	7,23E-03	1,29E-02	1,29E-02	2,30E-02	3,01E-02
05.15	0,00E+00	2,60E-02	2,21E-02	2,24E-02	2,10E-03	8,82E-03	1,76E-02	2,46E-02	2,58E-02	8,64E-02
05.20	0,00E+00	1,30E-02	1,43E-02	1,40E-02	3,33E-04	6,10E-03	1,16E-02	1,70E-02	2,74E-02	9,74E-02
05.25	0,00E+00	5,21E-03	1,09E-02	1,06E-02	3,44E-04	2,62E-03	6,01E-03	9,34E-03	1,48E-02	5,28E-02
05.30	0,00E+00	7,81E-03	1,20E-02	1,18E-02	4,21E-04	6,33E-03	1,27E-02	1,77E-02	2,34E-02	6,23E-02
05.35	0,00E+00	1,56E-02	2,11E-02	1,92E-02	1,56E-03	7,53E-03	1,56E-02	2,40E-02	2,64E-02	1,11E-01
05.40	0,00E+00	1,82E-02	1,69E-02	1,91E-02	3,33E-03	8,62E-03	1,41E-02	2,20E-02	2,93E-02	1,38E-01
05.45	1,98E-01	1,56E-02	2,06E-02	2,22E-02	2,78E-03	9,60E-03	2,03E-02	2,60E-02	3,68E-02	8,35E-02
05.50	0,00E+00	4,17E-02	3,75E-02	3,81E-02	6,51E-03	3,25E-02	5,24E-02	6,43E-02	9,47E-02	2,47E-01
05.55	0,00E+00	2,60E-02	3,98E-02	3,46E-02	3,91E-03	2,92E-02	6,05E-02	6,25E-02	1,14E-01	1,99E-01
06.00	0,00E+00	2,86E-02	3,31E-02	3,37E-02	9,43E-03	1,99E-02	3,71E-02	4,09E-02	4,27E-02	9,51E-02
06.05	0,00E+00	3,91E-02	4,17E-02	4,21E-02	3,57E-03	8,78E-03	2,04E-02	2,42E-02	2,44E-02	6,18E-02
06.10	1,98E-01	1,30E-02	1,93E-02	2,17E-02	2,55E-05	1,18E-03	3,90E-03	5,46E-03	4,45E-03	1,66E-02
06.15	0,00E+00	2,60E-02	2,14E-02	2,65E-02	5,90E-04	3,17E-03	7,70E-03	1,01E-02	1,67E-02	5,96E-02
06.20	0,00E+00	3,91E-02	5,83E-02	5,14E-02	2,31E-02	6,97E-02	1,20E-01	1,13E-01	1,23E-01	2,17E-01
06.25	0,00E+00	9,38E-02	9,58E-02	1,00E-01	2,85E-02	1,19E-01	2,38E-01	2,52E-01	2,47E-01	5,02E-01
06.30	1,98E-01	2,27E-01	1,63E-01	1,69E-01	2,37E-02	8,24E-02	1,33E-01	1,78E-01	2,12E-01	5,10E-01
06.35	0,00E+00	1,43E-01	1,42E-01	1,37E-01	1,94E-02	4,82E-02	7,95E-02	9,63E-02	1,12E-01	3,54E-01
06.40	1,98E-01	9,64E-02	1,13E-01	1,06E-01	1,46E-02	6,44E-02	1,55E-01	2,20E-01	2,33E-01	6,39E-01
06.45	0,00E+00	3,39E-02	4,97E-02	5,49E-02	1,29E-02	5,59E-02	1,01E-01	1,24E-01	1,67E-01	3,51E-01
06.50	1,98E-01	2,60E-02	4,37E-02	4,49E-02	1,64E-02	8,44E-02	1,64E-01	2,00E-01	2,49E-01	5,15E-01
06.55	0,00E+00	4,95E-02	5,00E-02	5,57E-02	3,61E-03	1,71E-02	2,95E-02	3,73E-02	4,73E-02	1,05E-01
07.00	0,00E+00	3,91E-02	3,85E-02	4,23E-02	6,18E-03	2,68E-02	3,76E-02	4,13E-02	5,47E-02	1,70E-01
07.05	1,98E-01	4,43E-02	4,53E-02	4,56E-02	1,14E-02	3,06E-02	6,33E-02	6,52E-02	1,13E-01	2,05E-01
07.10	0,00E+00	4,17E-02	5,08E-02	4,55E-02	1,99E-03	1,27E-02	2,08E-02	3,90E-02	3,85E-02	1,69E-01
07.15	1,98E-01	3,39E-02	4,24E-02	3,95E-02	1,01E-03	5,94E-03	1,42E-02	1,34E-02	3,29E-02	3,57E-02
07.20	0,00E+00	2,08E-02	3,49E-02	2,57E-02	6,13E-03	2,01E-02	4,16E-02	4,78E-02	1,05E-01	3,27E-01
07.25	0,00E+00	1,04E-02	1,33E-02	1,14E-02	2,51E-05	4,34E-04	1,76E-03	2,22E-03	6,78E-03	8,00E-03
07.30	1,98E-01	0,00E+00	5,21E-04	1,85E-03	0,00E+00	0,00E+00	0,00E+00	0,00E+00	0,00E+00	0,00E+00
07.35	0,00E+00	1,04E-02	4,17E-03	8,01E-03	5,22E-09	1,88E-05	3,52E-04	8,05E-03	6,36E-03	3,84E-02
07.40	0,00E+00	4,69E-02	3,96E-02	3,57E-02	1,85E-06	1,23E-04	3,69E-03	3,00E-02	4,76E-02	5,45E-01
07.45	0,00E+00	8,85E-02	4,32E-02	5,60E-02	3,55E-06	1,09E-03	2,49E-03	1,53E-02	1,41E-02	7,70E-02

Rainfall accumulation(mm) in point C , 22/6/2012 rainfall event

time	Rg	Pixel	Krig.	IDW	Dow. min.	Dow.1°q.	Dow.2°q.	Dow. Ave.	Dow.3°q.	Dow. max.
02.35	0,00E+00	3,39E-02	2,89E-02	3,57E-02	1,15E-04	1,55E-03	1,25E-02	5,29E-02	2,56E-02	2,03E-01
02.40	1,98E-01	8,07E-02	8,67E-02	8,13E-02	1,29E-04	2,89E-03	2,08E-02	1,23E-01	6,63E-02	6,98E-01
02.45	3,96E-01	9,64E-02	1,26E-01	1,14E-01	5,36E-04	1,71E-02	6,14E-02	1,92E-01	1,26E-01	1,20E+00
02.50	3,96E-01	1,98E-01	1,96E-01	1,82E-01	6,77E-04	2,32E-02	8,19E-02	2,31E-01	1,66E-01	1,47E+00
02.55	7,92E-01	2,97E-01	2,71E-01	2,54E-01	7,63E-04	2,60E-02	9,61E-02	2,72E-01	1,88E-01	1,60E+00
03.00	7,92E-01	3,59E-01	3,28E-01	3,10E-01	7,73E-04	2,80E-02	1,18E-01	3,84E-01	2,26E-01	2,26E+00
03.05	9,90E-01	4,48E-01	4,15E-01	3,85E-01	7,91E-04	2,95E-02	1,27E-01	4,24E-01	2,55E-01	2,52E+00
03.10	1,39E+00	5,29E-01	4,80E-01	4,53E-01	1,00E-03	3,23E-02	1,34E-01	4,33E-01	2,72E-01	2,57E+00
03.15	1,58E+00	5,99E-01	5,32E-01	5,08E-01	1,89E-03	3,58E-02	1,39E-01	4,41E-01	2,82E-01	2,62E+00
03.20	1,58E+00	6,33E-01	5,65E-01	5,42E-01	2,04E-03	3,67E-02	1,42E-01	4,43E-01	2,84E-01	2,62E+00
03.25	1,58E+00	6,35E-01	5,72E-01	5,50E-01	2,15E-03	3,78E-02	1,44E-01	4,49E-01	2,89E-01	2,65E+00
03.30	1,58E+00	6,35E-01	5,77E-01	5,54E-01	2,16E-03	3,81E-02	1,45E-01	4,56E-01	2,93E-01	2,71E+00
03.35	1,78E+00	6,46E-01	5,86E-01	5,64E-01	2,30E-03	3,96E-02	1,52E-01	4,71E-01	3,27E-01	2,79E+00
03.40	1,78E+00	6,54E-01	5,96E-01	5,75E-01	3,94E-03	4,36E-02	1,61E-01	4,81E-01	3,37E-01	2,81E+00
03.45	1,78E+00	6,64E-01	6,04E-01	5,92E-01	8,21E-03	5,26E-02	1,75E-01	4,96E-01	3,55E-01	2,86E+00
03.50	1,78E+00	6,80E-01	6,32E-01	6,21E-01	3,12E-02	1,07E-01	2,60E-01	5,83E-01	4,78E-01	3,03E+00
03.55	1,78E+00	7,37E-01	6,88E-01	6,83E-01	7,57E-02	1,72E-01	3,50E-01	6,71E-01	5,95E-01	3,17E+00
04.00	1,98E+00	9,04E-01	8,77E-01	8,52E-01	1,09E-01	2,71E-01	5,04E-01	8,32E-01	8,34E-01	3,50E+00
04.05	2,18E+00	1,10E+00	1,04E+00	1,02E+00	1,55E-01	4,08E-01	6,93E-01	1,07E+00	1,08E+00	4,02E+00
04.10	2,38E+00	1,35E+00	1,23E+00	1,23E+00	2,06E-01	5,56E-01	9,15E-01	1,29E+00	1,38E+00	4,65E+00
04.15	2,38E+00	1,52E+00	1,45E+00	1,42E+00	2,55E-01	7,41E-01	1,15E+00	1,58E+00	1,75E+00	5,47E+00
04.20	2,57E+00	1,70E+00	1,61E+00	1,58E+00	2,79E-01	8,22E-01	1,30E+00	1,71E+00	1,98E+00	5,84E+00
04.25	2,57E+00	1,75E+00	1,68E+00	1,65E+00	2,84E-01	8,43E-01	1,34E+00	1,75E+00	2,06E+00	5,93E+00
04.30	2,57E+00	1,77E+00	1,70E+00	1,68E+00	2,84E-01	8,45E-01	1,34E+00	1,76E+00	2,06E+00	5,96E+00
04.35	2,57E+00	1,78E+00	1,71E+00	1,70E+00	2,86E-01	8,58E-01	1,38E+00	1,82E+00	2,13E+00	6,22E+00
04.40	2,77E+00	1,82E+00	1,77E+00	1,74E+00	2,87E-01	8,68E-01	1,40E+00	1,86E+00	2,21E+00	6,35E+00
04.45	2,77E+00	1,84E+00	1,81E+00	1,78E+00	2,88E-01	8,80E-01	1,43E+00	1,89E+00	2,25E+00	6,62E+00
04.50	2,77E+00	1,85E+00	1,82E+00	1,80E+00	2,89E-01	8,90E-01	1,45E+00	1,92E+00	2,28E+00	6,74E+00
04.55	2,77E+00	1,86E+00	1,85E+00	1,83E+00	2,92E-01	9,10E-01	1,51E+00	2,00E+00	2,35E+00	7,01E+00
05.00	2,77E+00	1,89E+00	1,88E+00	1,85E+00	3,04E-01	9,51E-01	1,58E+00	2,07E+00	2,43E+00	7,16E+00
05.05	2,97E+00	1,93E+00	1,92E+00	1,89E+00	3,07E-01	9,64E-01	1,61E+00	2,09E+00	2,48E+00	7,21E+00
05.10	2,97E+00	1,94E+00	1,93E+00	1,91E+00	3,09E-01	9,71E-01	1,62E+00	2,11E+00	2,50E+00	7,24E+00
05.15	2,97E+00	1,96E+00	1,95E+00	1,93E+00	3,11E-01	9,80E-01	1,64E+00	2,13E+00	2,53E+00	7,33E+00
05.20	2,97E+00	1,98E+00	1,97E+00	1,95E+00	3,11E-01	9,86E-01	1,65E+00	2,15E+00	2,55E+00	7,43E+00
05.25	2,97E+00	1,98E+00	1,98E+00	1,96E+00	3,12E-01	9,88E-01	1,66E+00	2,16E+00	2,57E+00	7,48E+00
05.30	2,97E+00	1,99E+00	1,99E+00	1,97E+00	3,12E-01	9,95E-01	1,67E+00	2,18E+00	2,59E+00	7,54E+00
05.35	2,97E+00	2,01E+00	2,01E+00	1,99E+00	3,14E-01	1,00E+00	1,69E+00	2,20E+00	2,62E+00	7,65E+00
05.40	2,97E+00	2,02E+00	2,03E+00	2,01E+00	3,17E-01	1,01E+00	1,70E+00	2,22E+00	2,65E+00	7,79E+00
05.45	3,17E+00	2,04E+00	2,05E+00	2,03E+00	3,20E-01	1,02E+00	1,72E+00	2,25E+00	2,68E+00	7,87E+00
05.50	3,17E+00	2,08E+00	2,09E+00	2,07E+00	3,26E-01	1,05E+00	1,77E+00	2,31E+00	2,78E+00	8,12E+00
05.55	3,17E+00	2,11E+00	2,13E+00	2,10E+00	3,30E-01	1,08E+00	1,83E+00	2,37E+00	2,89E+00	8,32E+00
06.00	3,17E+00	2,14E+00	2,16E+00	2,14E+00	3,40E-01	1,10E+00	1,87E+00	2,42E+00	2,93E+00	8,42E+00
06.05	3,17E+00	2,17E+00	2,20E+00	2,18E+00	3,43E-01	1,11E+00	1,89E+00	2,44E+00	2,96E+00	8,48E+00
06.10	3,37E+00	2,19E+00	2,22E+00	2,20E+00	3,43E-01	1,11E+00	1,89E+00	2,45E+00	2,96E+00	8,49E+00
06.15	3,37E+00	2,21E+00	2,24E+00	2,23E+00	3,44E-01	1,12E+00	1,90E+00	2,46E+00	2,98E+00	8,55E+00
06.20	3,37E+00	2,25E+00	2,30E+00	2,28E+00	3,67E-01	1,18E+00	2,02E+00	2,57E+00	3,10E+00	8,77E+00
06.25	3,37E+00	2,35E+00	2,40E+00	2,38E+00	3,95E-01	1,30E+00	2,26E+00	2,82E+00	3,35E+00	9,27E+00
06.30	3,56E+00	2,57E+00	2,56E+00	2,55E+00	4,19E-01	1,39E+00	2,39E+00	3,00E+00	3,56E+00	9,78E+00

06.35	3,56E+00	2,72E+00	2,70E+00	2,69E+00	4,38E-01	1,43E+00	2,47E+00	3,09E+00	3,67E+00	1,01E+01
06.40	3,76E+00	2,81E+00	2,81E+00	2,79E+00	4,53E-01	1,50E+00	2,63E+00	3,31E+00	3,91E+00	1,08E+01
06.45	3,76E+00	2,85E+00	2,86E+00	2,85E+00	4,66E-01	1,55E+00	2,73E+00	3,44E+00	4,07E+00	1,11E+01
06.50	3,96E+00	2,87E+00	2,91E+00	2,89E+00	4,82E-01	1,64E+00	2,89E+00	3,64E+00	4,32E+00	1,16E+01
06.55	3,96E+00	2,92E+00	2,96E+00	2,95E+00	4,86E-01	1,66E+00	2,92E+00	3,67E+00	4,37E+00	1,17E+01
07.00	3,96E+00	2,96E+00	3,00E+00	2,99E+00	4,92E-01	1,68E+00	2,96E+00	3,72E+00	4,43E+00	1,19E+01
07.05	4,16E+00	3,01E+00	3,04E+00	3,04E+00	5,04E-01	1,71E+00	3,02E+00	3,78E+00	4,54E+00	1,21E+01
07.10	4,16E+00	3,05E+00	3,09E+00	3,08E+00	5,06E-01	1,73E+00	3,04E+00	3,82E+00	4,58E+00	1,23E+01
07.15	4,36E+00	3,08E+00	3,13E+00	3,12E+00	5,07E-01	1,73E+00	3,06E+00	3,83E+00	4,61E+00	1,23E+01
07.20	4,36E+00	3,10E+00	3,17E+00	3,15E+00	5,13E-01	1,75E+00	3,10E+00	3,88E+00	4,71E+00	1,27E+01
07.25	4,36E+00	3,11E+00	3,18E+00	3,16E+00	5,13E-01	1,75E+00	3,10E+00	3,88E+00	4,72E+00	1,27E+01
07.30	4,55E+00	3,11E+00	3,18E+00	3,16E+00	5,13E-01	1,75E+00	3,10E+00	3,88E+00	4,72E+00	1,27E+01
07.35	4,55E+00	3,12E+00	3,19E+00	3,17E+00	5,13E-01	1,75E+00	3,10E+00	3,89E+00	4,73E+00	1,27E+01
07.40	4,55E+00	3,17E+00	3,23E+00	3,20E+00	5,13E-01	1,75E+00	3,11E+00	3,92E+00	4,78E+00	1,32E+01
07.45	4,55E+00	3,26E+00	3,27E+00	3,26E+00	5,13E-01	1,75E+00	3,11E+00	3,94E+00	4,79E+00	1,33E+01